Computational Design of Multi-targeting Lead-Compounds to Disrupt Quorum Sensing Pathway for Combating Drug-resistant Gram-negative Bacteria Superbugs.

By

Dilip Kumar Yadav

Under the supervision of

Dr. N Arul Murugan & Dr. D K Sharma

Submitted in partial fulfilment of the requirements

for the degree of Master of Technology,

Computational Biology

Centre for Computational Biology Indraprastha

Institute of Information Technology - Delhi

December 2023

Certificate

This is to certify that the thesis titled "Computational Design of Multi-targeting Lead-Compounds to Disrupt Quorum Sensing Pathway for Combating Drug-resistant Gram-negative Bacteria Superbugs." being submitted by Dilip Kumar Yadav to the Indraprastha Institute of Information Technology Delhi, for the award of the Master of Technology is an original research work carried out by him under my supervision. In my opinion, the thesis has reached the standards fulfilling the requirements of the regulations relating to the degree.

The results contained in this thesis have not been submitted in part or full to any other university or institute for the award of any degree/diploma.

December, 2023

Dr. N Arul Murugan & Dr. D K Sharma
Department of Computational Biology & SSH
Indraprastha Institute of Information Technology Delhi
New Delhi 110020

Acknowledgements

I am deeply grateful to Dr. Docent N Arul Murugan & Dr. D K Sharma for his unwavering guidance and mentorship throughout this journey. His encouragement and push for excellence have been instrumental in shaping this work. Even during his busiest days, he generously offered his time to help me with any issues and clarify doubts, for which I am truly thankful.

I extend my heartfelt thanks to my mother, brother, and sister, whose unwavering support and understanding allowed me to fully focus on my thesis. Their constant encouragement has been a source of strength throughout my academic journey. I am indebted to my PhD mentor, Anshul Yadav, for his invaluable advice and insights that have greatly enriched my thesis work. His creative suggestions and ideas have played a significant role in shaping the project.

Gratitude also goes to my friends Amit Samal, Shivansh Verma, and Nishant Singh for their support. Their camaraderie made the ups and downs of the project easier to navigate. I thank my fellow batch mates for their continuous support and camaraderie. Their willingness to help and share knowledge has been a great source of inspiration.

A special mention goes to all the faculty members and staff of the Department of Computational Biology and IIIT Delhi, who have supported us throughout our college journey. I would also like to thank Mr Adarsh from the IT department for his invaluable assistance in providing access to college IT infrastructure and facilitating our web server deployment.

Contents

List of Figures

List of Tables

Chapter 1

1. (a) Introduction

Density sensing, or quorum sensing, is a vital process that regulates a variety of physiological behaviours in bacteria. Both Gram-positive and Gram-negative bacteria have this mechanism, although they use different signal molecules to communicate. Signal molecules, or self-inducing chemicals, are produced and released by bacteria to affect the population's overall behaviour. Certain genes are activated, which controls the bacterial population's adaptability, when the concentration of these signal molecules reaches a threshold determined by the density of the bacterial population. Monitoring a number of cellular functions, including the regulation of bacterial luminescence, virulence factors, resistance to disinfectants, spore formation, toxin production, motility, Biofilm formation and development of resistance to drugs [1]. Despite the fact that antibiotics are now a universal necessity, antibiotic resistance is spreading faster than ever before [2,3]. Ever since antibiotics were introduced, the extensive use of millions of tons of these drugs has exerted selective pressure, leading to the development of resistance in nearly all pathogenic bacteria against commonly employed antibiotics [4]. The majority of antibiotics in current use are formulated to actively eliminate pathogenic bacteria. They achieve this by disrupting cell membranes and disrupting vital protein synthesis. This kind of "life or death" selection pressure encourages the development of microbial resistance, and the widespread application of antibiotics has given rise to significant challenges in dealing with microbial resistance. Over the past few years, there has been a global emergence of "superbugs" that possess the ability to withstand a range of commonly utilized antibiotics. The growing resistance of bacteria to antibacterial substances and the dissemination of these resistant pathogens pose substantial threats to human health. Currently, the majority of antibacterial substances focus on essential bacterial physiological activities, which, in turn, apply significant selection pressure on bacteria and encourage the development and dissemination of drug-resistant strains. Antimicrobial resistance is a worldwide concern that continues to place a growing strain on public health. This is due to the swift development of antibiotic resistance, primarily driven by the excessive and inappropriate use of antibacterial agents. The reduced involvement of many leading pharmaceutical companies in antibiotic research and their shift towards addressing chronic, non-communicable illnesses highlights the challenges involved in creating innovative antibacterial treatments and the substantial expenses associated with bringing new therapies to market. The crisis related to antibiotics is connected to the emergence of multidrug-resistant pathogens, commonly known as "superbugs." These superbugs can survive antibiotic treatments, as demonstrated by the

group of pathogens referred to as "ESKAPE," including Enterococcus faecium, Staphylococcus aureus, Klebsiella pneumoniae, Acinetobacter baumannii, *Pseudomonas aeruginosa*, and Enterobacter species. According to the World Health Organization (WHO), *Pseudomonas aeruginosa* is classified as a "critical priority pathogen" that demands immediate attention because of its multidrug resistance (MDR) to a wide range of antibiotics, including carbapenems and third-generation cephalosporins [5]. *Pseudomonas aeruginosa* is a frequent cause of infections in various parts of the body, including the lungs, skin, eyes, wounds, bloodstream, and urinary tract. These infections can occur in both hospital and community settings [6,7]. This Gram-negative bacterium is a frequent instigator of infections acquired in healthcare facilities (nosocomial infections). It also plays a significant role as a pathogen in patients with cystic fibrosis (CF), those with weakened immune systems, individuals with burns and open fractures, and those who have implanted medical devices like catheters [8].

1. (b) Mechanisms of Microbial Resistance

Extensive antibiotic utilization in clinical therapy has resulted in the development of concurrent multi-resistance mechanisms in microorganisms against antibiotic receptors. The primary mechanisms involve the inactivation of antibiotics via chemical alterations, the active efflux of antibiotics through systemic pumps, and the modification of genes responsible for drug receptors.

Simultaneously, numerous pathogenic bacteria have the capability to generate a dense biofilm, which significantly enhances their resistance [9].

(a) Chemical modification is a process that disrupts the mechanism of antibiotic action by releasing modified enzymes capable of altering the chemical structure of antibiotic drugs. This, in turn, renders the antibiotics inactive and devoid of their therapeutic properties. The enzymatic mechanism behind this involves the degradation and chemical modification of antibiotic groups. A highly effective strategy for combating antibiotic presence involves the production of enzymes. By introducing specific compounds to inactivate the drugs or dismantle the molecules themselves, the antibiotics lose their capacity to interact with their intended receptors.

(b) Microorganisms can also employ antibiotic efflux mechanisms to expel antibiotics. Typically, antibiotic drugs need to traverse the microorganism's cell membrane to effectively receptors specific components. Antibiotic efflux resistance represents a significant mechanism of microbial resistance facilitated by drug efflux pumps. Microorganisms construct efflux pump proteins on the cell membrane to remove antibiotic drugs from within the cell. This expulsion process often outpaces the rate of drug penetration, thereby regulating the intracellular drug concentration to a non-sensitive

level. Various microbial efflux pump systems have been identified, including lipophilic and hydrophilic efflux systems, each designed to address drugs with distinct chemical properties.

(c) Another significant resistance mechanism involves the alteration of Drug receptors genes. This mechanism primarily entails the modification of Drug receptors genes, resulting in the loss of drug efficacy as it can no longer bind to the receptor. Bacteria employ various common strategies to develop antibiotic resistance, including evading the impact of antibiotics by disrupting the receptors site. Consequently, bacteria have developed diverse tactics, such as shielding the Receptors(preventing the antibiotic from reaching its binding site) and modifying the receptors site, which reduces the affinity for antibiotic molecules. In the context of β-lactam antibiotics, they exert a bactericidal effect by inhibiting mucopeptide synthase and the penicillin-binding proteins (PBPs) involved in the bacterial cell wall's transpeptidation process. This inhibition prevents the bacteria from forming a complete cell wall, ultimately leading to their demise.

(d) Drug resistance results from the cellular adaptations that have evolved over time. Bacteria have developed intricate mechanisms to adapt to environmental stressors, enabling them to survive even in challenging conditions, such as within the human body. To gain a competitive edge, bacteria must actively compete for essential nutrients while also defending against assaults from molecules produced by other competing organisms.

Within a specific host, bacteria consistently face challenges from the host's immune system. To successfully establish themselves in a particular biological environment, it is imperative for bacteria to adapt and endure these stressful circumstances. Consequently, bacteria have devised intricate mechanisms to safeguard essential cellular processes, including the synthesis of cell walls and the maintenance of membrane stability. The development of resistance to antibiotics like daptomycin (DAP) and vancomycin (at low levels in Staphylococcus aureus) represents a clinically significant example of a resistance phenotype arising from an overarching cellular adaptive response to bacterial threats [11].

The presence of numerous mechanisms of multidrug resistance has posed significant challenges in addressing and resolving the issue of microbial resistance. In the ongoing battle between microorganisms and antibiotics, an increasing number of microorganisms have developed multiple resistance mechanisms, leading to the emergence of "super bacteria." As an illustration, the highly resistant bacterium Staphylococcus aureus exhibits the capability to specifically degrade penicillin through the production of β-lactamase. Conversely, it can also nullify methicillin's ability to bind to cell wall mucin synthase by producing the PBP2a protein [10]. In the case of another highly resistant bacterium, *Pseudomonas aeruginosa*, it possesses the ability to generate diverse drug efflux pumps to withstand various classes of antibiotics. Furthermore, resistance genes can be acquired through

horizontal gene transfer. The alteration in bacterial morphology and the formation of dense biofilms allow it to exhibit resistance to nearly all antibiotics available in the market [11].

1. (c) The Disease-Causing Potential of *Pseudomonas Aeruginosa*

Pseudomonas aeruginosa's clinical relevance arises from its ability to produce a wide array of virulence factors that facilitate the invasion and damage of host tissues. Among these factors, flagella and pili play roles in adhering to tissue surfaces and promoting tissue migration through swarming and twitching movements. Furthermore, P. aeruginosa releases various exoenzymes, exotoxins, and proteins that disrupt host defense mechanisms, all of which are pivotal for its virulence and overall survival. In addition, *Pseudomonas aeruginosa* produces numerous secondary metabolites, including hydrogen cyanide (HCN). It can also affect the host's response to oxidative stress through the use of the redox-reactive pigment pyocyanin. Furthermore, the bacterium acquires essential nutrients, such as iron, from host proteins like transferrin and lactoferrin using siderophores like pyoverdine and pyochelin. In chronic infections, *Pseudomonas aeruginosa* develops biofilms, which are bacterial communities typically anchored to a surface and enclosed within an extracellular matrix containing various substances like exopolysaccharides, proteins, nucleic acids, and lipids. Biofilms possess a high resistance to antibiotics and the immune system. Consequently, the diverse range of virulence elements, comprising secreted large molecules and secondary metabolites in *Pseudomonas aeruginosa*'s arsenal, presents it as a formidable opportunistic pathogen, posing significant challenges [14]. In recent years, investigators have highlighted the significance of bacterial biofilm formation in conferring resistance against microbes. The drug resistance stemming from bacterial biofilms represents a systematic and intricate resistance mechanism. This resistance principle can be broken down into at least three key components [14].

(a) The biofilm structure itself serves as an efficient barrier against drugs, leading to a considerable reduction in antibiotic penetration. Bacteria within the biofilm are interconnected through proteins and DNA, particularly extracellular polysaccharides. This interconnection forms an impenetrable barrier that significantly diminishes the permeability of antibiotic drugs, thereby enhancing the bacterial survival rate within the biofilm.

(b) The unique microenvironment within the biofilm induces bacterial heterogeneity in the membrane and governs the antibiotic resistance of these bacteria. Research has shown that nutrient concentrations and bacterial secretions within various regions of the biofilm are not uniform. Consequently, this results in varying growth conditions among bacterial cells in different areas of the

biofilm, ultimately causing bacterial heterogeneity and leading to distinct levels of drug resistance among the bacterial population.

(c) The highly challenging conditions existing outside the biofilm foster drug resistance within the bacterial membrane. Significant environmental fluctuations external to the biofilm, including alterations in temperature, pH levels, and the concentration of specific chemicals, can influence the bacteria's functions within the biofilm. These influences can result in the regulation of their physiological and biochemical processes, leading to reduced growth efficiency and the development of a state of antibiotic resistance. Hence, it proves beneficial to investigate bacterial resistance by receptors strategies that inhibit the formation of bacterial biofilms, suppress bacterial quorum sensing, mitigate the barrier effects of biofilms, and inhibit the phenotypic alterations of bacteria within biofilms. These approaches aim to diminish the antibiotic resistance exhibited by bacterial biofilms [12].

Mechanism of Resistance	Mechanism of Action
Chemical Alteration	Alter the chemical composition of antibiotic medications
Efflux Pump Mechanism	Efflux of Intracellular Antibiotics
Alteration of Genes Involved in Drug Receptors	Modify Genes Related to Drug Receptors
Comprehensive Cellular Adaptation	Adapt and Respond to Environmental Stressors
The Biofilm Structure Itself	Diminish the Penetration of Antibiotics
Unique Internal Environment within the Biofilm	Intracellular Structures Generate Variability
Harsh External Conditions Beyond the Biofilm	Intracellular Structures Foster Resistance

Table.1. (c): Deciphering the Battle: Mechanism of Resistance and Mechanism of Action in *Pseudomonas aeruginosa* – A Comprehensive Analysis.

1. (d) *Pseudomonas aeruginosa* as a Highly Resistant Pathogen

Pseudomonas aeruginosa displays a high degree of antimicrobial resistance attributed to intrinsic, acquired, and evolved mechanisms. In the case of intrinsic resistance, P. aeruginosa's outer membrane has low permeability, and it boasts a repertoire of at least 12 efflux pumps capable of

ejecting diverse antibiotics, encompassing cephalosporins, carbapenems, fluoroquinolones, and aminoglycosides [13]. Furthermore, β-lactamase genes are often encoded within the chromosomal DNA of P. aeruginosa, rendering the bacterium resistant to penicillins and cephalosporins. In *Pseudomonas aeruginosa*, acquired resistance primarily occurs through horizontal gene transfer, wherein genes responsible for particular resistance traits are transmitted from one bacterium to another. Acquired resistance can also emerge through mutational alterations, such as those affecting DNA gyrase, which leads to reduced affinity for fluoroquinolones [14]. A third avenue for the development of resistance is termed evolved resistance. In this process, *Pseudomonas aeruginosa* responds to various stimuli, including subinhibitory levels of antibiotics, nutrient scarcity, pH fluctuations, and temperature variations. This response involves the activation of genes that enhance specific functions, such as efflux pump mechanisms, and those that modify the composition of the cell envelope [14]. Hence, the efficacy of compounds designed to receptors *Pseudomonas aeruginosa* infections can be considerably hindered by these bacterial defense mechanisms. Therefore, it is crucial to take into account the understanding of prevailing resistance mechanisms when incorporating new molecular structures into the rational development of inhibitors Receptors bacterial quorum sensing regulatory pathways [14].

1. (e) Receptors Quorum Sensing for Drug Discovery

Quorum sensing (QS) is a cellular communication mechanism employed by bacteria, involving the generation and perception of diffusible signaling molecules known as quorum sensing signal molecules (QSSMs) or autoinducers (AIs). When a bacterial population attains a specific threshold, as indicated by the concentration of QSSMs in the nearby milieu, it triggers the coordinated transcription of numerous genes, allowing the population to exhibit collective behavior. The regulation facilitated by diffusible signaling molecules oversees a diverse array of processes, including swarming and swimming motility, biofilm maturation, the production of virulence factors, secondary metabolites, and the development of antibiotic resistance. In recent times, endeavors to create novel antimicrobial compounds have encompassed the focus on particular virulence factors or the regulatory mechanisms of virulence, rather than solely Receptors cell viability. This approach is aimed at reducing the selective pressures that give rise to the development of resistance. One of these tactics involves the disruption of bacterial communication by Receptors QS-mediated signaling. This disruption aims to reduce virulence, allowing the host's defense mechanisms to eliminate the infecting bacteria. Therefore, the utilization of QS inhibitors (QSIs), which do not directly impact bacterial viability, is expected to exert lower selective pressure in terms of resistance compared to

traditional antibiotics. QS inhibitors (QSIs) alone might not be entirely effective in eradicating infections, particularly in individuals with compromised immune systems. However, they are likely to work synergistically when combined with growth-inhibiting antibiotics. Nevertheless, QSIs can prove highly effective as preventive measures [15].

1. (f) Mechanisms of Quorum Sensing Employed by *Pseudomonas aeruginosa*

Pseudomonas aeruginosa houses three prominent quorum sensing (QS) systems: las, rhl, and pqs. These systems exhibit intricate interconnections and substantial integration. Each system is autoregulatory and, concurrently, influences the functions of the others. For instance, the las system plays a positive regulatory role in both the rhl and pqs system genes, which encode QSSM receptors (rhlR and pqsR) and synthase genes (rhlI and pqsH). Nevertheless, specific receptors genes are exclusively controlled by either the las or rhl system, while some necessitate the combined activation of both of these quorum sensing systems for full functionality [16]. The las and rhl systems utilize distinct N-acyl-L-homoserine lactone (AHL) type signal molecules. The third quorum sensing circuit, known as pqs, employs 2-alkyl-4-quinolones (such as 2-heptyl-4-hydroxyquinoline (HHQ) or 2-heptyl-3-hydroxy-4(1H)-quinolone (PQS)) as quorum sensing signal molecules (QSSMs). *Pseudomonas aeruginosa* strains with mutations in critical QS genes from the las, rhl, or pqs systems exhibit significantly reduced pathogenicity in experimental infection models. This highlights the potential of QS as a receptors for novel antibacterial agents [17]. In each quorum sensing system, the binding of the respective QS signal molecule to the receptor protein (LasR, RhlR, and PqsR) triggers the expression of biosynthetic genes, creating an autoinduction loop that produces additional signal molecules. Simultaneously, this activation is responsible for the upregulation of various genes related to virulence, secondary metabolism, and the development of biofilms [17].

1. (g) The pqs System in Pseudomonas (Pseudomonas Quinolone System)

The *Pseudomonas aeruginosa* pqs quorum sensing (QS) system utilizes 2-alkyl-4-quinolone signal molecules instead of AHLs. These molecules interact with their specific receptor, PqsR (also known as MvfR), which belongs to the LysR family of transcriptional regulators. PqsR typically comprises an N-terminal DNA-binding domain and a C-terminal ligand-binding domain. *Pseudomonas aeruginosa* synthesizes a diverse array of more than 50 quinolone molecules falling into three primary classes: 2-alkyl-4-hydroxyquinolines, 2-alkyl-3-hydroxy-4-quinolones, and 2-alkyl-4-hydroxyquinoline-N-oxides, including HHQ (2-heptyl-4-hydroxyquinolone) and Pseudomonas quinolone signal (PQS) (2-heptyl-3-hydroxy-4(1H)-quinolone). PQS/HHQ and their C-9 derivatives can activate PqsR. In contrast to HHQ, PQS acts as an iron chelator and regulates the expression of

genes associated with the iron-starvation response and the production of virulence factors through both PqsR-dependent and PqsR-independent pathways [18]. The biosynthesis of AQ involves the fusion of 70 and β-keto fatty acids, a process facilitated by the heterodimeric enzyme PqsBC. This fusion results in the formation of HHQ, which can then undergo hydroxylation at the 3-position catalyzed by PqsH to produce PQS [19]. The Co-A derivative is the result of reactions involving PqsA and PqsD, initiated from anthranilic acid. Both PQS and HHQ can engage with PqsR to create a PqsR/AQ protein complex. This complex subsequently binds to the pqsA promoter, resulting in the activation of the pqsABCDEphnAB operon. This activation triggers the autoinduction response, a characteristic feature of many quorum sensing systems [20]. Recent research has uncovered that while PqsE serves as a thioesterase involved in AQ biosynthesis, the precise mechanism by which PqsE regulates specific virulence factors, such as pyocyanin, remains unclear [21]. The AQ system is interconnected with the las and rhl QS systems, as LasR positively influences it, while RhlR has a negative effect on PqsR by binding to its promoter. Furthermore, pqsH experiences positive regulation by LasR/3OC12-HSL, which leads to an increase in the quantity of PQS [21].

1.1 Thesis Organisation

Chapter 2 [Methodology] - This chapter delineates the all-encompassing methodology employed in the research, encompassing data collection and processing procedures. It elucidates the acquisition and analysis of data related to protein receptors in *Pseudomonas aeruginosa*, along with their inhibitors for quorum sensing. Furthermore, the chapter provides insights into the modeling of proteins and the meticulous selection of compounds for the further study.

Chapter 3, 4 & 5 [Results and Discussion] - In this chapter, the research findings take center stage, encompassing thorough data analysis, the identification of shared molecules exhibiting inhibitory properties, and the outcomes of protein modeling and molecular docking. The discussion delves into the significance of these results, unraveling their implications for the broader research topic.

Chapter 6 [Conclusion and Future Directions] - The concluding chapter encapsulates the pivotal discoveries of the study, emphasizing their significance in the context of quorum sensing in *Pseudomonas aeruginosa* and their potential implications for therapeutic interventions. The chapter adeptly addresses the study's limitations and offers valuable recommendations for future research, thereby underscoring its substantial contribution to the investigation of *Pseudomonas aeruginosa* and the enhancement of patient treatment methodologies.

Chapter 2

2.1 Introduction

The investigation into the quorum sensing pathways of *Pseudomonas aeruginosa* in this study is underpinned by a meticulous and multifaceted approach. *Pseudomonas aeruginosa*, a pathogenic bacterium notorious for its role in nosocomial infections and its intrinsic resistance to multiple drugs, relies significantly on quorum sensing to coordinate virulence and population dynamics. To unravel the intricacies of this system, the study focuses on four major quorum sensing systems: LAS, RHL, PQS, and IQS. The methodology employed in this study integrates cutting-edge computational tools and databases to comprehensively explore and dissect the quorum sensing pathways. The utilization of a Linux operating system provides a robust and secure foundation for the research. Python, a versatile programming language, is harnessed for scripting and data analysis. Jupyter notebooks facilitate an interactive and organized environment for seamless code execution and documentation. This amalgamation of cutting-edge computational tools, databases, and bioinformatics methodologies forms the bedrock of a systematic and rigorous exploration into the quorum sensing pathways of *Pseudomonas aeruginosa*. The integration of these tools enables a holistic understanding of bacterial communication networks, providing a foundation for the identification of potential inhibitors and the development of targeted strategies against *Pseudomonas aeruginosa* infections [22].

2.2 Computational Requirements

By effectively meeting the essential computational requirements, we were able to fulfill the study objectives and carry out the necessary analyses, data processing, and derive meaningful findings within the designated timeframe. The successful completion of our investigation was facilitated by resolving these computational needs.

2.2.1 Linux Operating System Setup

IIIT Delhi employed the open-source, Unix-based Linux operating system to process data for this investigation. The selection of Linux was based on its reliability, adaptability, and resilience in handling data-intensive tasks, making it an ideal choice for data processing and analysis. The robust command-line interface and comprehensive support for scientific computing further contributed to its suitability. The Linux operating system provided by IIIT Delhi's Dr. Docent N Arul Murugan Lab

(Neurocare – e Lab) met all the specified requirements for the study. During the design and development of data processing scripts, careful consideration was given to operating system compatibility, with a particular focus on supporting the Windows platform. Although the subsequent data preparation operations were executed on the Linux operating system, the script design aimed at ensuring seamless execution and optimal performance on Windows platforms. This interoperability enhances accessibility and flexibility, allowing researchers to utilize the scripts on various operating systems. The initial configuration of workstations involved the installation and setup of the Linux operating system using available resources to establish the Linux environment. Administrative access to the computer system was necessary to facilitate a smooth setup process. The use of the Linux operating system was deemed essential for researchers, as it played a crucial role in ensuring the reliable and secure completion of data processing tasks [23].

2.2.2 Python Environment Setup

Python was selected for its simplicity and versatility as a widely used programming language. Introduced in 1991 in homage to the British comedy group Monty Python, Python has evolved into a user-friendly language. Its popularity in data analysis and scientific computing is attributed to its straightforward syntax, extensive standard library, and a thriving ecosystem of third-party packages. This study utilized Python 3, the latest version of the language, chosen for its stability and compatibility with contemporary libraries. To ensure a seamless workflow, the Python environment was configured on Linux workstations. Installation and setup were performed through the command line, with an update to ensure Python 3 ran at its most recent version. Depending on the project's setup, either the pip package manager or the conda package manager was employed to install essential Python packages and libraries, such as Pandas and NumPy, Matplotlib, Plotly, Seaborn. These packages provide robust tools for data analysis, computing, and manipulation, enhancing the functionality of the Python environment. The meticulous configuration of the Python environment and the Linux operating system established a reliable and effective platform for conducting the study. The scripts developed for the study can be adapted for other operating systems by incorporating Windows compatibility, promoting accessibility and enabling researchers to work with their preferred setups. The adoption of Python streamlined data analysis tasks, offering a flexible and adaptable programming environment, thanks to its simplicity and extensive libraries [24].

2.2.3 Jupyter notebook

Jupyter Notebook stands out as a robust and widely embraced web-based application catering to data analysis, scientific computing, and machine learning endeavors. This open-source software empowers users to construct interactive documents that seamlessly integrate live code, mathematical expressions, images, and textual content. Its notable strength lies in its ability to amalgamate code execution, data visualization, and documentation within a unified environment, making it a favored tool among academics and educators. The unique feature of Jupyter Notebook lies in its capability to seamlessly integrate code execution, data visualization, and documentation, resembling a virtual laboratory. Users can create and execute code, visualize data, and document their entire workflow, all within a single platform. Jupyter notebooks are saved with the .ipynb extension, encapsulating source code, results, and explanations for easy sharing and duplication of work. Before utilizing Jupyter Notebook, it needs to be installed on the user's PC, a straightforward process achieved by running the pip command, which automatically takes care of all necessary dependencies. Once installed, launching Jupyter Notebook is a simple task from the computer's terminal, initiating the application in the user's default web browser, ready for them to embark on their data analysis endeavors [25].

2.3 Tools and web server (Biological databases, web servers and software are used in the thesis)

2.3.1 NCBI PubMed

The National Center for Biotechnology Information (NCBI) PubMed stands as a cornerstone in the field of biomedical research, offering an extensive and freely accessible database of scientific literature. PubMed serves as an invaluable resource for researchers, healthcare professionals, and the broader scientific community, facilitating access to a vast repository of peer-reviewed articles and biomedical literature. NCBI PubMed stands as an indispensable resource in the realm of biomedical literature, playing a pivotal role in advancing scientific knowledge, supporting evidence-based practices, and fostering collaboration within the global scientific community. Researchers and healthcare professionals alike benefit from the wealth of information provided by PubMed, contributing to the ongoing progress of biomedical research [26].

2.3.2 PDB RCSB

PDB RCSB, likely an abbreviation for "Protein Data Bank at the Research Collaboratory for Structural Bioinformatics," signifies a specialized platform dedicated to the comprehensive

collection and dissemination of three-dimensional structural data pertaining to biological macromolecules, with a primary focus on proteins. The RCSB, or Research Collaboratory for Structural Bioinformatics, serves as the custodian of this valuable resource, emphasizing its commitment to advancing structural biology research. This platform plays a pivotal role in providing researchers, scientists, and the broader scientific community with access to a vast array of structural information, enabling in-depth exploration and analysis of macromolecular structures. The collaborative nature of the RCSB underscores its dedication to fostering advancements in structural bioinformatics, thereby contributing to the broader understanding of biological processes and supporting research endeavors across various scientific disciplines [27].

2.3.3 UNIPROT

UniProt, short for Universal Protein Resource, is a comprehensive and widely utilized database that serves as a centralized hub for information related to protein sequences and functional annotation. Established through collaborative efforts, UniProt provides a wealth of data essential for various biological and biochemical research endeavors. UniProt consolidates information from multiple sources, including experimental data, computational predictions, and curated literature, to offer a comprehensive overview of protein sequences and their associated functions. The database is a vital resource for researchers, bioinformaticians, and scientists working in diverse fields such as genomics, proteomics, and systems biology. Key features of UniProt include its three main components: UniProtKB (Knowledgebase), UniRef (Sequence Clusters), and UniParc (Sequence Archive). Researchers often turn to UniProt for its user-friendly interface, powerful search capabilities, and the wealth of information it provides about individual proteins, including their functions, subcellular locations, and involvement in biological pathways. The database plays a crucial role in advancing scientific understanding by facilitating the exploration of protein structure and function on a global scale. So, UniProt stands as a cornerstone resource in the field of bioinformatics, offering a centralized platform that empowers researchers worldwide with accurate and up-to-date information on protein sequences and their functional annotations [28].

2.3.4 SWISS – MODEL

Swiss-Model is a widely used and reputable automated protein structure homology-modeling server. Swiss-Model is an online resource designed to predict and model the three-dimensional structure of a protein based on its amino acid sequence. It operates on the principle of homology modeling, leveraging the known structures of related proteins (homologs) to predict the structure of a receptor protein.

Key features and aspects of Swiss-Model include:

I. Homology Modeling: Swiss-Model employs homology modeling, a technique that assumes proteins with similar sequences share similar structures. If a protein's sequence closely resembles that of a known structure, Swiss-Model generates a model of the receptor protein based on the template structure.

II. Automated Process: One of the strengths of Swiss-Model is its automation. Users can submit a protein sequence to the server, and the platform performs the modeling process, generating a predicted 3D structure without the need for extensive user intervention.

III. Template Selection: Swiss-Model selects appropriate templates for modeling based on sequence similarity and other factors. The reliability of the predictions depends on the availability and quality of suitable template structures.

IV. Visualization and Analysis: The platform typically provides tools for users to visualize and analyze the generated protein models. This aids researchers in assessing the quality of the predicted structure and gaining insights into the potential function of the receptor protein.

V. Integration with Other Resources: Swiss-Model may integrate with other bioinformatics resources, databases, and tools to enhance the accuracy and utility of the modeling process.

Overall, Swiss-Model plays a valuable role in the field of structural bioinformatics by providing a user-friendly and automated platform for predicting the three-dimensional structures of proteins based on homology modeling principles [29].

2.3.5 AutoDock Vina: Molecular Docking Software

AutoDock Vina is widely used and efficient molecular docking software designed for predicting the binding modes of small ligands to macromolecular Receptors. Molecular docking is a crucial computational technique in the field of structural bioinformatics, helping researchers understand and predict the interactions between small molecules, such as drug candidates, and their receptors proteins. Researchers and drug discovery professionals often utilize AutoDock Vina in the early stages of drug development to identify potential lead compounds and understand their binding interactions with receptors proteins. It has proven valuable in virtual screening campaigns, where large compound libraries are computationally screened to prioritize candidates for further experimental validation [30].

Key Features of AutoDock Vina:

I. Molecular Docking: AutoDock Vina performs molecular docking simulations, predicting how a ligand (small molecule) binds to a receptors (typically a protein). The software

explores different conformations and orientations of the ligand within the binding site to estimate the most energetically favourable binding mode.

II. Scoring Function: AutoDock Vina employs a scoring function to evaluate and rank potential binding poses. The scoring function estimates the binding affinity between the ligand and the receptor, helping researchers identify the most likely binding configurations.

III. Efficiency: One of the notable features of AutoDock Vina is its computational efficiency. The software is designed to provide accurate results with relatively shorter computational times compared to some other docking programs, making it a popular choice for virtual screening campaigns.

IV. User-Friendly Interface: AutoDock Vina is often appreciated for its user-friendly interface, which allows users to set up and run docking simulations with relative ease. The software typically supports command-line usage as well as graphical interfaces for improved accessibility.

V. Open-Source: AutoDock Vina is open-source software, fostering collaboration and allowing researchers to modify and customize the code to suit their specific needs. This open nature has contributed to the widespread adoption and continuous improvement of the software.

VI. Versatility: While AutoDock Vina is commonly used for protein-ligand docking, it is versatile enough to handle various types of macromolecular Receptors, including nucleic acids.

2.3.6 PyMOL

PyMOL is powerful and widely used molecular visualization software designed for the analysis and representation of three-dimensional molecular structures. Developed by Warren L. DeLano, PyMOL is known for its versatility and user-friendly interface, making it a popular tool among researchers, structural biologists, and chemists. Researchers often employ PyMOL for tasks such as analyzing protein-ligand interactions, visualizing macromolecular complexes, and generating insightful structural representations for scientific communication [31].

Key Features of PyMOL:

I. Molecular Visualization: PyMOL excels in visually representing molecular structures, including proteins, nucleic acids, small molecules, and other complex biomolecular assemblies. It provides high-quality graphical representations that aid researchers in understanding the spatial arrangement and conformation of molecular entities.

II. Publication-Quality Graphics: PyMOL is often utilized for generating publication-quality images and figures. Its rendering capabilities enable the creation of visually appealing

representations, facilitating the communication of complex structural information in scientific publications and presentations.

III. Scripting and Automation: PyMOL supports a scripting language that allows users to automate tasks and customize the visualization process. This scripting capability is valuable for creating reproducible workflows and efficiently handling large datasets.

IV. Integration with Other Tools: PyMOL can be integrated with other computational tools and software, enhancing its utility in structural biology workflows. It supports various file formats for importing and exporting molecular structures, promoting interoperability with other bioinformatics resources.

2.3.7 MGL Tool

"MGL Tools" likely refers to a set of software tools developed by the Molecular Graphics Laboratory (MGL) for molecular modeling and visualization. Specifically, MGL Tools are associated with the AutoDock suite, which includes tools for molecular docking simulations [32].

MGL Tools in the Context of AutoDock:

I. Preparation of Input Files: MGL Tools typically provide utilities for preparing input files for molecular docking simulations. This includes the conversion of molecular structures, such as proteins and ligands, into formats compatible with AutoDock.

II. Graphical User Interface (GUI): MGL Tools often come with a graphical user interface to facilitate the setup of molecular docking experiments. The GUI makes it more accessible for users to define parameters, set up simulations, and visualize the structures.

III. Grid Generation: Molecular docking often involves the generation of grids that define the search space for ligand binding. MGL Tools may include features for generating these grids, considering factors like the binding site and possible ligand orientations.

IV. Analysis and Visualization: After running molecular docking simulations, MGL Tools may offer functionalities for the analysis and visualization of results. This can include examining binding poses, calculating binding energies, and generating visual representations of the interactions between ligands and proteins.

V. Integration with AutoDock Suite: MGL Tools are closely associated with the AutoDock suite of software. AutoDock is a widely used molecular docking program for predicting ligand-receptor interactions, and MGL Tools provide a user-friendly interface for preparing input files and analyzing output files generated by AutoDock.

VI. Scripting Capabilities: MGL Tools may offer scripting capabilities, allowing users to automate tasks and customize workflows according to their specific needs. This scripting support enhances the flexibility and reproducibility of molecular modeling analyses.

2.3.8 CASTp: Computed Atlas of Surface Topography of proteins

CASTp, which stands for Computed Atlas of Surface Topography of proteins, is a valuable computational tool designed for the identification and analysis of pockets and voids on the surfaces of protein structures. Developed to aid researchers in understanding the functional characteristics of proteins, CASTp provides insights into the spatial arrangement of concave regions, binding sites, and potential ligand-binding pockets within three-dimensional protein structures [33].

Key Features of CASTp:

I. Surface Topography Analysis: CASTp specializes in the computation of the surface topography of proteins. It identifies and characterizes concave regions, cavities, and pockets on the protein surface, which are often crucial for understanding the protein's function, such as ligand binding sites or active sites.

II. Identification of Binding Sites: One of the primary applications of CASTp is the identification of potential binding sites on protein surfaces. This information is essential for drug discovery and the design of ligands or inhibitors that can interact with specific regions of the protein.

III. Volume and Area Calculations: CASTp provides quantitative measurements, including volume and area calculations, for the identified pockets and voids. These metrics offer valuable quantitative insights into the size and accessibility of potential binding sites.

IV. Visualization Tools: The tool often comes equipped with visualization capabilities, allowing users to interactively explore and analyze the three-dimensional structures of proteins along with the identified pockets. Visual representations aid in the interpretation of structural features.

V. Accessibility and Web Interface: CASTp is often accessible through a web interface, making it convenient for researchers to submit protein structures for analysis without the need for extensive software installation or computational expertise.

VI. Versatility: CASTp is versatile and applicable to a wide range of protein structures. It can be used for the analysis of both small proteins and large macromolecular complexes, providing insights into the structural features of diverse biological molecules.

2.3.9 Open Babel

Open Babel is an open-source chemical toolbox designed to facilitate molecular informatics and computational chemistry tasks. Serving as a versatile and powerful software, Open Babel allows users to interconvert chemical file formats, perform molecular manipulation, and carry out diverse cheminformatics operations. It is widely utilized by researchers, computational chemists, and developers in the field of chemistry and related disciplines.

Key Features of Open Babel:

I. Chemical File Format Conversion: Open Babel excels in converting chemical file formats, providing a seamless means of interoperability between different molecular structure representations. It supports a vast array of file formats, allowing users to convert molecular structures into a format suitable for their specific needs.

II. Molecular Structure Manipulation: Users can employ Open Babel to perform various operations on molecular structures, such as adding or removing hydrogen atoms, generating 3D coordinates, and optimizing molecular geometries. These manipulations are essential for preparing structures for computational studies and analyses.

III. Chemical Informatics: Open Babel facilitates cheminformatics tasks, including the calculation of molecular descriptors, molecular fingerprints, and other quantitative measures that aid in the characterization and comparison of chemical compounds.

IV. Scripting and Programming Interface: Open Babel provides a scripting interface and programming API (Application Programming Interface), enabling users to automate tasks and integrate Open Babel functionalities into their workflows. This flexibility is valuable for users who wish to customize their analyses or perform batch processing.

V. Interoperability: The software promotes interoperability in cheminformatics research by supporting integration with other tools and software packages. Its open nature allows for collaboration and compatibility within the broader computational chemistry community.

VI. 3D Structure Generation: Open Babel includes tools for generating 3D molecular structures, a crucial step in preparing molecules for molecular dynamics simulations, quantum chemistry calculations, and other computational studies.

VII. Accessibility: Open Babel is often accessible through a command-line interface, making it straightforward for users to incorporate it into scripts or use it in a computational pipeline. Additionally, it may have graphical user interfaces (GUIs) for those who prefer a more interactive experience.

Overall, Open Babel plays a pivotal role in the field of computational chemistry and molecular informatics by providing a reliable and open-source platform for diverse chemical data manipulation and analysis tasks. Researchers leverage its capabilities for tasks ranging from virtual screening in drug discovery to the preparation of input files for quantum chemistry simulations [34].

2.3.10 PubChem Sketcher

The PubChem Sketcher is a web-based molecular structure drawing tool provided by PubChem, a comprehensive chemical database maintained by the National Center for Biotechnology Information (NCBI), part of the United States National Library of Medicine (NLM). The Sketcher is designed to enable users to draw, modify, and submit chemical structures interactively through a user-friendly graphical interface [35].

Key Features of PubChem Sketcher:

I. Molecular Structure Drawing: The primary functionality of the PubChem Sketcher is to allow users to draw molecular structures directly within the web interface. This feature is valuable for researchers, students, and professionals who need to input chemical structures for various purposes, such as searching for chemical information or submitting structures for prediction.

II. Chemical Structure Editing: Users can edit and modify drawn structures using a range of tools provided by the Sketcher. This includes adding or removing atoms, changing bond types, and adjusting the overall structure to represent the desired chemical compound accurately.

III. Real-Time Structure Validation: The Sketcher often includes real-time validation features, helping users ensure that the drawn structures are chemically valid. This can be particularly useful in preventing common errors and ensuring the accuracy of the entered chemical information.

IV. Integration with PubChem Database: The PubChem Sketcher is integrated with the larger PubChem database, allowing users to search for information related to the drawn structures. This integration enhances the utility of the Sketcher for users interested in exploring existing chemical data or contributing their structures to the PubChem repository.

V. Export and Sharing: Once a structure is drawn or edited, users can typically export the structure in various chemical file formats. This facilitates the sharing of structures with colleagues or using them in other computational chemistry tools and software.

VI. Accessibility: As a web-based tool, the PubChem Sketcher is easily accessible from standard web browsers without the need for additional software installation. This accessibility makes it

a convenient choice for users who require a quick and efficient way to draw and manipulate chemical structures.

2.3.11 NovoPro Bioscience

NovoPro Bioscience is a dynamic and innovative company operating in the bioscience sector. Established with a commitment to advancing scientific discovery and improving life sciences research, NovoPro Bioscience has emerged as a notable player in the field.

Key Features and Offerings:

I. Product Portfolio: NovoPro Bioscience is recognized for its diverse range of [e.g., antibodies, proteins, assays] designed to meet the evolving needs of the scientific community.

II. Cutting-Edge Technology: At the forefront of bioscience, NovoPro Bioscience leverages cutting-edge technologies and methodologies to deliver reliable and high-quality solutions. This commitment to innovation positions the company as a trusted partner in the advancement of research.

III. Research and Development: A strong emphasis on research and development underscores NovoPro Bioscience's dedication to staying abreast of the latest advancements in the bioscience field. This commitment is reflected in the continuous improvement and expansion of their product offerings.

IV. Global Reach: With a global perspective, NovoPro Bioscience caters to the needs of researchers and scientists worldwide. The company's products are distributed internationally, contributing to scientific endeavors on a global scale.

V. Customer-Centric Approach: NovoPro Bioscience places a high value on customer satisfaction. The company is known for its customer-centric approach, providing support and expertise to researchers, institutions, and industries engaged in life sciences.

2.3.12 LigPlot+

LigPlot+ is a powerful and widely used software tool designed for the visualization and analysis of protein-ligand interactions in molecular structures. Developed to aid researchers in the field of structural biology and drug discovery, LigPlot+ provides a user-friendly interface to generate detailed and insightful visual representations of the interactions between proteins and ligands [36].

Key Features of LigPlot+:

I. Intermolecular Interaction Visualization: LigPlot+ excels in visualizing the intricate network of interactions between proteins and ligands. It generates 2D schematic diagrams that

illustrate various types of interactions, including hydrogen bonds, hydrophobic contacts, and water bridges.

II. Interactivity: The tool often includes interactive features that enable users to explore the LigPlot diagrams in a dynamic and user-friendly manner. This interactivity facilitates a more in-depth analysis of the interactions and their significance in the context of molecular recognition.

III. Compatibility with Structural Files: LigPlot+ is designed to work with various structural file formats commonly used in structural biology, including Protein Data Bank (PDB) files. This compatibility ensures that researchers can easily input their structural data into LigPlot+ for analysis.

2.4 Data Collection, Preprocessing, and Visualisation

2.4.1(a) Literature mining

- After an extensive review of the literature in NCBI [37], I focused on exploring the differences between Gram-positive and Gram-negative bacteria, which include A. baumannii, E. coli, P. aeruginosa, and K. pneumonia (Gram-negative), along with S. aureus, S. pneumoniae, E. faecium, and E. faecalis (Gram-positive). Subsequently, my research delved deeper into Gram-negative strains, particularly those exhibiting high levels of multiple drug resistance (MDR). Following an exhaustive survey of various Gram-negative bacteria, I narrowed down my investigation to *Pseudomonas aeruginosa* [38]. A comprehensive review of research papers pertaining to *Pseudomonas aeruginosa* led me to identify four distinct pathways. These pathways were analyzed in detail to determine their potential as receptors for inhibiting bacterial growth and disrupting virulence and population expansion. The pathways identified were the LAS system, RHL system, PQS system, and IQS system, each comprising sub-divisions that were subsequently Receptorsed for further study. In the pursuit of inhibiting *Pseudomonas aeruginosa*'s growth, I meticulously studied these pathways, seeking potential points of intervention. The LAS system, RHL system, PQS system, and IQS system emerged as major pathways with significant implications for bacterial virulence and population dynamics. To advance my research, I systematically examined each pathway's sub-divisions, aiming to pinpoint specific components that could be potentially inhibited. This strategic approach is crucial in developing Receptorsed interventions that can halt *Pseudomonas aeruginosa*'s growth and mitigate its virulence. In conclusion, my study has identified the LAS system, RHL system, PQS system, and IQS system as key pathways in *Pseudomonas aeruginosa*. By focusing on specific components within these pathways, there is potential for the development of novel

interventions to inhibit bacterial growth and mitigate the associated virulence and population expansion. This research contributes to our understanding of bacterial pathogenicity and opens avenues for the development of Receptorised therapies against *Pseudomonas aeruginosa* [39].

2.4.1(b) Structural Profiling of Key Receptors Across Four Major Pathways of *Pseudomonas aeruginosa*

After an extensive literature mining endeavor, I identified four major pathways in *Pseudomonas aeruginosa*, namely LAS, RHL, PQS, and IQS. Delving further into the subdivisions of these pathways, I commenced the search for potential receptors and subsequently identified a spectrum of promising Receptors. Within the LAS system, LASI and LASR were Receptorsed, while RHLR represented the key receptor in the RHL system. The PQS system presented a multifaceted set of potential Receptors, including PQSE, PQSD, PQSA, PQSR (MVFR), and PQSH. Additionally, in the IQS system, AMBE, AMBB, and the LuxR-type transcription factor QscR were identified. To elucidate the three-dimensional structures of these potential Receptors, I consulted the Protein Data Bank (PDB) at the RCSB (Research Collaboratory for Structural Bioinformatics). Remarkably, 10 out of the 11 receptors had available structures on the PDB, facilitating a comprehensive understanding of their molecular architectures. The lone exception was the PQSH receptor from the PQS system. To bridge this gap, the Swiss Model server was employed to generate the three-dimensional structure of PQSH. This step ensured a complete dataset for all selected Receptors, laying a solid foundation for the subsequent phases of my investigation. Armed with the structural information of these Receptors, each identified as potential Receptors, I now possess the tools to explore inhibition strategies. This insight holds significant promise for impeding *Pseudomonas aeruginosa*'s growth, virulence factors, and population dynamics. The culmination of this research contributes to the arsenal of knowledge essential for developing Receptorsed interventions against this opportunistic pathogen [40].

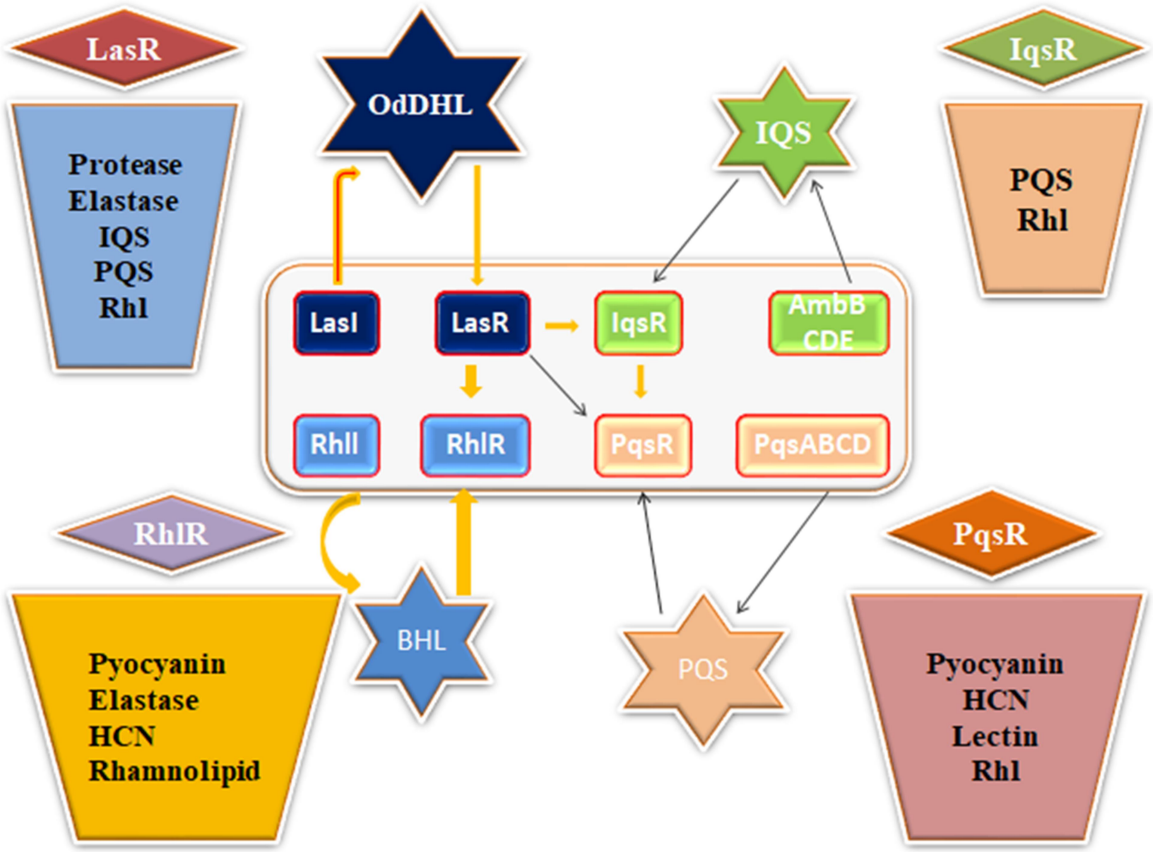

Fig.2.4.1 (b) Deciphering Pseudomonas aeruginosa's Virulent Symphony: Pathways, Protein Interactions, and Enzyme Release in Host Takeover.

S. No	Receptor Name	PDB & UniProt id's	Structure	Sequence Length	Missing Residues/Homology Modelling
1.	LASI	1RO5	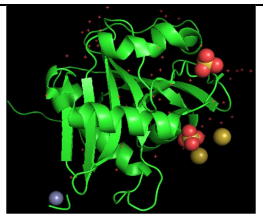	201	Yes/No
2.	PQSE	2Q0I	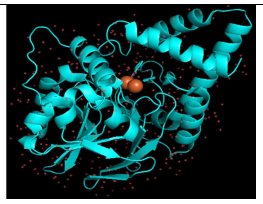	303	Yes/No

3.	PQSD	3H77	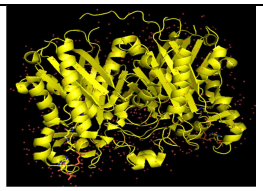	359	No/No
4.	LASR	4NG2	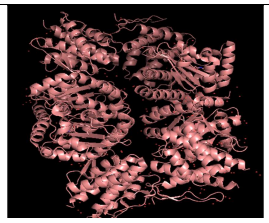	184	Yes/No
5.	PQSA	5OE3	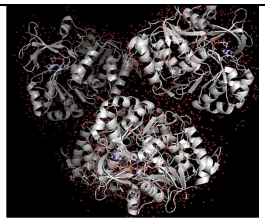	407	Yes/No
6.	QSCR	6CC0	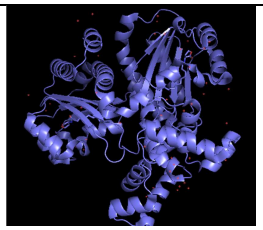	237	Yes/No
7.	MVFR	7QA0		332	Yes/Yes
8.	RHLR	7R3J	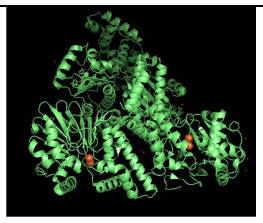	318	No/No
9.	AMBE	7R9X	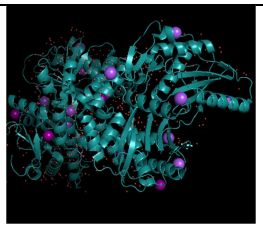	438	Yes/No

10.	AMBB	7X17	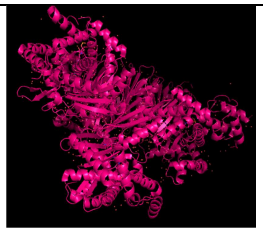	523	Yes/No
11.	PQSH	Q02N79 (UniProt Id)	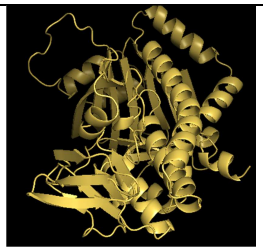	382	Homology Modelling using Swiss Model

Table 2.4.1.(b): Comprehensive Analysis of Virulence-Associated Receptors: PDB ID Exploration, Structural Characteristics, Sequence Length, Missing Residues, and Homology Modeling Insights

2.4.1 (c) Exploration of Compound Databases for Potential Inhibitors

In the pursuit of identifying potential inhibitors for the 11 key receptors across *Pseudomonas aeruginosa* quorum sensing pathways, I systematically explored several compound databases, including ZINC15[41], PubChem[42], ChEMBL[43], ChemSpider[44]. The initial analysis revealed a vast number of compounds within these databases. However, considering constraints such as time, cost, and resources, utilizing the entirety of these databases was not feasible. To optimize the search for potential inhibitors, I turned my attention to databases specifically focused on natural products. Through an exhaustive examination, databases such as IMPATT[45], DRUG BANK[46], NATURAL products atlas[47], and Super natural II [48] were considered. Following careful consideration, I narrowed down my focus to IMPATT due to their extensive coverage of natural compounds and Drug Bank for drug repurposing. This strategic decision was driven by the recognition of the rich repository of natural products within these databases. By leveraging the unique chemical diversity present in natural compounds, I aimed to identify molecules with the potential to act as inhibitors for the selected Receptors. This shift in approach aligns with the objective of harnessing nature's own chemical arsenal to develop Receptorsed interventions against *Pseudomonas aeruginosa*. The utilization of natural product databases offers a nuanced perspective in the quest for inhibitors, as these compounds often possess bioactive properties with potential therapeutic applications. This refined strategy enhances the efficiency of the inhibitor search, directing the research towards a promising avenue for developing novel strategies to impede the quorum sensing mechanisms of *Pseudomonas aeruginosa*.

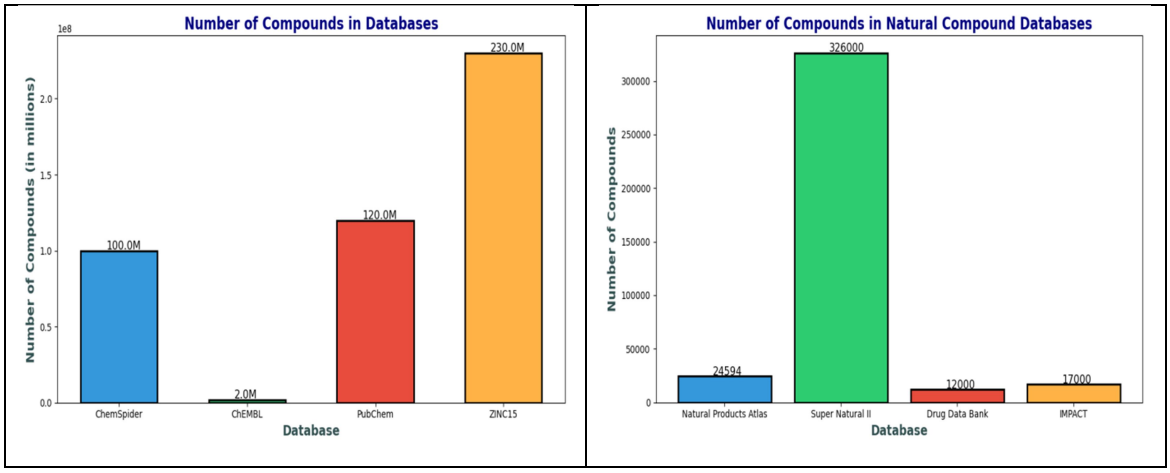

Fig.2.4.1(c): Comparative Analysis of Compound Counts in Various Databases (I) and Natural Compound Database (II)

2.4.2.(a) Preprocessing for Structural Profiling: Investigating Key Receptors Across Four Major Pathways of *Pseudomonas aeruginosa*

In the investigation of *Pseudomonas aeruginosa* quorum sensing pathways, four major systems were identified: LAS, RHL, PQS, and IQS. Within these systems, LASI and LASR were Receptorsed in the LAS system, RHLR represented the key receptor in the RHL system, and the PQS system included potential receptors such as PQSE, PQSD, PQSA, PQSR (MVFR), and PQSH. Additionally, the IQS system featured AMBE, AMBB, and the LuxR-type transcription factor QscR as identified components. Subsequently, the 3D structures of the receptors were obtained from the Protein Data Bank (PDB) using the following PDB IDs: 1RO5, 2Q0I, 3H77, 4NG2, 5OE3, 6CC0, 7QA0, 7R3J, 7R9X, and 7X17. However, the structure of PQSH was unavailable in the PDB, leading to its modeling through the SWISS-MODEL server using the Pseudomonas genome sequence from UNIPROT. After obtaining the structures, visualization and examination of the receptors were performed using PYMOL. Active site information was crucial, and while 8 receptors had available active site data, 3 receptors (1RO5, 7R9X, and Q02N79.PQSH) required further investigation. The CASTP server was utilized to determine the active site information for these Receptors. Following the identification of missing residues in 7 Receptors, the SWISS-MODEL server was employed once again to fill these gaps. Subsequently, the receptors were pre-processed, and molecules bound to the active sites were removed to ensure a clean and accurate dataset. The resulting 11 receptor structures, free from missing residues and non-essential bound molecules, were then saved as separate PDB files for subsequent utilization in chapters 3, 4, and 5 of the study, particularly for docking analyses. This meticulous process ensures the integrity and accuracy of the receptor structures, providing a

solid foundation for further chapters in the study, contributing to the understanding of potential inhibitory interactions for *Pseudomonas aeruginosa* [49].

2.4.2.(b) Unveiling Potential Inhibitors: Preprocessing Natural Compound Databases for Structural Profiling Across Multiple Biological Pathways

Having successfully prepared the receptor structures, the next phase involved obtaining compounds from the IMPATT and DRUG BANK databases. To streamline this process, I developed a Python script and executed it on a Linux server to download compounds from both databases. The downloaded compounds were available in different formats on each database, and for uniformity, I opted to download them in Structure Data File (SDF) format. The IMPATT database yielded a total of 17,976 compounds, while the DRUG BANK database provided approximately 12,000 compounds. Subsequently, I applied the Open Babel tool to convert the downloaded SDF files into PDBQT format, ensuring compatibility with the AutoDock suite for docking studies. To achieve this, I implemented a concise script, which was executed on the Linux server. This conversion process enabled a standardized format for both receptor and compound files. Upon completion, the compounds were now ready in PDBQT format, aligning seamlessly with the receptor structures. The integration of the receptor structures and compounds marked a crucial milestone in preparing the dataset for subsequent phases of the research. This meticulous approach ensures consistency and compatibility within the dataset, setting the stage for comprehensive docking studies and analyses. The use of standard file formats facilitates seamless integration with molecular docking tools, enhancing the accuracy and reliability of the subsequent computational experiments in the research study [50].

2.4.3.(a) Comprehensive Visualization and Validation of 3D Receptor Structures

This research meticulously presents the visualization and validation of 11 *Pseudomonas aeruginosa* quorum sensing Receptors, encompassing LASI, LASR, RHLR, PQSE, PQSD, PQSA, PQSR (MVFR), PQSH, AMBE, AMBB, and QscR. Leveraging PYMOL, a thorough analysis of the 3D structures was conducted to identify potential missing residues and evaluate the presence of bound molecules post a comprehensive cleaning process. The visualization aimed at ensuring the structural integrity of the Receptors, establishing a reliable foundation for subsequent molecular docking studies. This intricate examination significantly augments the accuracy of the dataset, fostering a more profound comprehension of potential inhibitory interactions against *Pseudomonas aeruginosa*. The study particularly emphasizes the unveiling of missing residues and cleaned ligand-binding sites

as pivotal contributors to an enhanced understanding, setting the stage for advanced molecular docking investigations [51].

2.4.3 (b) Unveiling Structural Transformations: Visualization of IMPATT and DRUG BANK Compounds in PDBQT Format via Open Babel Conversion

This study intricately examines the transformation of compounds sourced from the IMPATT and DRUG BANK databases, initially presented in Structure Data File (SDF) format, into the PDBQT format. Utilizing the Open Babel tool, the conversion process undergoes meticulous scrutiny to ensure the precise and consistent preparation of compounds, optimizing them for subsequent molecular docking studies. Through this detailed visualization, the study provides valuable insights into the successful harmonization of diverse compound structures into a standardized PDBQT format, laying the groundwork for advanced computational analyses. The methodology presented herein contributes significantly to the reliability and reproducibility of results, thereby advancing the exploration of potential inhibitors against *Pseudomonas aeruginosa* quorum sensing Receptors. This standardized approach enhances the robustness of computational experiments, offering a reliable platform for the investigation of inhibitory interactions in the context of *Pseudomonas aeruginosa* quorum sensing pathways [52].

Chapter 3

In Chapter 2, we successfully generated the PDB files for 11 *Pseudomonas aeruginosa* quorum sensing Receptors, comprising LASI, LASR, RHLR, PQSE, PQSD, PQSA, PQSR (MVFR), PQSH, AMBE, AMBB, and QscR, alongside potential inhibitors sourced from the IMPPAT and DRUG BANK databases. Now, the next step involves preparing the PDB files of these 11 receptors in PDBQT format for docking studies. To accomplish this, we utilized the MGL (Molecular Graphics Laboratory) tool to generate the necessary grid and configuration files essential for conducting docking experiments. For each of the 11 Receptors, a grid box size of 40x40x40 was selected. Leveraging the functionalities offered by the MGL tool, the conversion of all receptor PDB files to PDBQT format was completed. These files are pivotal for setting up the docking simulations, facilitating the investigation of potential interactions between the receptors and the identified inhibitors. This step marks a critical advancement in our research, enabling us to proceed with docking studies aimed at elucidating the binding affinities and interactions between the receptors and the candidate inhibitors. The uniformity in file formats ensures consistency and accuracy in subsequent computational analyses, contributing significantly to the reliability of our findings in exploring potential inhibitory mechanisms against *Pseudomonas aeruginosa* quorum sensing Receptors. Following the completion of the docking simulations, the focus shifted to extracting meaningful insights from the results. Initially, the top molecules exhibiting the most negative binding energies for each of the 11 receptors were visualized using the LigPlot+ tool. The corresponding ligand interactions were analyzed and are presented in the table below. Subsequently, an in-depth analysis was conducted for all docked molecules from the IMPATT database. Density plots and box plots were generated to visualize the distribution of binding energies, providing a comprehensive overview of the binding affinities of the molecules. Further refinement involved a detailed examination of the top 40 molecules for each receptor, as depicted in the table below. Heatmap and frequency distribution graphs were employed to visually represent the binding affinities of these molecules across the Receptors. To discern commonality and assess consistency, a comparative analysis of the top 40 molecules was conducted for each receptor. The results highlighted molecules that exhibited inhibitory effects across multiple Receptors, underscoring their potential as broad-spectrum inhibitors. Finally, a comprehensive examination of the majority consensus was performed. A Receptor was compiled, identifying molecules that demonstrated inhibitory effects across a significant proportion of the Receptors. This analysis serves as a valuable guidepost in prioritizing molecules for further investigation and potential therapeutic development. These systematic analyses contribute to a nuanced understanding of the interactions between receptors and inhibitors, providing

insights that are pivotal for the development of Receptorsed strategies against *Pseudomonas aeruginosa* quorum sensing pathways. The presented results lay the groundwork for subsequent experimental validations and hold promise for the advancement of anti-pathogenic interventions [53].

Results:

S. No	Receptors& Ligand	Receptors Ligand Interaction (Ligplot+)	Binding Energy(Kcal/mol)
1.	1RO5 & IMPHY013460	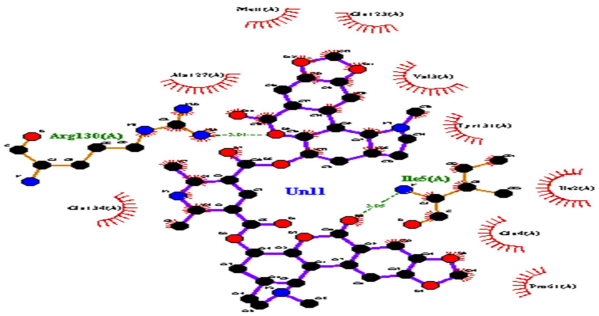	-10.384 (Kcal/mol)
2.	2Q0I & IMPHY000624	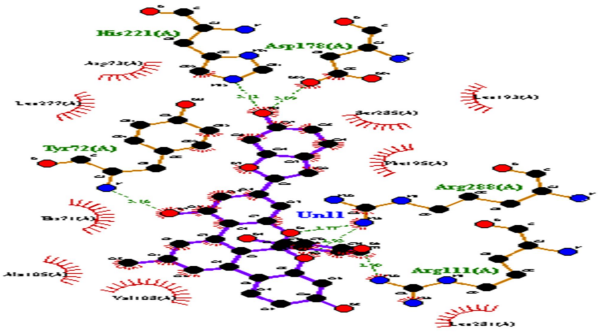	-11.724 (Kcal/mol)
3.	3H77 & IMPHY009207	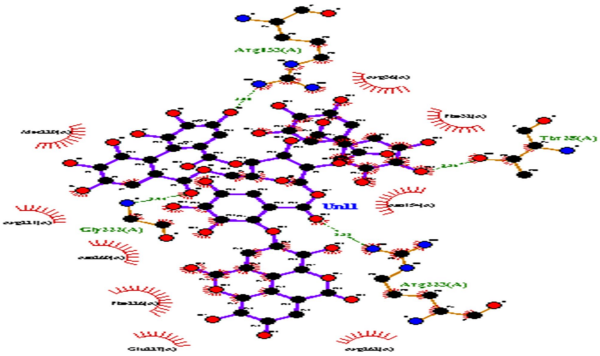	-11.855 (Kcal/mol)

4.	4ng2 & IMPHY006927	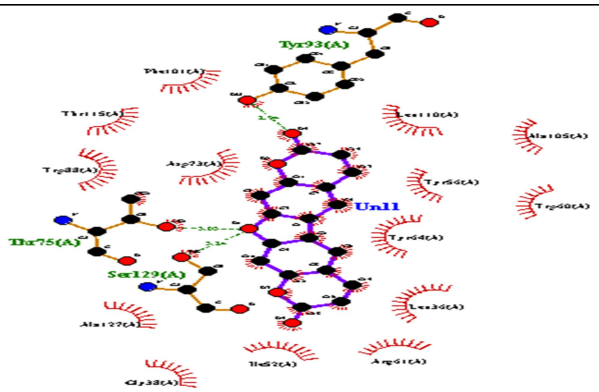	-13.131 (Kcal/mol)
5.	5OE3 & IMPHY008591	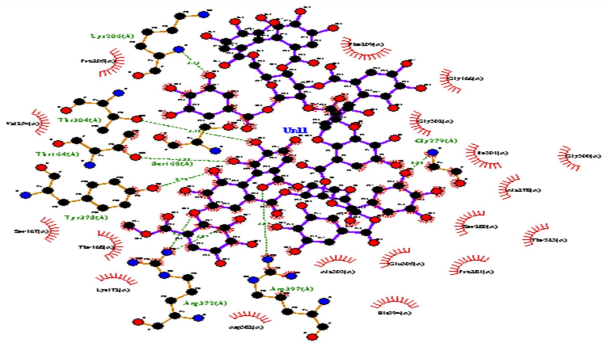	-14.541 (Kcal/mol)
6.	6CC0 & IMPHY000296	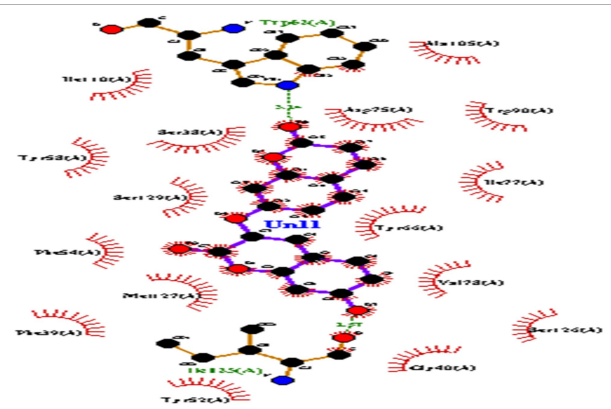	-11.247 (Kcal/mol)
7.	7QA0 & IMPHY002351	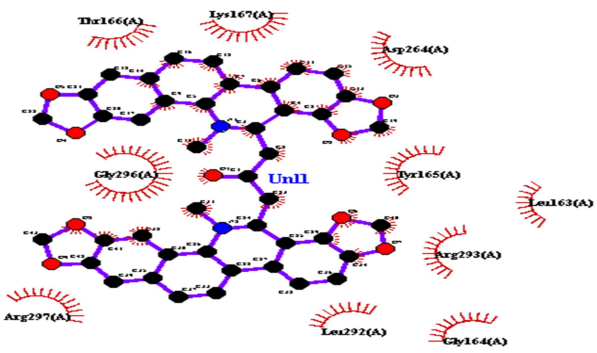	-12.646 (Kcal/mol)

8.	7r3j & IMPHY008591	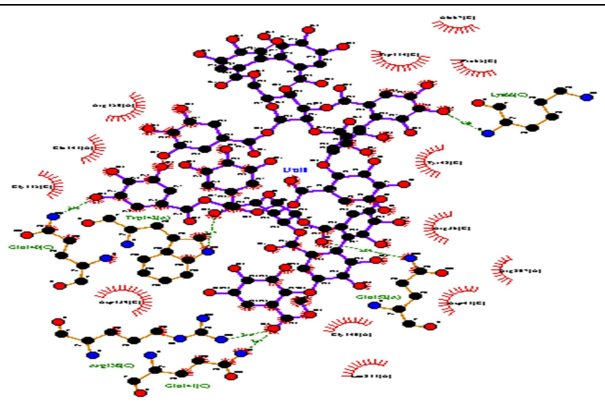	-11.804 (Kcal/mol)
9.	7R9X & IMPHY002351	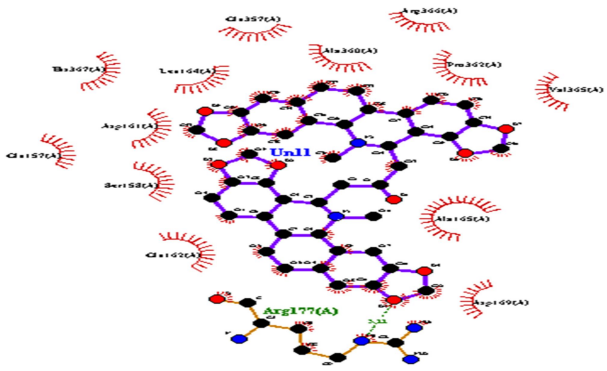	-11.632 (Kcal/mol)
10.	7x17 & IMPHY013460	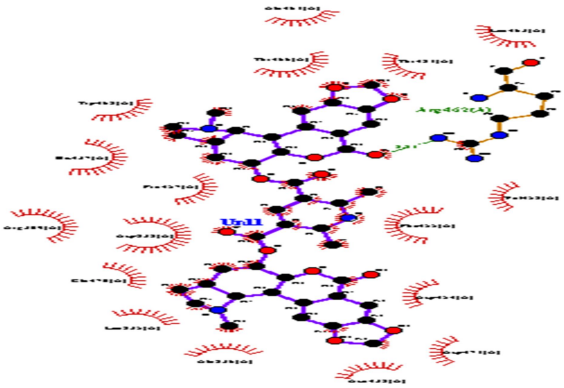	-14.42 (Kcal/mol)
11.	Q02N79 & IMPHY009207	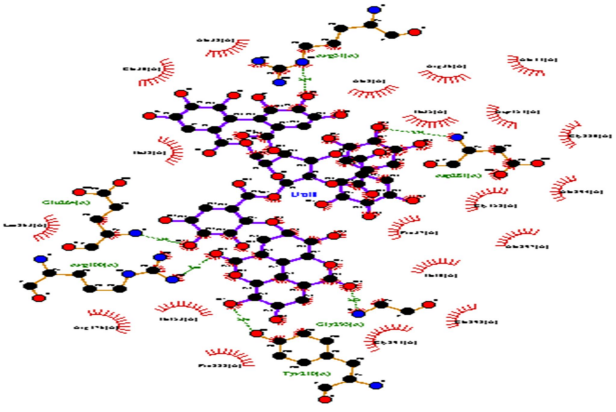	-13.368 (Kcal/mol)

Table.3.(A): Quantifying Inhibitory Potency: Top Molecules with Peak Binding Energy and Detailed Receptor-Ligand Interactions Across All 11 Receptors, Visualized Using LigPlot.

1. 1RO5

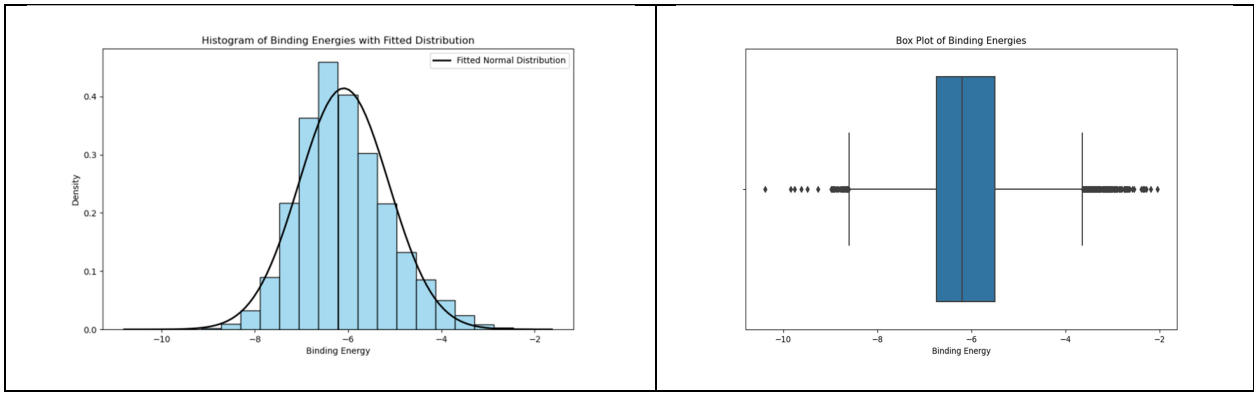

Figure.3.1.1: Statistical Insights into Novel Quorum Sensing Inhibitors — (a) Histogram with Fitted Normal Distribution Density Plot and (b) Box Plot of Binding Energies for all molecules of IMPPAT Database.

Ligand Name	Binding Energy (Kcal/mol)
IMPHY013460	-10.384
IMPHY008591	-9.847
IMPHY014498	-9.761
IMPHY014605	-9.612
IMPHY014959	-9.487
IMPHY012392	-9.268
IMPHY007982	-8.98
IMPHY007725	-8.974
IMPHY006572	-8.955
IMPHY001398	-8.948
IMPHY005216	-8.933
IMPHY009357	-8.922
IMPHY000270	-8.913
IMPHY001778	-8.877
IMPHY010857	-8.858
IMPHY008804	-8.855
IMPHY008302	-8.829
IMPHY002478	-8.793

IMPHY011118	-8.766
IMPHY009721	-8.743
IMPHY010783	-8.74
IMPHY013237	-8.727
IMPHY003674	-8.721
IMPHY010697	-8.72
IMPHY013247	-8.718
IMPHY011404	-8.714
IMPHY002714	-8.686
IMPHY007776	-8.684
IMPHY012222	-8.666
IMPHY008170	-8.665
IMPHY008712	-8.663
IMPHY015101	-8.66
IMPHY008124	-8.634
IMPHY013458	-8.633
IMPHY003226	-8.631
IMPHY014362	-8.626
IMPHY006183	-8.626
IMPHY004411	-8.613
IMPHY013531	-8.61
IMPHY014103	-8.603

Table.3.1.1: Pinnacle of Potency — Top 40 Molecules Showcasing Highest Binding Energies among all molecules of IMPPAT database.

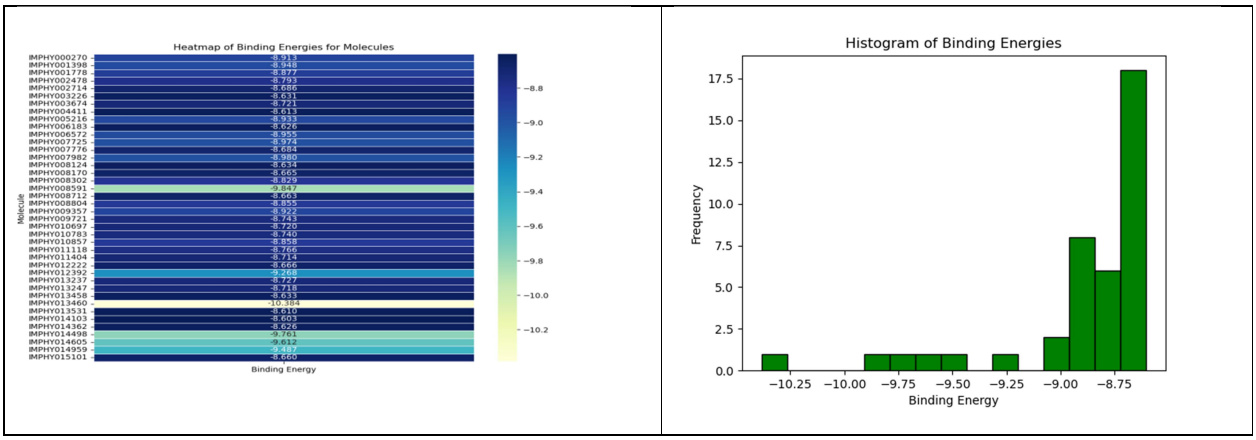

Figure.3.1.2: Insightful Visualization — (a) Heatmap and (b) Frequency distribution Illustrating the Binding Energies of the Top 40 Molecules among a Set of all molecules of IMPPAT Database.

2. 2Q0I

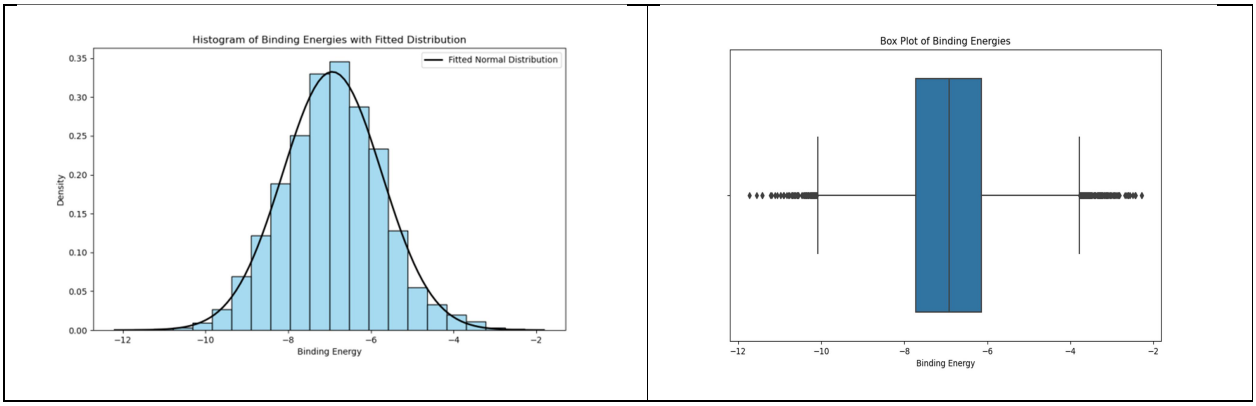

Figure.3.2.1: Statistical Insights into Novel Quorum Sensing Inhibitors — (a) Histogram with Fitted Normal Distribution Density Plot and (b) Box Plot of Binding Energies for all molecules of IMPPAT Database.

Ligand Name	Binding Energies (Kcal/mol)
IMPHY007887	-11.416
IMPHY013701	-11.421
IMPHY004355	-11.55
IMPHY000624	-11.724
IMPHY007725	-11.187
IMPHY014191	-11.218
IMPHY003932	-11.106
IMPHY006158	-11.061
IMPHY008403	-10.98

IMPHY005216	-10.978
IMPHY009207	-10.908
IMPHY005887	-10.892
IMPHY007791	-10.832
IMPHY006927	-10.793
IMPHY006882	-10.765
IMPHY009488	-10.71
IMPHY015394	-10.704
IMPHY007991	-10.694
IMPHY000358	-10.68
IMPHY013529	-10.65
IMPHY011108	-10.631
IMPHY009234	-10.628
IMPHY008591	-10.624
IMPHY004849	-10.582
IMPHY008512	-10.57
IMPHY005634	-10.564
IMPHY008234	-10.553
IMPHY010362	-10.55
IMPHY014362	-10.465
IMPHY013460	-10.445
IMPHY011378	-10.418
IMPHY012772	-10.399
IMPHY012536	-10.379
IMPHY004899	-10.375
IMPHY008618	-10.372
IMPHY000296	-10.371
IMPHY006572	-10.358
IMPHY015035	-10.341
IMPHY002246	-10.324
IMPHY013247	-10.319

Table.3.2.1: Pinnacle of Potency — Top 40 Molecules Showcasing Highest Binding Energies among all molecules of IMPPAT database.

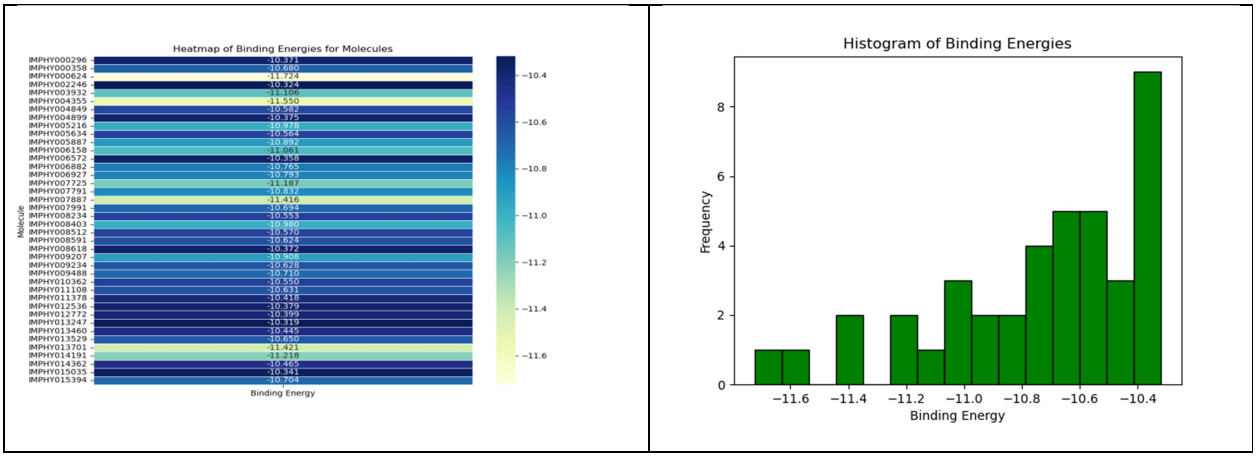

Figure.3.2.2: Insightful Visualization — (a) Heatmap and (b) Frequency distribution Illustrating the Binding Energies of the Top 40 Molecules among a Set of all molecules of IMPPAT Database.

3. 3H77

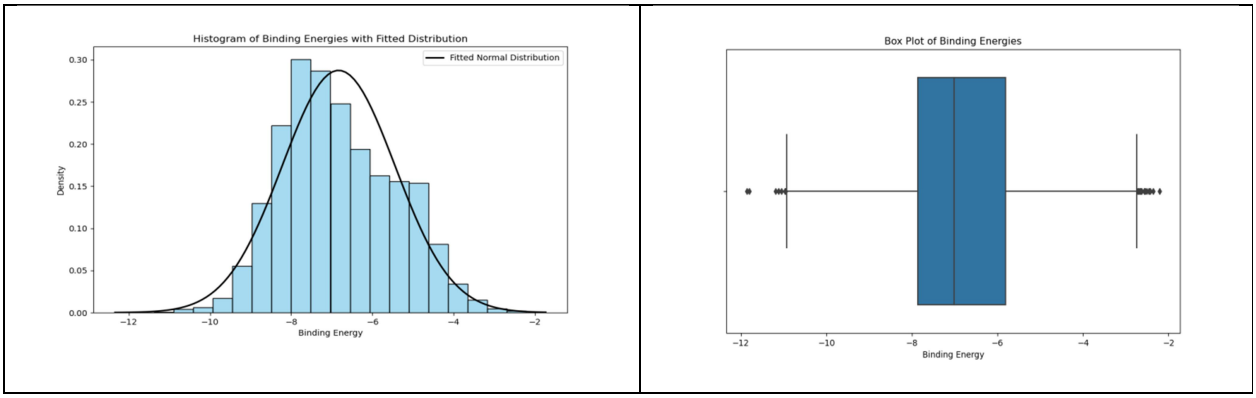

Figure.3.3.1: Statistical Insights into Novel Quorum Sensing Inhibitors — (a) Histogram with Fitted Normal Distribution Density Plot and (b) Box Plot of Binding Energies for all molecules of IMPPAT Database.

Ligands Name	Binding Energies (Kcal/mol)
IMPHY009207	-11.855
IMPHY010480	-11.806
IMPHY005887	-11.194
IMPHY008329	-11.119
IMPHY004849	-11.056
IMPHY014186	-10.967

IMPHY007725	-10.954
IMPHY015060	-10.949
IMPHY014191	-10.932
IMPHY010661	-10.89
IMPHY009004	-10.836
IMPHY010832	-10.824
IMPHY010511	-10.817
IMPHY006882	-10.817
IMPHY005599	-10.805
IMPHY003938	-10.787
IMPHY003592	-10.774
IMPHY002709	-10.767
IMPHY014362	-10.744
IMPHY014103	-10.69
IMPHY005533	-10.67
IMPHY011807	-10.642
IMPHY005595	-10.628
IMPHY003272	-10.623
IMPHY006688	-10.62
IMPHY002714	-10.612
IMPHY012331	-10.597
IMPHY010362	-10.575
IMPHY004103	-10.564
IMPHY004969	-10.56
IMPHY012556	-10.538
IMPHY007718	-10.527
IMPHY002354	-10.508
IMPHY013314	-10.501
IMPHY012887	-10.488
IMPHY015394	-10.483
IMPHY000715	-10.463
IMPHY009690	-10.461

IMPHY008366	-10.457

Table.3.3.1: Pinnacle of Potency — Top 40 Molecules Showcasing Highest Binding Energies among all molecules of IMPPAT database:

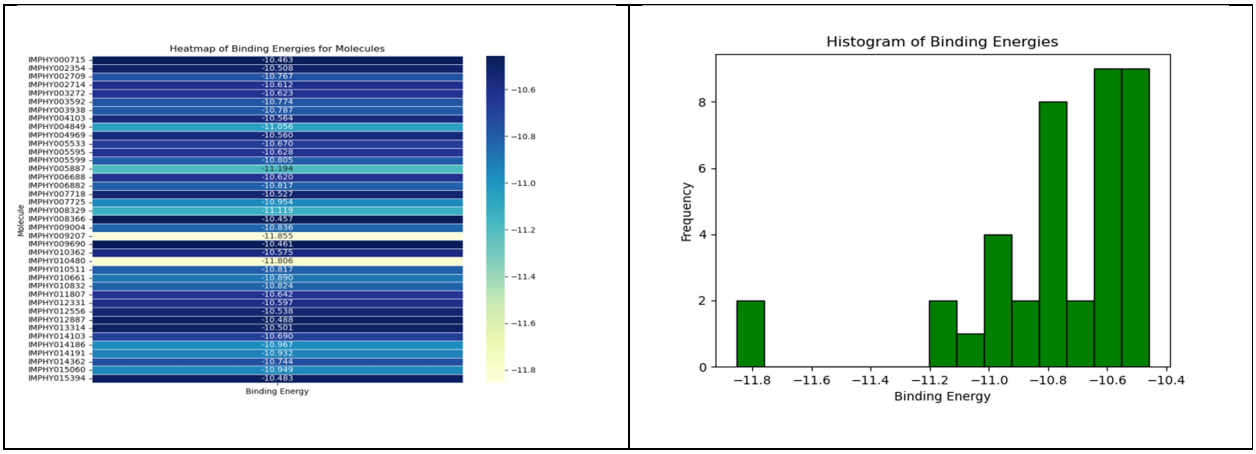

Figure.3.3.2: Insightful Visualization — (a) Heatmap and (b) Frequency distribution Illustrating the Binding Energies of the Top 40 Molecules among a Set of all molecules of IMPPAT Database.

4. 4ng2

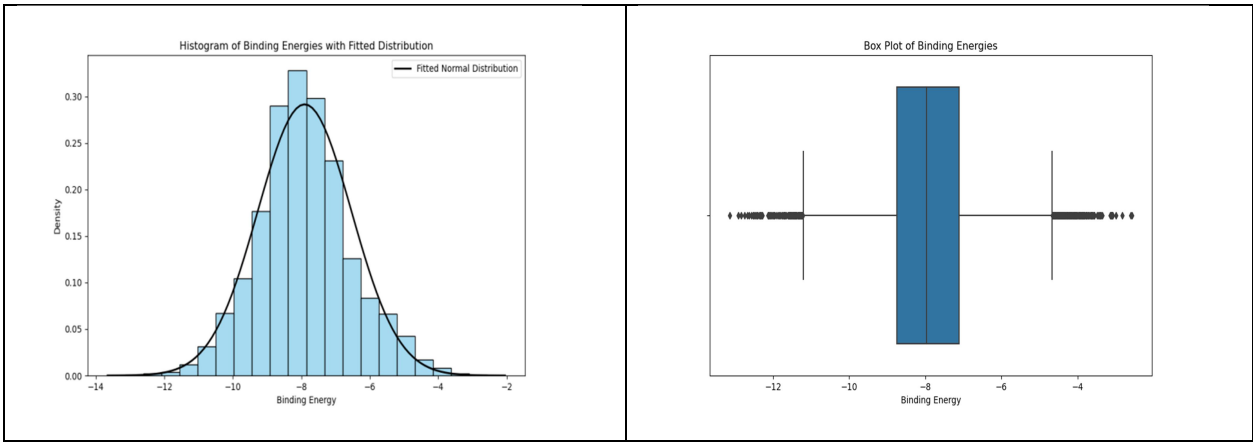

Figure.3.4.1: Statistical Insights into Novel Quorum Sensing Inhibitors — (a) Histogram with Fitted Normal Distribution Density Plot and (b) Box Plot of Binding Energies for all molecules of IMPPAT Database.

Ligands Name	Binding Energies (Kcal/mol)
IMPHY006927	-13.131
IMPHY004849	-12.911
IMPHY004491	-12.842

IMPHY007736	-12.748
IMPHY007501	-12.669
IMPHY004128	-12.621
IMPHY008771	-12.565
IMPHY004193	-12.516
IMPHY002805	-12.504
IMPHY011665	-12.481
IMPHY000159	-12.441
IMPHY002068	-12.409
IMPHY007725	-12.404
IMPHY014498	-12.354
IMPHY005061	-12.333
IMPHY014011	-12.321
IMPHY000086	-12.31
IMPHY007463	-12.277
IMPHY007663	-12.276
IMPHY006882	-12.13
IMPHY000151	-12.108
IMPHY000296	-12.099
IMPHY008324	-12.074
IMPHY010828	-12.067
IMPHY007459	-12.038
IMPHY007798	-12.015
IMPHY004731	-11.98
IMPHY014442	-11.976
IMPHY013015	-11.967
IMPHY007888	-11.96
IMPHY010048	-11.925
IMPHY005264	-11.872
IMPHY011550	-11.847
IMPHY005064	-11.822
IMPHY004103	-11.81

IMPHY004397	-11.77
IMPHY004395	-11.752
IMPHY014101	-11.725
IMPHY002638	-11.718
IMPHY012046	-11.703

Table.3.4.1: Pinnacle of Potency — Top 40 Molecules Showcasing Highest Binding Energies among all molecules of IMPPAT database:

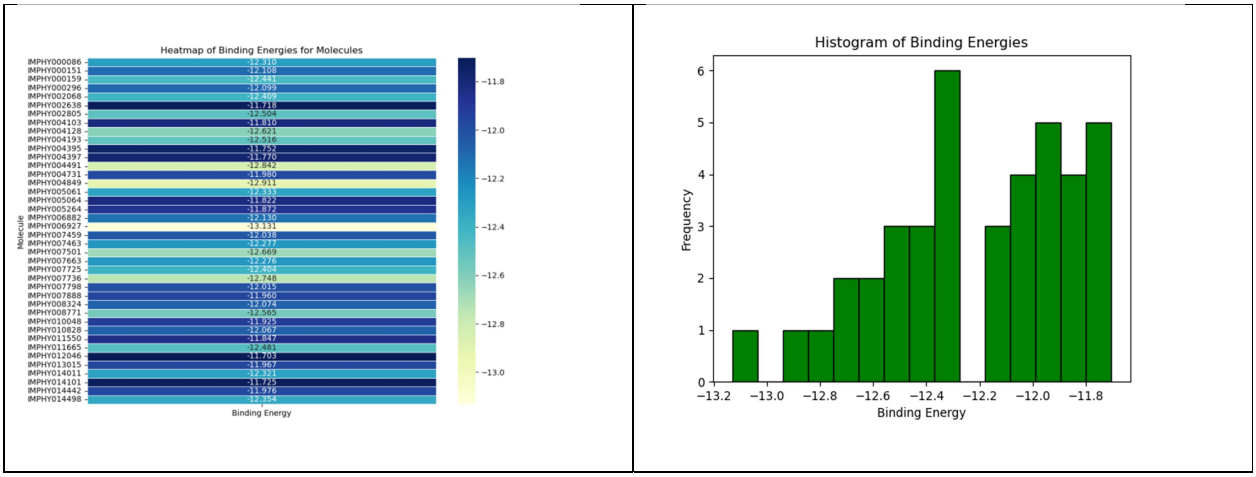

Figure.3.4.2: Insightful Visualization — (a) Heatmap and (b) Frequency distribution Illustrating the Binding Energies of the Top 40 Molecules among a Set of all molecules of IMPPAT Database.

5. 5OE3

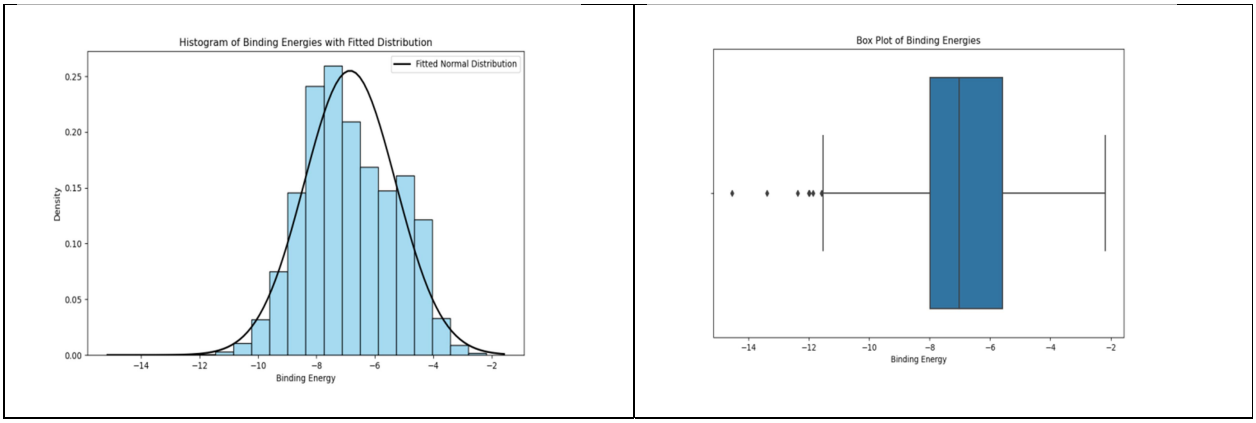

Figure.3.5.1: Statistical Insights into Novel Quorum Sensing Inhibitors — (a) Histogram with Fitted Normal Distribution Density Plot and (b) Box Plot of Binding Energies for all molecules of IMPPAT Database.

Ligands Name	Binding Energies (Kcal/mol)
IMPHY013480	-13.387
IMPHY008591	-14.541
IMPHY007725	-12.364
IMPHY009207	-12.007
IMPHY007991	-11.981
IMPHY010353	-11.869
IMPHY007982	-11.584
IMPHY006658	-11.535
IMPHY011092	-11.499
IMPHY000624	-11.475
IMPHY008628	-11.439
IMPHY000426	-11.38
IMPHY013460	-11.379
IMPHY008302	-11.369
IMPHY005795	-11.346
IMPHY014498	-11.282
IMPHY013479	-11.261
IMPHY005180	-11.26
IMPHY001698	-11.253
IMPHY014959	-11.243
IMPHY013928	-11.219
IMPHY000697	-11.212
IMPHY004411	-11.154
IMPHY000783	-11.148
IMPHY010360	-11.052
IMPHY013622	-11.028
IMPHY000715	-11.011
IMPHY005824	-11.008
IMPHY001646	-11
IMPHY013237	-10.999
IMPHY004011	-10.978

IMPHY002430	-10.978
IMPHY010219	-10.96
IMPHY014129	-10.954
IMPHY001398	-10.942
IMPHY004179	-10.939
IMPHY004177	-10.903
IMPHY013287	-10.887
IMPHY010113	-10.884
IMPHY002832	-10.879

Table.3.5.1: Pinnacle of Potency — Top 40 Molecules Showcasing Highest Binding Energies among all molecules of IMPPAT database.

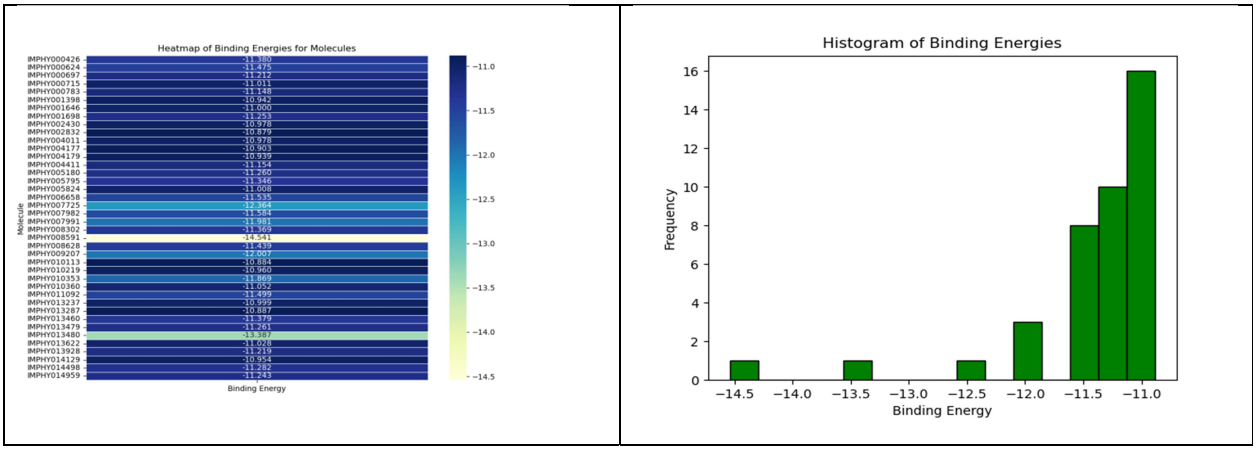

Figure.3.5.2: Insightful Visualization — (a) Heatmap and (b) Frequency distribution Illustrating the Binding Energies of the Top 40 Molecules among a Set of all molecules of IMPPAT Database.

6. 6CC0

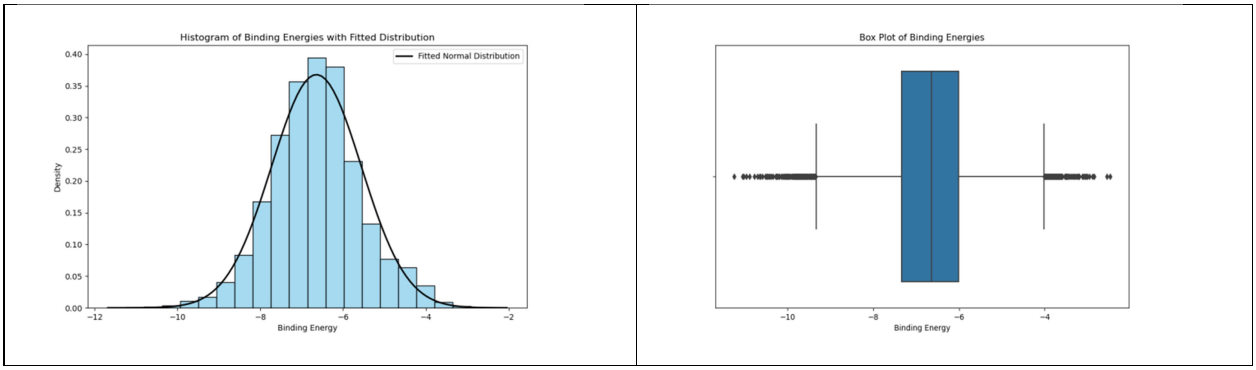

Figure.3.6.1: Statistical Insights into Novel Quorum Sensing Inhibitors — (a) Histogram with Fitted Normal Distribution Density Plot and (b) Box Plot of Binding Energies for all molecules of IMPPAT Database.

Ligands Name	Binding Energies (Kcal/mol)
IMPHY000296	-11.247
IMPHY002348	-11.055
IMPHY008542	-11.028
IMPHY012102	-10.962
IMPHY009808	-10.886
IMPHY013996	-10.773
IMPHY000991	-10.699
IMPHY011147	-10.654
IMPHY005061	-10.639
IMPHY000782	-10.596
IMPHY014032	-10.521
IMPHY013176	-10.515
IMPHY006505	-10.51
IMPHY014605	-10.481
IMPHY002836	-10.469
IMPHY010647	-10.434
IMPHY005850	-10.419
IMPHY009207	-10.374
IMPHY010878	-10.345
IMPHY006967	-10.274
IMPHY004943	-10.266
IMPHY001994	-10.254
IMPHY002993	-10.247
IMPHY000643	-10.236
IMPHY008591	-10.201
IMPHY014373	-10.196
IMPHY003379	-10.19
IMPHY002205	-10.141
IMPHY012106	-10.115

IMPHY000984	-10.114
IMPHY006258	-10.076
IMPHY013049	-10.066
IMPHY006066	-10.025
IMPHY004614	-10.04
IMPHY006092	-10.025
IMPHY007982	-10.023
IMPHY000837	-10.01
IMPHY000578	-9.985
IMPHY013402	-9.966
IMPHY008563	-9.965

Table.3.6.1: Pinnacle of Potency — Top 40 Molecules Showcasing Highest Binding Energies among all molecules of IMPPAT database.

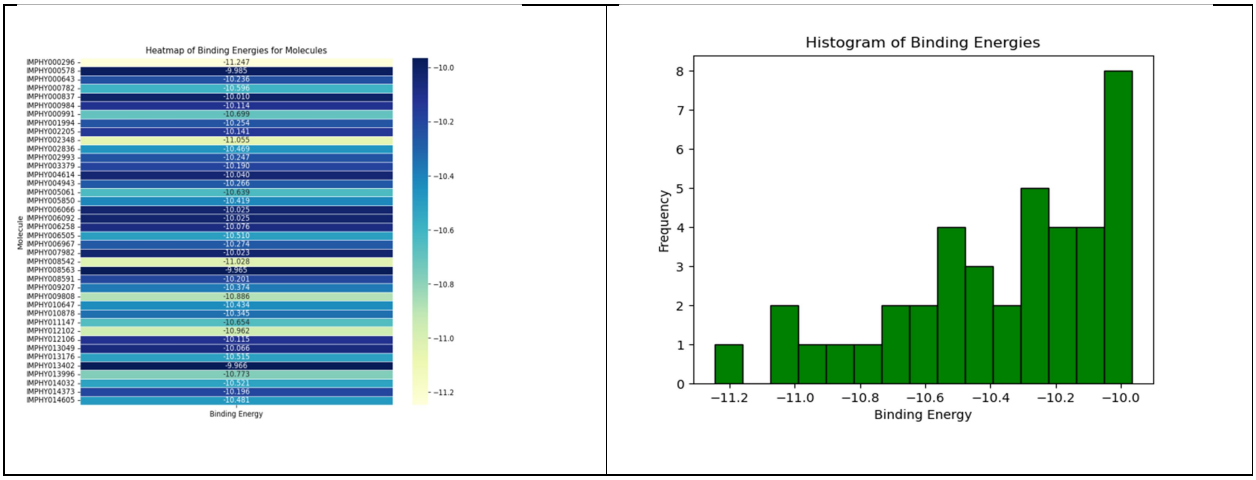

Figure.3.6.2: Insightful Visualization — (a) Heatmap and (b) Frequency distribution Illustrating the Binding Energies of the Top 40 Molecules among a Set of all molecules of IMPPAT Database.

7. 7QA0

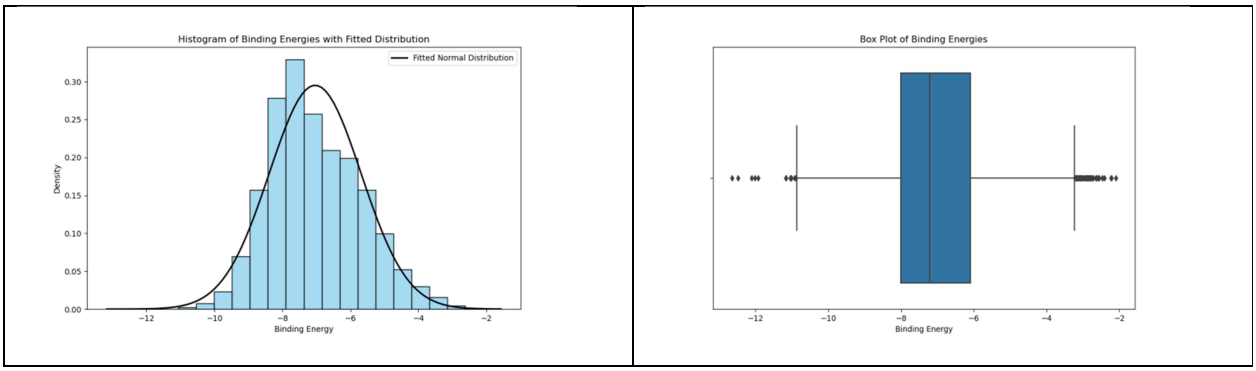

Figure.3.7.1: Statistical Insights into Novel Quorum Sensing Inhibitors — (a) Histogram with Fitted Normal Distribution Density Plot and (b) Box Plot of Binding Energies for all molecules of IMPPAT Database.

Ligands Name	Binding Energies (Kcal/mol)
IMPHY002351	-12.646
IMPHY014498	-12.483
IMPHY009721	-12.11
IMPHY003226	-12.025
IMPHY014605	-11.93
IMPHY010617	-11.174
IMPHY011528	-11.164
IMPHY006129	-11.163
IMPHY002830	-11.046
IMPHY005319	-11.04
IMPHY009207	-11.021
IMPHY012856	-10.922
IMPHY006882	-10.905
IMPHY009247	-10.895
IMPHY003932	-10.862
IMPHY010846	-10.835
IMPHY000715	-10.822
IMPHY005718	-10.779
IMPHY013368	-10.767
IMPHY008329	-10.739

IMPHY003388	-10.738
IMPHY014146	-10.704
IMPHY011622	-10.696
IMPHY013554	-10.669
IMPHY001365	-10.617
IMPHY013479	-10.602
IMPHY009888	-10.585
IMPHY000062	-10.578
IMPHY006788	-10.576
IMPHY013306	-10.573
IMPHY004623	-10.557
IMPHY012536	-10.549
IMPHY004962	-10.529
IMPHY008124	-10.522
IMPHY002828	-10.522
IMPHY007665	-10.505
IMPHY005086	-10.487
IMPHY004920	-10.478
IMPHY015117	-10.462
IMPHY007679	-10.453

Table.3.7.1: Pinnacle of Potency — Top 40 Molecules Showcasing Highest Binding Energies among all molecules of IMPPAT database.

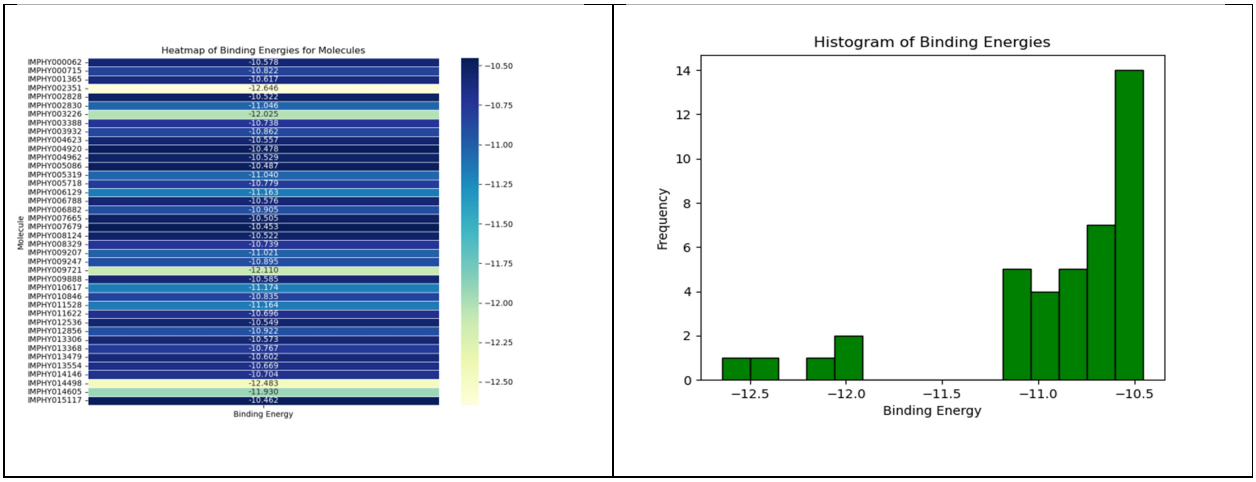

Figure.3.7.2: Insightful Visualization — (a) Heatmap and (b) Frequency distribution Illustrating the Binding Energies of the Top 40 Molecules among a Set of all molecules of IMPPAT Database.

8. 7r3j

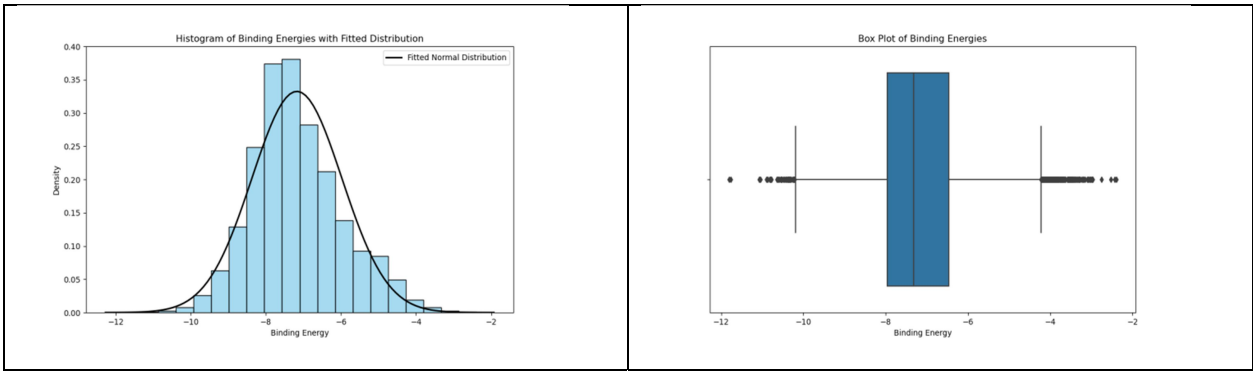

Figure.3.8.1: Statistical Insights into Novel Quorum Sensing Inhibitors — (a) Histogram with Fitted Normal Distribution Density Plot and (b) Box Plot of Binding Energies for all molecules of IMPPAT Database.

Ligands Name	Binding Energies (Kcal/mol)
IMPHY008591	-11.804
IMPHY012522	-11.764
IMPHY012391	-11.071
IMPHY009015	-11.066
IMPHY013479	-11.044
IMPHY009795	-10.901
IMPHY010488	-10.873
IMPHY009207	-10.868
IMPHY013287	-10.82
IMPHY012397	-10.808
IMPHY010180	-10.803
IMPHY009033	-10.792
IMPHY010360	-10.782
IMPHY000991	-10.642
IMPHY002148	-10.626
IMPHY000062	-10.604
IMPHY001316	-10.588
IMPHY013460	-10.558

IMPHY015781	-10.552
IMPHY009794	-10.542
IMPHY004198	-10.529
IMPHY002214	-10.519
IMPHY003379	-10.479
IMPHY015473	-10.478
IMPHY000954	-10.467
IMPHY003938	-10.431
IMPHY001837	-10.428
IMPHY011099	-10.421
IMPHY007669	-10.386
IMPHY000058	-10.377
IMPHY015740	-10.373
IMPHY002272	-10.36
IMPHY010353	-10.357
IMPHY005815	-10.342
IMPHY001349	-10.324
IMPHY003846	-10.319
IMPHY009686	-10.302
IMPHY005319	-10.258
IMPHY003757	-10.25
IMPHY006116	-10.232

Table.3.8.1: Pinnacle of Potency — Top 40 Molecules Showcasing Highest Binding Energies among all molecules of IMPPAT database.

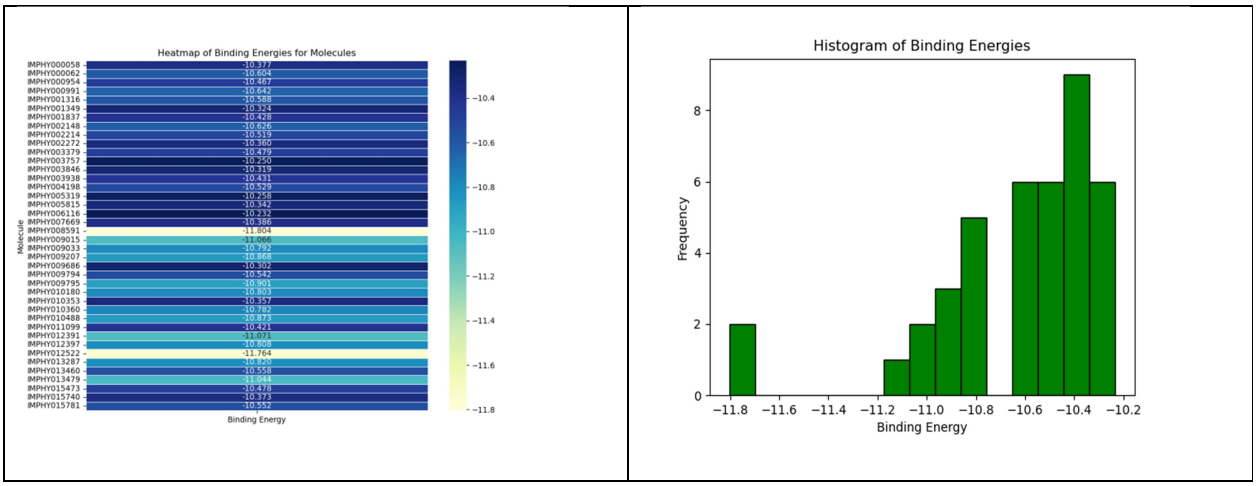

Figure.3.8.2: Insightful Visualization — (a) Heatmap and (b) Frequency distribution Illustrating the Binding Energies of the Top 40 Molecules among a Set of all molecules of IMPPAT Database.

9. 7R9X

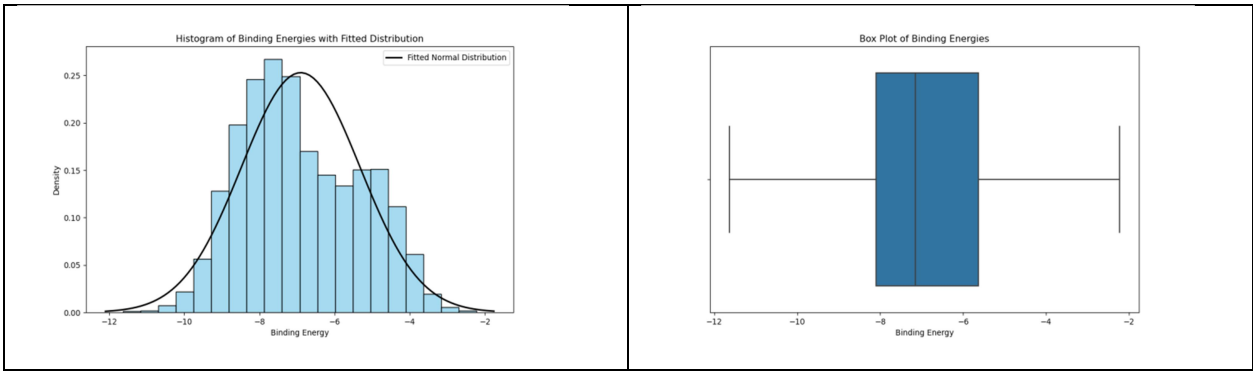

Figure.3.9.1: Statistical Insights into Novel Quorum Sensing Inhibitors — (a) Histogram with Fitted Normal Distribution Density Plot and (b) Box Plot of Binding Energies for all molecules of IMPPAT Database.

Ligands Name	Binding Energies (Kcal/mol)
IMPHY002351	-11.632
IMPHY013460	-11.463
IMPHY007725	-11.458
IMPHY007982	-11.377
IMPHY012397	-11.213
IMPHY008591	-11.203
IMPHY000569	-11.185
IMPHY007447	-11.14

IMPHY002214	-11.094
IMPHY004198	-11.065
IMPHY011625	-11.026
IMPHY009015	-10.975
IMPHY013314	-10.946
IMPHY000439	-10.942
IMPHY014353	-10.94
IMPHY002035	-10.924
IMPHY014498	-10.906
IMPHY006134	-10.831
IMPHY005412	-10.804
IMPHY003932	-10.802
IMPHY012522	-10.801
IMPHY002009	-10.775
IMPHY003792	-10.702
IMPHY004411	-10.687
IMPHY003226	-10.678
IMPHY003592	-10.672
IMPHY003277	-10.657
IMPHY000062	-10.603
IMPHY013445	-10.596
IMPHY010554	-10.554
IMPHY014959	-10.541
IMPHY002395	-10.538
IMPHY000624	-10.519
IMPHY009218	-10.506
IMPHY014605	-10.503
IMPHY011870	-10.501
IMPHY008815	-10.496
IMPHY001857	-10.485
IMPHY010298	-10.48
IMPHY010360	-10.475

Table.3.9.1: Pinnacle of Potency — Top 40 Molecules Showcasing Highest Binding Energies among all molecules of IMPPAT database.

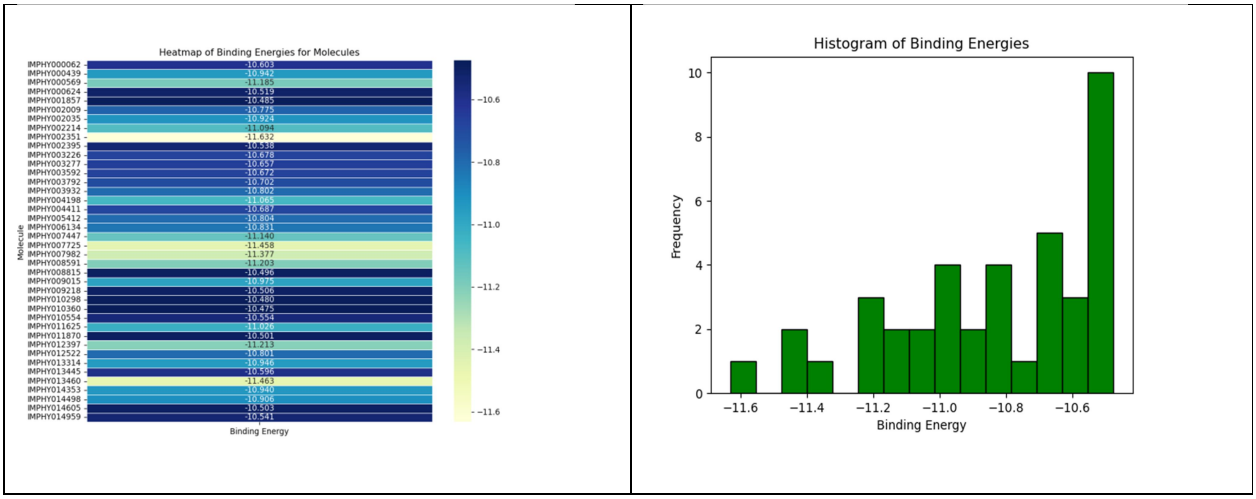

Figure.3.9.2: Insightful Visualization — (a) Heatmap and (b) Frequency distribution Illustrating the Binding Energies of the Top 40 Molecules among a Set of all molecules of IMPPAT Database.

10.7X17

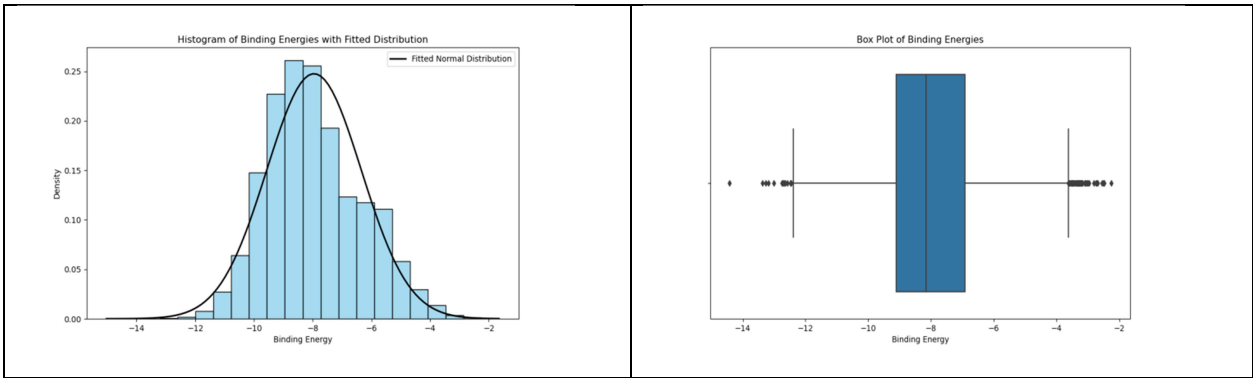

Figure.3.10.1: Statistical Insights into Novel Quorum Sensing Inhibitors — (a) Histogram with Fitted Normal Distribution Density Plot and (b) Box Plot of Binding Energies for all molecules of IMPPAT Database.

Ligands Name	Binding Energies (Kcal/mol)
IMPHY013460	-14.42
IMPHY009015	-13.269
IMPHY013479	-13.188
IMPHY010353	-13.016
IMPHY007991	-12.758

IMPHY002214	-12.735
IMPHY001857	-12.702
IMPHY012397	-12.662
IMPHY008712	-12.651
IMPHY007982	-12.584
IMPHY010691	-12.477
IMPHY010488	-12.469
IMPHY003447	-12.465
IMPHY002655	-12.46
IMPHY010360	-12.393
IMPHY007353	-12.269
IMPHY009062	-12.238
IMPHY004198	-12.235
IMPHY003938	-12.208
IMPHY010846	-12.202
IMPHY000732	-12.199
IMPHY008947	-12.176
IMPHY001707	-12.144
IMPHY014183	-12.103
IMPHY001192	-11.996
IMPHY008302	-11.983
IMPHY004411	-11.981
IMPHY003735	-11.969
IMPHY009219	-11.957
IMPHY013475	-11.95
IMPHY014076	-11.939
IMPHY011333	-11.934
IMPHY002104	-11.922
IMPHY011499	-11.917
IMPHY006572	-11.884
IMPHY001016	-11.877
IMPHY013314	-11.864

IMPHY010112	-11.856
IMPHY006737	-11.856

Table.3.10.1: Pinnacle of Potency — Top 40 Molecules Showcasing Highest Binding Energies among all molecules of IMPPAT database.

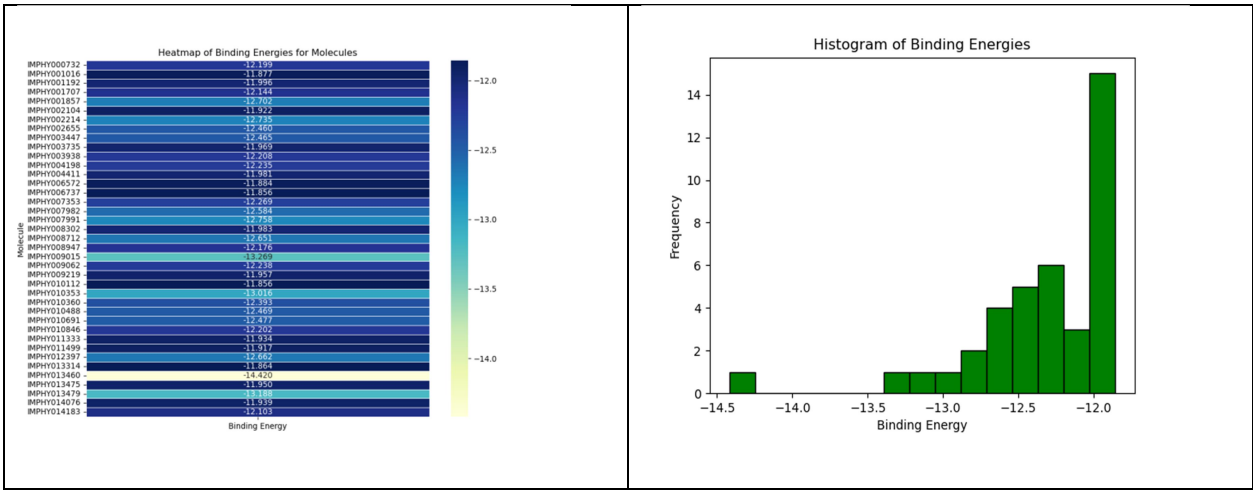

Figure.3.10.2: Insightful Visualization — (a) Heatmap and (b) Frequency distribution Illustrating the Binding Energies of the Top 40 Molecules among a Set of all molecules of IMPPAT Database.

11.Q02N79

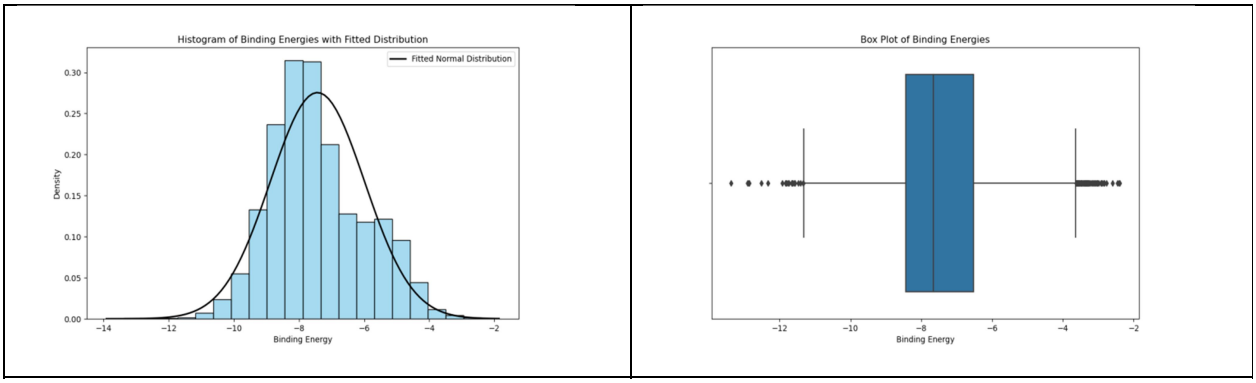

Figure.3.11.1: Statistical Insights into Novel Quorum Sensing Inhibitors — (a) Histogram with Fitted Normal Distribution Density Plot and (b) Box Plot of Binding Energies for all molecules of IMPPAT Database.

Ligands Name	**Binding Energies (Kcal/mol)**
IMPHY002351	-12.517
IMPHY011092	-12.86

IMPHY005795	-12.881
IMPHY004791	-12.909
IMPHY009207	-13.368
IMPHY013460	-12.334
IMPHY007725	-11.919
IMPHY005599	-11.831
IMPHY013479	-11.825
IMPHY013287	-11.799
IMPHY013380	-11.746
IMPHY000954	-11.744
IMPHY013480	-11.652
IMPHY009623	-11.643
IMPHY006658	-11.632
IMPHY002752	-11.582
IMPHY013458	-11.559
IMPHY010214	-11.467
IMPHY010511	-11.406
IMPHY009004	-11.337
IMPHY007496	-11.329
IMPHY009147	-11.324
IMPHY002366	-11.303
IMPHY010476	-11.196
IMPHY013480	-11.158
IMPHY013622	-11.138
IMPHY013382	-11.137
IMPHY009794	-11.122
IMPHY000426	-11.086
IMPHY002714	-11.065
IMPHY007982	-11.06
IMPHY003226	-11.038
IMPHY012880	-11.025
IMPHY010793	-11.022

IMPHY005216	-11.015
IMPHY000509	-11.014
IMPHY000467	-11.014
IMPHY007698	-10.995
IMPHY005533	-10.989
IMPHY002270	-10.977
IMPHY003938	-10.976

Table.3.11.1: Pinnacle of Potency — Top 40 Molecules Showcasing Highest Binding Energies among all molecules of IMPPAT database.

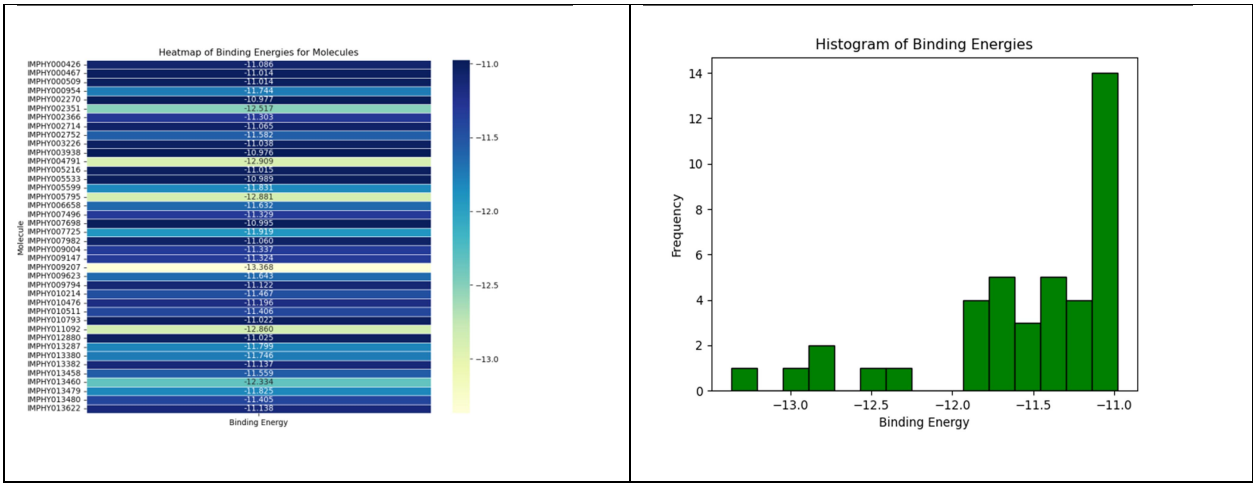

Figure.3.11.2: Insightful Visualization — (a) Heatmap and (b) Frequency distribution Illustrating the Binding Energies of the Top 40 Molecules among a Set of all molecules of IMPPAT Database.

Receptors	Ligands
Common Compounds between Receptor 1 and Receptor 2	[IMPHY007725, IMPHY008591, IMPHY013247, IMPHY013460, IMPHY014362, IMPHY005216, IMPHY006572]
Common Compounds between Receptor 1 and Receptor 3	[IMPHY014103, IMPHY002714, IMPHY007725, IMPHY014362]
Common Compounds between Receptor 1 and Receptor 4	[IMPHY014498, IMPHY007725]
Common Compounds between Receptor 1 and Receptor 5	[IMPHY014959, IMPHY014498, IMPHY007725, IMPHY008591, IMPHY004411, IMPHY013237, IMPHY013460, IMPHY007982, IMPHY008302, IMPHY001398]

Common Compounds between Receptor 1 and Receptor 6	[IMPHY014605, IMPHY007982, IMPHY008591]
Common Compounds between Receptor 1 and Receptor 7	[IMPHY009721, IMPHY014498, IMPHY003226, IMPHY014605, IMPHY008124]
Common Compounds between Receptor 1 and Receptor 8	[IMPHY008591, IMPHY013460]
Common Compounds between Receptor 1 and Receptor 9	[IMPHY014959, IMPHY014498, IMPHY007725, IMPHY008591, IMPHY004411, IMPHY013460, IMPHY003226, IMPHY014605, IMPHY007982]
Common Compounds between Receptor 1 and Receptor 10	[IMPHY008712, IMPHY004411, IMPHY013460, IMPHY007982, IMPHY008302, IMPHY006572]
Common Compounds between Receptor 1 and Receptor 11	[IMPHY007725, IMPHY002714, IMPHY013458, IMPHY013460, IMPHY003226, IMPHY005216, IMPHY007982]
Common Compounds between Receptor 2 and Receptor 3	[IMPHY009207, IMPHY004849, IMPHY005887, IMPHY007725, IMPHY006882, IMPHY014191, IMPHY010362, IMPHY014362, IMPHY015394]
Common Compounds between Receptor 2 and Receptor 4	[IMPHY004849, IMPHY007725, IMPHY006927, IMPHY006882, IMPHY000296]
Common Compounds between Receptor 2 and Receptor 5	[IMPHY009207, IMPHY007991, IMPHY007725, IMPHY008591, IMPHY000624, IMPHY013460]
Common Compounds between Receptor 2 and Receptor 6	[IMPHY009207, IMPHY008591, IMPHY000296]
Common Compounds between Receptor 2 and Receptor 7	[IMPHY009207, IMPHY003932, IMPHY006882, IMPHY012536]
Common Compounds between Receptor 2 and Receptor 8	[IMPHY009207, IMPHY008591, IMPHY013460]
Common Compounds between Receptor 2 and Receptor 9	[IMPHY007725, IMPHY008591, IMPHY000624, IMPHY003932, IMPHY013460]
Common Compounds between Receptor 2 and Receptor 10	[IMPHY007991, IMPHY013460, IMPHY006572]
Common Compounds between Receptor 2 and Receptor 11	[IMPHY009207, IMPHY005216, IMPHY007725, IMPHY013460]

Common Compounds between Receptor 3 and Receptor 4	[IMPHY004849, IMPHY007725, IMPHY004103, IMPHY006882]
Common Compounds between Receptor 3 and Receptor 5	[IMPHY009207, IMPHY007725, IMPHY000715]
Common Compounds between Receptor 3 and Receptor 6	[IMPHY009207]
Common Compounds between Receptor 3 and Receptor 7	[IMPHY009207, IMPHY008329, IMPHY000715, IMPHY006882]
Common Compounds between Receptor 3 and Receptor 8	[IMPHY009207, IMPHY003938]
Common Compounds between Receptor 3 and Receptor 9	[IMPHY007725, IMPHY003592, IMPHY013314]
Common Compounds between Receptor 3 and Receptor 10	[IMPHY013314, IMPHY003938]
Common Compounds between Receptor 3 and Receptor 11	[IMPHY009207, IMPHY007725, IMPHY002714, IMPHY005533, IMPHY005599, IMPHY009004, IMPHY010511, IMPHY003938]
Common Compounds between Receptor 4 and Receptor 5	[IMPHY014498, IMPHY007725]
Common Compounds between Receptor 4 and Receptor 6	[IMPHY005061, IMPHY000296]
Common Compounds between Receptor 4 and Receptor 7	[IMPHY014498, IMPHY006882]
Common Compounds between Receptor 4 and Receptor 8	set()
Common Compounds between Receptor 4 and Receptor 9	[IMPHY014498, IMPHY007725]
Common Compounds between Receptor 4 and Receptor 10	set()
Common Compounds between Receptor 4 and Receptor 11	[IMPHY007725]
Common Compounds between Receptor 5 and Receptor 6	[IMPHY009207, IMPHY007982, IMPHY008591]
Common Compounds between Receptor 5 and Receptor 7	[IMPHY009207, IMPHY014498, IMPHY000715, IMPHY013479]
Common Compounds between Receptor 5 and Receptor 8	[IMPHY009207, IMPHY008591, IMPHY010360, IMPHY013479, IMPHY013287, IMPHY013460, IMPHY010353]
Common Compounds between Receptor 5 and Receptor 9	[IMPHY014959, IMPHY014498, IMPHY007725, IMPHY008591, IMPHY010360, IMPHY004411, IMPHY000624, IMPHY013460, IMPHY007982]
Common Compounds between Receptor 5 and Receptor 10	[IMPHY007991, IMPHY010360, IMPHY013479, IMPHY004411, IMPHY013460, IMPHY007982, IMPHY008302, IMPHY010353

	]
Common Compounds between Receptor 5 and Receptor 11	[IMPHY009207, IMPHY013480, IMPHY007725, IMPHY000426, IMPHY013479, IMPHY006658, IMPHY013287, IMPHY005795, IMPHY013622, IMPHY013460, IMPHY007982, IMPHY011092]
Common Compounds between Receptor 6 and Receptor 7	[IMPHY009207, IMPHY014605]
Common Compounds between Receptor 6 and Receptor 8	[IMPHY009207, IMPHY003379, IMPHY000991, IMPHY008591]
Common Compounds between Receptor 6 and Receptor 9	[IMPHY014605, IMPHY007982, IMPHY008591]
Common Compounds between Receptor 6 and Receptor 10	[IMPHY007982]
Common Compounds between Receptor 6 and Receptor 11	[IMPHY009207, IMPHY007982]
Common Compounds between Receptor 7 and Receptor 8	[IMPHY009207, IMPHY000062, IMPHY013479, IMPHY005319]
Common Compounds between Receptor 7 and Receptor 9	[IMPHY014498, IMPHY000062, IMPHY002351, IMPHY003932, IMPHY003226, IMPHY014605]
Common Compounds between Receptor 7 and Receptor 10	[IMPHY010846, IMPHY013479]
Common Compounds between Receptor 7 and Receptor 11	[IMPHY009207, IMPHY002351, IMPHY013479, IMPHY003226]
Common Compounds between Receptor 8 and Receptor 9	[IMPHY009015, IMPHY002214, IMPHY008591, IMPHY010360, IMPHY000062, IMPHY012397, IMPHY012522, IMPHY013460, IMPHY004198]
Common Compounds between Receptor 8 and Receptor 10	[IMPHY009015, IMPHY002214, IMPHY010360, IMPHY013479, IMPHY012397, IMPHY010488, IMPHY013460, IMPHY003938, IMPHY010353, IMPHY004198]
Common Compounds between Receptor 8 and Receptor 11	[IMPHY009207, IMPHY013479, IMPHY013287, IMPHY013460, IMPHY003938, IMPHY009794, IMPHY000954]
Common Compounds between Receptor 9 and Receptor 10	[IMPHY009015, IMPHY002214, IMPHY013314, IMPHY010360, IMPHY012397, IMPHY004411, IMPHY001857, IMPHY013460, IMPHY007982, IMPHY004198]

Common Compounds between Receptor 9 and Receptor 11	[IMPHY007725, IMPHY002351, IMPHY013460, IMPHY003226, IMPHY007982]
Common Compounds between Receptor 10 and Receptor 11	[IMPHY007982, IMPHY003938, IMPHY013460, IMPHY013479]

Table.3.(B): Comprehensive Analysis — Comparison List of Molecules Demonstrating Common Inhibitory Properties Across 11 Receptors, Derived from all molecules of IMPPAT database.

Receptors	**Ligands**
Common compounds in the majority	[IMPHY009207, IMPHY007725, IMPHY008591, IMPHY013460, IMPHY007982]

Table.3.(C): Unified Potency — Common Inhibitory Compounds Across 11 Receptors, Unveiling Consistency across all molecules of IMPPAT database.

S.NO	**IMPATT Ligands**	**Ligands Structure**
1.	IMPHY009207	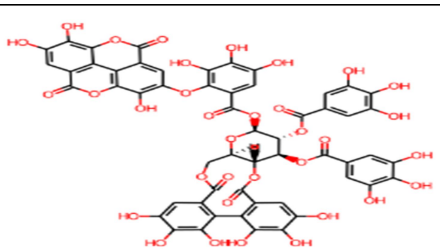
2.	IMPHY007725	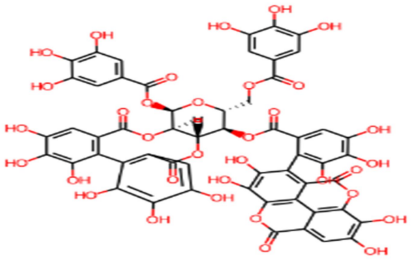
3.	IMPHY008591	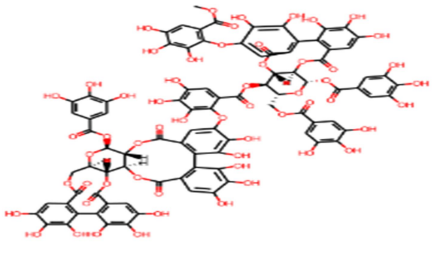

4.	IMPHY013460	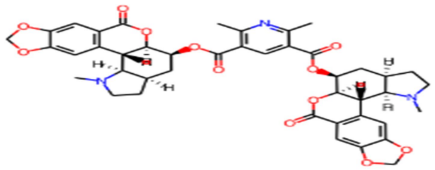
5.	IMPHY007982	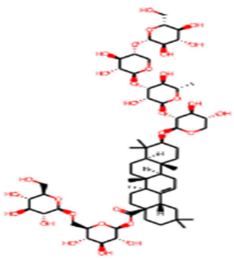

Table.3.(D): Unified Potency — Common Inhibitory Compounds with Structures Across 11 Receptors, Unveiling Consistency across all molecules of IMPPAT database.

Chapter 4

In Chapter 4, the focus of the study shifted to explore the inhibitory potential of compounds from the DRUG BANK database. Retaining the same experimental setup as Chapter 3, the study utilized the previously generated PDBQT files, grid files, and configuration files with a consistent grid box size of 40x40x40 for the molecular docking simulations. This chapter aimed to investigate whether compounds from the DRUG BANK database exhibit similar or divergent inhibitory effects compared to those identified in Chapter 3 using the IMPATT database. By maintaining a standardized methodology across both chapters, the study seeks to discern database-specific nuances in potential inhibitors against *Pseudomonas aeruginosa* quorum sensing Receptors. The systematic comparison between the two databases enhances the robustness of the findings, allowing for a comprehensive evaluation of potential inhibitory molecules across different compound repositories. This approach ensures a nuanced understanding of the variability in inhibitory profiles, providing valuable insights for future drug development endeavors Receptors quorum sensing pathways in *Pseudomonas aeruginosa*. Following the completion of the docking simulations, the focus shifted to extracting meaningful insights from the results. Initially, the top molecules exhibiting the most negative binding energies for each of the 11 receptors were visualized using the LigPlot+ tool. The corresponding ligand interactions were analyzed and are presented in the table below. Subsequently, an in-depth analysis was conducted for all docked molecules from the IMPATT database. Density plots and box plots were generated to visualize the distribution of binding energies, providing a comprehensive overview of the binding affinities of the molecules. Further refinement involved a detailed examination of the top 40 molecules for each receptor, as depicted in the table below. Heatmaps and frequency distribution graphs were employed to visually represent the binding affinities of these molecules across the Receptors. To discern commonality and assess consistency, a comparative analysis of the top 40 molecules was conducted for each receptor. The results highlighted molecules that exhibited inhibitory effects across multiple Receptors, underscoring their potential as broad-spectrum inhibitors. Finally, a comprehensive examination of the majority consensus was performed. A Receptor was compiled, identifying molecules that demonstrated inhibitory effects across a significant proportion of the Receptors. This analysis serves as a valuable guidepost in prioritizing molecules for further investigation and potential therapeutic development. These systematic analyses contribute to a nuanced understanding of the interactions between receptors and inhibitors, providing insights that are pivotal for the development of Receptorsed strategies against *Pseudomonas aeruginosa* quorum sensing pathways. The presented results lay the groundwork for subsequent experimental validations and hold promise for the advancement of anti-pathogenic interventions.

Results:

S. No	Receptors& Ligand	Receptors Ligand Interaction (Ligplot+)	Binding Energy(Kcal/mol)
1.	1RO5 & ligand4670	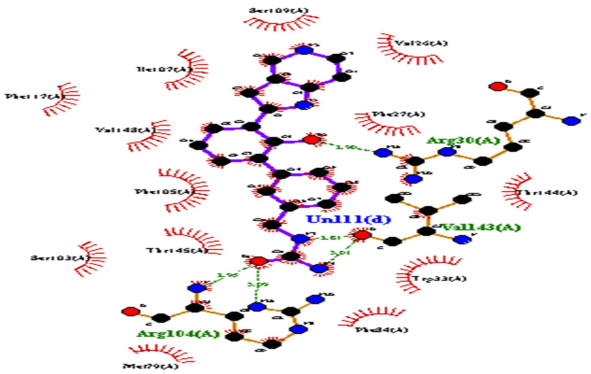	-10.441 (Kcal/mol)
2.	2Q0I & ligand6877	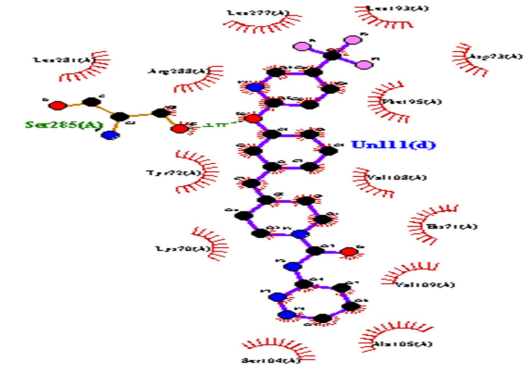	-11.825 (Kcal/mol)
3.	3H77 & ligand1610	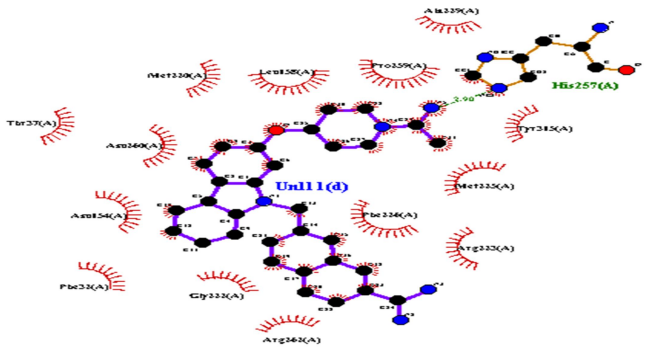	-11.415 (Kcal/mol)

4.	4ng2 & ligand6880	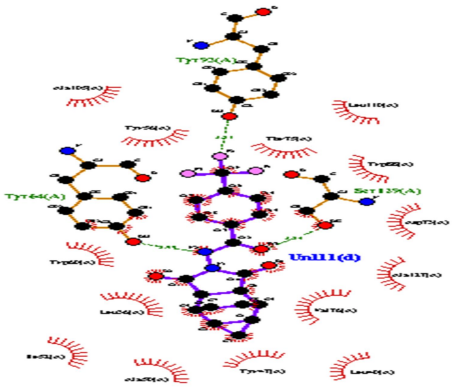	-13.781 (Kcal/mol)
5.	5OE3 & ligand8831	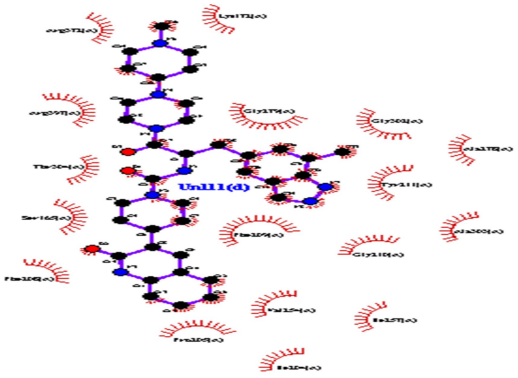	-11.455 (Kcal/mol)
6.	6CC0 & ligand6885	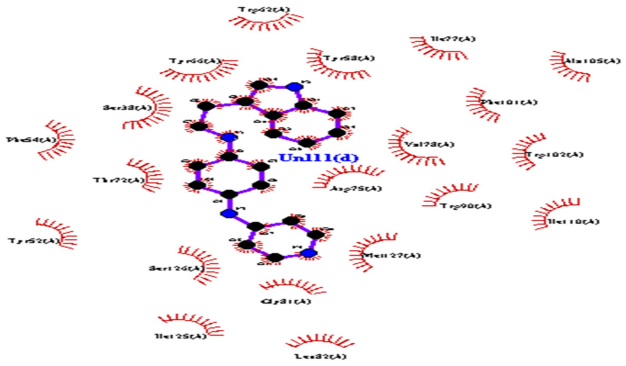	-11.639 (Kcal/mol)
7.	7QA0 & ligand7530	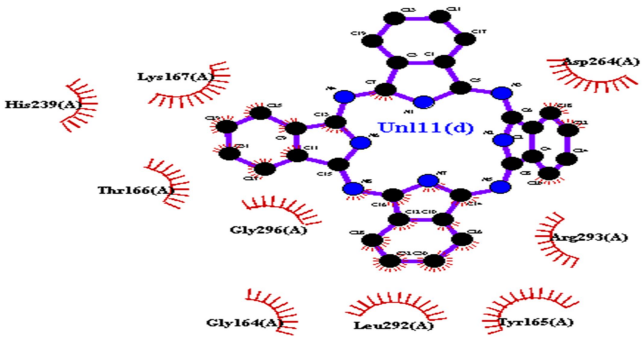	-11.379 (Kcal/mol)

8.	7r3j & ligand3764	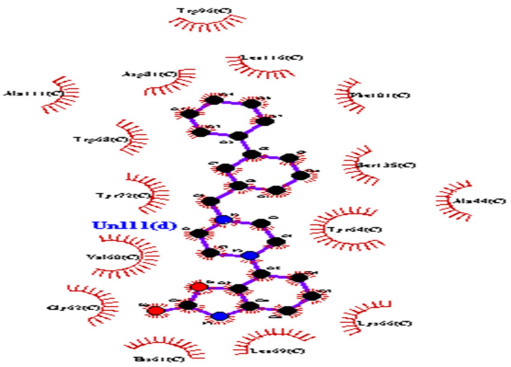	-11.669 (Kcal/mol)
9.	7R9X & ligand7530	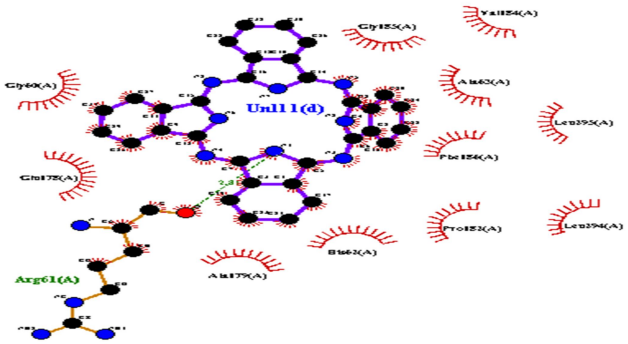	-11.275 (Kcal/mol)
10.	7x17 & ligand7530	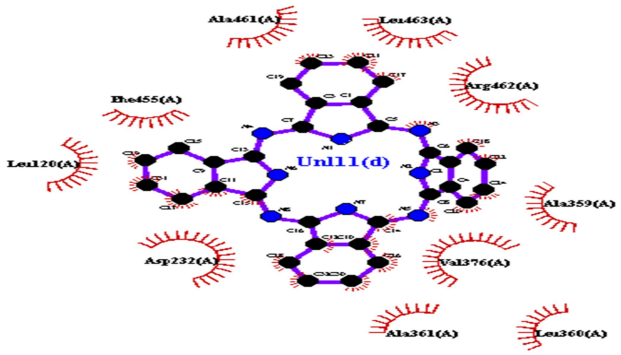	-13.468 (Kcal/mol)
11.	Q02N79 & ligand184	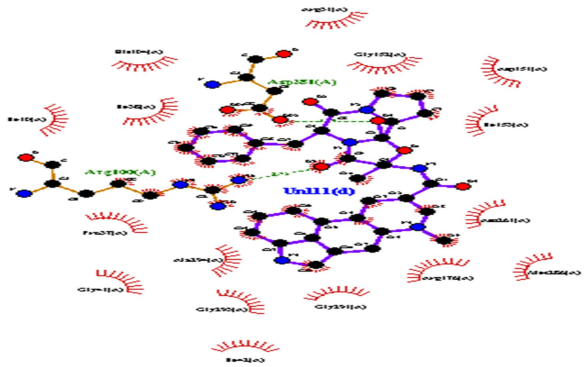	-11.758 (Kcal/mol)

Table.3.(A): Quantifying Inhibitory Potency: Top Molecules with Peak Binding Energy and Detailed Receptor-Ligand Interactions Across All 11 Receptors, Visualized Using LigPlot.

1. 1RO5

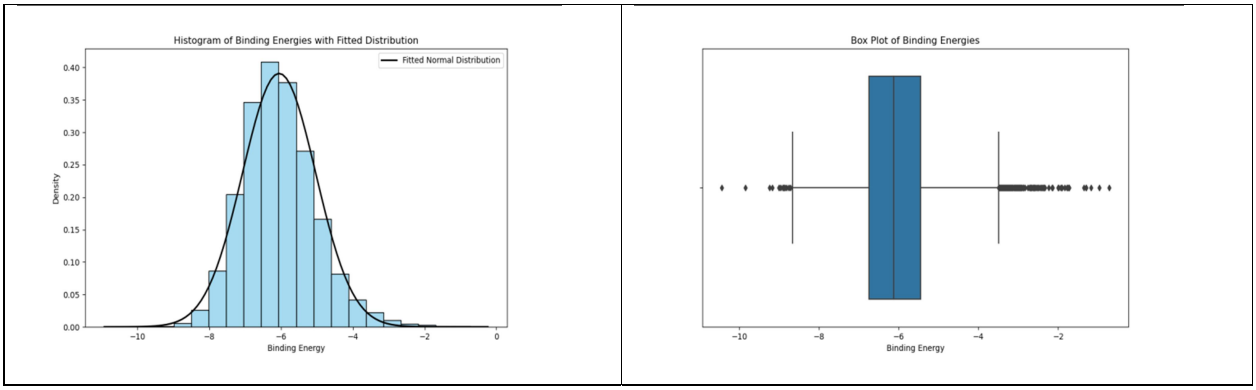

Figure.4.1.1: Statistical Insights into Novel Quorum Sensing Inhibitors — (a) Histogram with Fitted Normal Distribution Density Plot and (b) Box Plot of Binding Energies for all molecules of IMPPAT Database.

Ligands Name	Binding Energies (Kcal/mol)
ligand4670	-10.441
ligand3749	-9.849
ligand7530	-9.242
ligand8831	-9.179
ligand252	-9.008
ligand9012	-8.965
ligand6342	-8.915
ligand8106	-8.879
ligand7763	-8.856
ligand8549	-8.816
ligand7159	-8.76
ligand8484	-8.719
ligand7478	-8.66
ligand5720	-8.645
ligand7074	-8.628
ligand2385	-8.628
ligand6767	-8.624
ligand8441	-8.614
ligand8529	-8.608
ligand7344	-8.603

ligand7465	-8.592
ligand6877	-8.592
ligand8993	-8.586
ligand2215	-8.581
ligand125	-8.566
ligand4179	-8.55
ligand8436	-8.547
ligand1444	-8.528
ligand4403	-8.526
ligand3083	-8.506
ligand8699	-8.495
ligand7412	-8.491
ligand9072	-8.486
ligand3976	-8.477
ligand1433	-8.477
ligand6857	-8.476
ligand8492	-8.475
ligand8722	-8.47
ligand6075	-8.456
ligand2106	-8.889

Table.3.1.1: Pinnacle of Potency — Top 40 Molecules Showcasing Highest Binding Energies among all molecules of IMPPAT database.

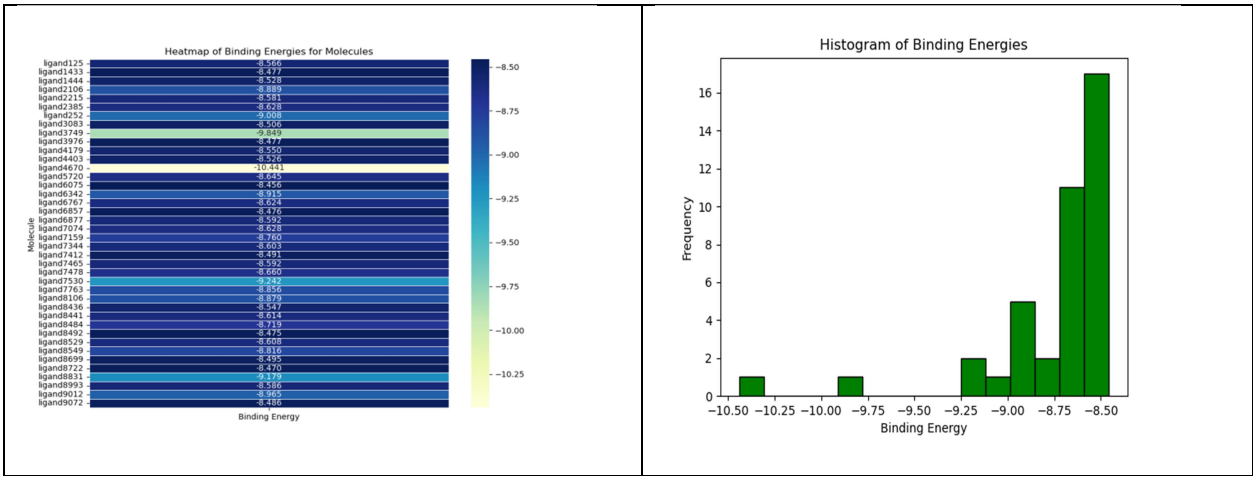

Figure.4.1.2: Insightful Visualization — (a) Heatmap and (b) Frequency distribution Illustrating the Binding Energies of the Top 40 Molecules among a Set of all molecules of IMPPAT Database.

2. 2Q0I

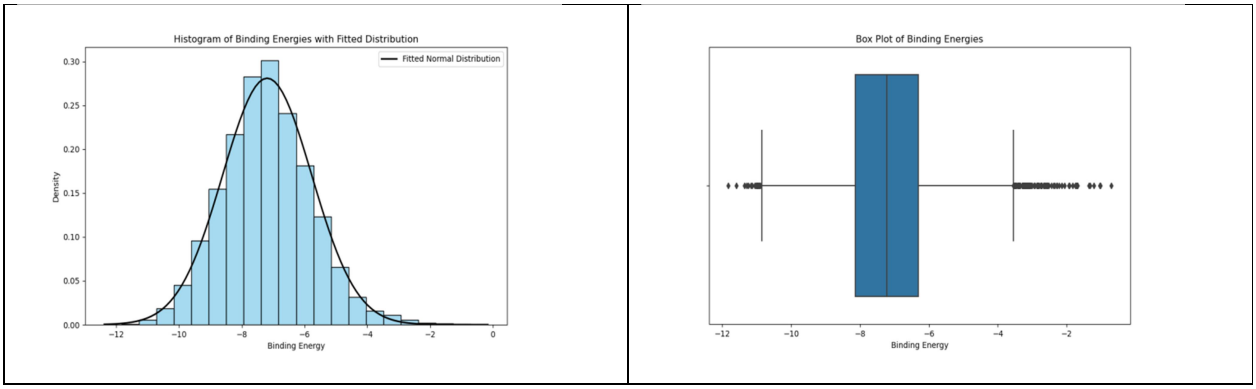

Figure.4.2.1: Statistical Insights into Novel Quorum Sensing Inhibitors — (a) Histogram with Fitted Normal Distribution Density Plot and (b) Box Plot of Binding Energies for all molecules of IMPPAT Database.

Ligands Name	Binding Energies (Kcal/mol)
ligand6877	-11.825
ligand8441	-11.598
ligand6767	-11.348
ligand8538	-11.286
ligand4096	-11.241
ligand8831	-11.173
ligand7047	-11.127
ligand4472	-11.05
ligand4087	-11.021
ligand7408	-11.008
ligand3883	-10.999
ligand4209	-10.975
ligand8488	-10.974
ligand4038	-10.965
ligand7196	-10.961
ligand526	-10.954
ligand9084	-10.926
ligand8689	-10.906

ligand5336	-10.897
ligand9053	-10.858
ligand8946	-10.838
ligand4162	-10.823
ligand1444	-10.821
ligand5660	-10.815
ligand3526	-10.814
ligand6185	-10.771
ligand3660	-10.763
ligand6777	-10.761
ligand3976	-10.732
ligand5779	-10.718
ligand8658	-10.716
ligand1730	-10.706
ligand3834	-10.704
ligand5326	-10.689
ligand5589	-10.677
ligand7467	-10.664
ligand8492	-10.66
ligand984	-10.65
ligand5662	-10.62
ligand6961	-10.617

Table.3.2.1: Pinnacle of Potency — Top 40 Molecules Showcasing Highest Binding Energies among all molecules of IMPPAT database.

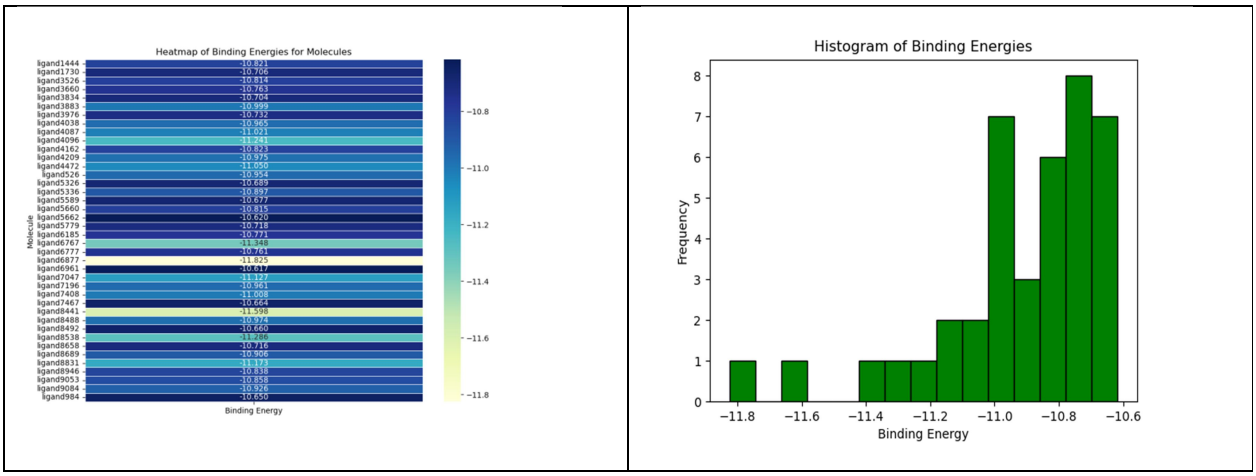

Figure.4.2.2: Insightful Visualization — (a) Heatmap and (b) Frequency distribution Illustrating the Binding Energies of the Top 40 Molecules among a Set of all molecules of IMPPAT Database.

3. 3H77

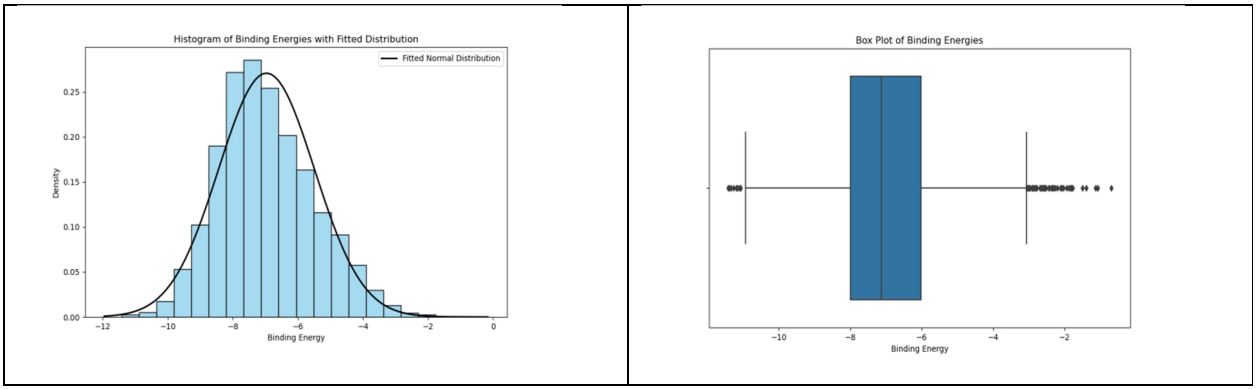

Figure.4.3.1: Statistical Insights into Novel Quorum Sensing Inhibitors — (a) Histogram with Fitted Normal Distribution Density Plot and (b) Box Plot of Binding Energies for all molecules of IMPPAT Database.

Ligands Name	Binding Energies (Kcal/mol)
ligand1610	-11.415
ligand1444	-11.395
ligand8441	-11.35
ligand4113	-11.273
ligand3883	-11.196
ligand8401	-11.161
ligand6767	-11.156
ligand6723	-11.094

ligand6893	-11.091
ligand5203	-11.062
ligand8831	-10.936
ligand4209	-10.906
ligand4096	-10.899
ligand7003	-10.882
ligand8484	-10.867
ligand3817	-10.835
ligand5185	-10.803
ligand5589	-10.779
ligand5772	-10.759
ligand4834	-10.753
ligand6857	-10.724
ligand9021	-10.71
ligand9053	-10.628
ligand6851	-10.602
ligand2839	-10.596
ligand5304	-10.582
ligand7537	-10.565
ligand7234	-10.547
ligand6950	-10.531
ligand5718	-10.512
ligand3736	-10.512
ligand7530	-10.497
ligand3749	-10.48
ligand8459	-10.46
ligand2461	-10.457
ligand6194	-10.433
ligand3385	-10.421
ligand3638	-10.4
ligand3102	-10.361
ligand3607	-10.35

Table.3.3.1: Pinnacle of Potency — Top 40 Molecules Showcasing Highest Binding Energies among all molecules of IMPPAT database.

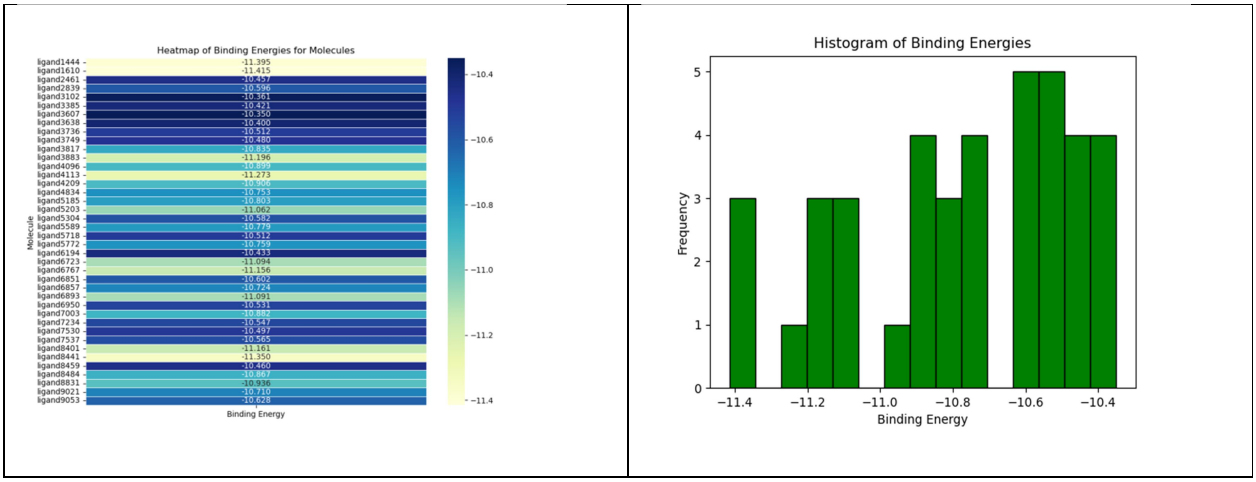

Figure.4.3.2: Insightful Visualization — (a) Heatmap and (b) Frequency distribution Illustrating the Binding Energies of the Top 40 Molecules among a Set of all molecules of IMPPAT Database.

4. 4NG2

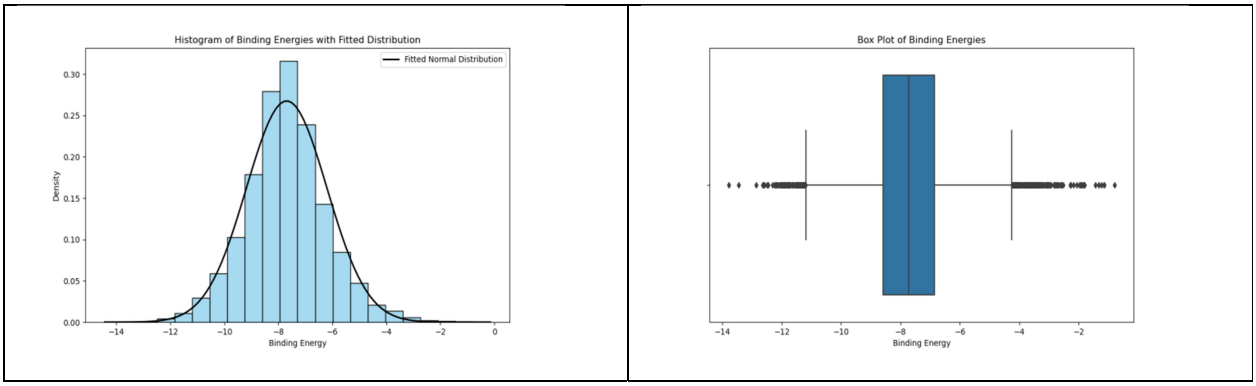

Figure.4.4.1: Statistical Insights into Novel Quorum Sensing Inhibitors — (a) Histogram with Fitted Normal Distribution Density Plot and (b) Box Plot of Binding Energies for all molecules of IMPPAT Database.

Ligands Name	Binding Energies (Kcal/mol)
ligand6880	-13.781
ligand5638	-13.457
ligand5336	-12.864
ligand3773	-12.646
ligand4121	-12.627

ligand7133	-12.584
ligand6533	-12.486
ligand3373	-12.453
ligand7420	-12.318
ligand6743	-12.239
ligand6102	-12.237
ligand5431	-12.192
ligand8133	-12.166
ligand5694	-12.166
ligand4612	-12.1
ligand5365	-12.071
ligand6725	-12.053
ligand4251	-12.01
ligand4096	-12.009
ligand4854	-11.999
ligand8788	-11.996
ligand5202	-11.982
ligand1267	-11.97
ligand3797	-11.962
ligand3768	-11.946
ligand6283	-11.923
ligand5036	-11.922
ligand5772	-11.913
ligand7146	-11.879
ligand5179	-11.87
ligand9010	-11.836
ligand4933	-11.832
ligand5545	-11.823
ligand4511	-11.804
ligand7918	-11.775
ligand7401	-11.768
ligand1503	-11.768

ligand4583	-11.743
ligand4804	-11.735
ligand4429	-11.729

Table.3.4.1: Pinnacle of Potency — Top 40 Molecules Showcasing Highest Binding Energies among all molecules of IMPPAT database.

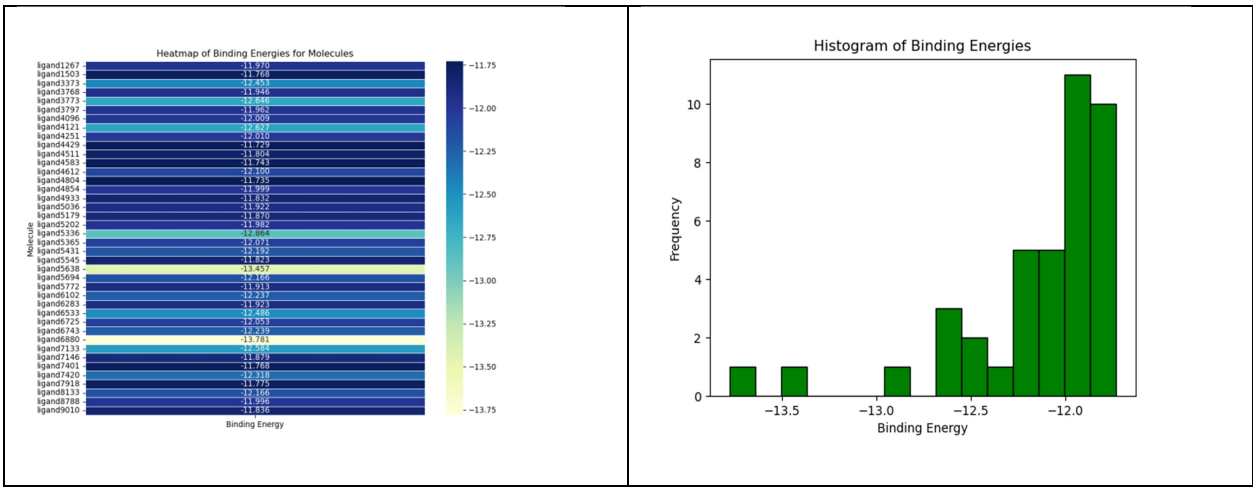

Figure.4.4.2: Insightful Visualization — (a) Heatmap and (b) Frequency distribution Illustrating the Binding Energies of the Top 40 Molecules among a Set of all molecules of IMPPAT Database.

5. 5OE3

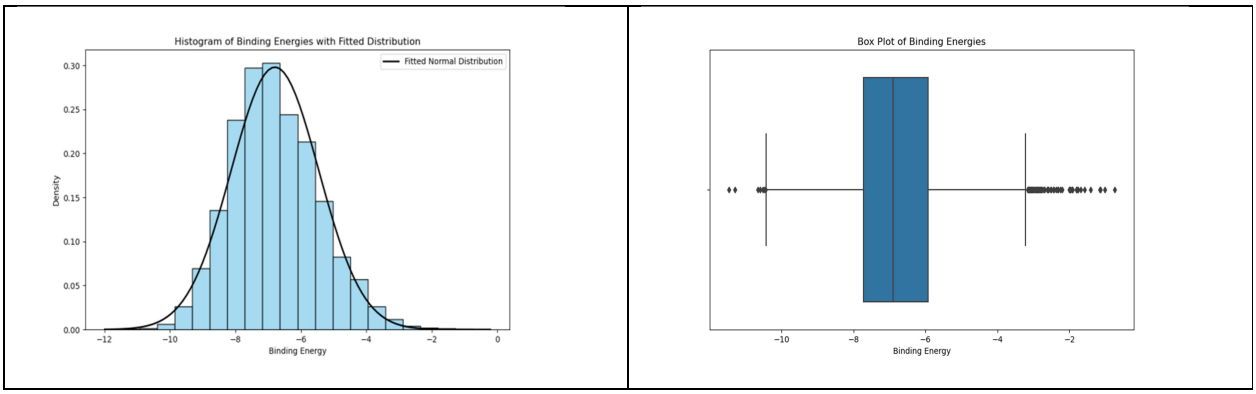

Figure.4.5.1: Statistical Insights into Novel Quorum Sensing Inhibitors — (a) Histogram with Fitted Normal Distribution Density Plot and (b) Box Plot of Binding Energies for all molecules of IMPPAT Database.

Ligands Name	Binding Energies (Kcal/mol)
ligand8831	-11.455

ligand8480	-11.293
ligand7412	-10.658
ligand8681	-10.588
ligand8469	-10.519
ligand7471	-10.469
ligand5064	-10.444
ligand1433	-10.423
ligand6730	-10.37
ligand8677	-10.363
ligand3976	-10.303
ligand8441	-10.287
ligand7536	-10.285
ligand6893	-10.271
ligand7844	-10.216
ligand3749	-10.166
ligand1444	-10.16
ligand184	-10.119
ligand7530	-10.11
ligand7099	-10.105
ligand1669	-10.092
ligand6042	-10.077
ligand4197	-10.075
ligand6656	-10.059
ligand7159	-10.057
ligand1274	-10.038
ligand1399	-10.009
ligand3638	-10.003
ligand6485	-10.003
ligand7169	-9.985
ligand1290	-9.968
ligand984	-9.967
ligand6681	-9.966

ligand9125	-9.941
ligand1934	-9.933
ligand8946	-9.901
ligand3146	-9.88
ligand6504	-9.866
ligand4145	-9.847
ligand4968	-9.845

Table.3.5.1: Pinnacle of Potency — Top 40 Molecules Showcasing Highest Binding Energies among all molecules of IMPPAT database.

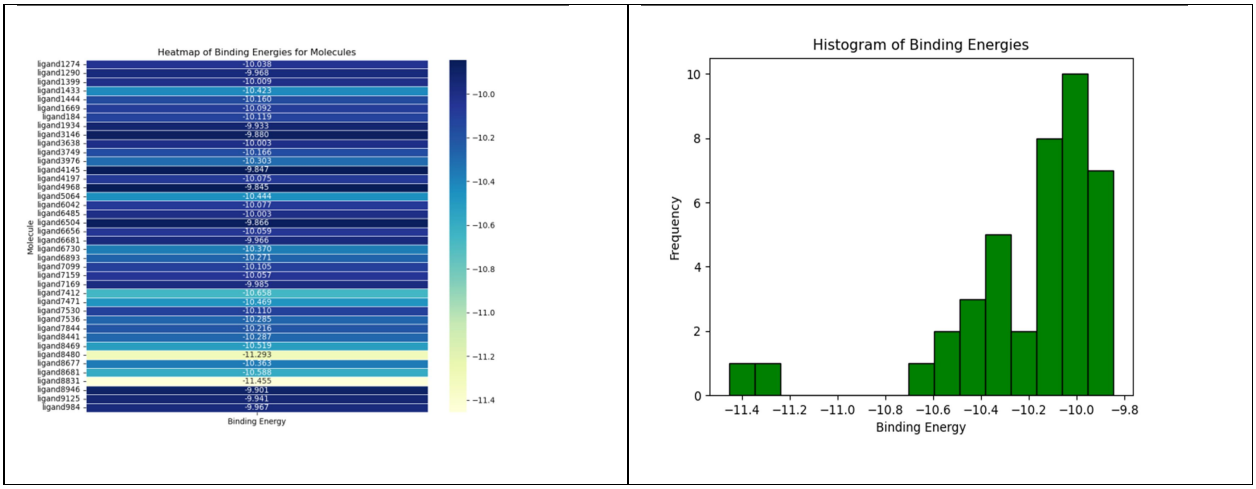

Figure.4.5.2: Insightful Visualization — (a) Heatmap and (b) Frequency distribution Illustrating the Binding Energies of the Top 40 Molecules among a Set of all molecules of IMPPAT Database.

6. 6CC0

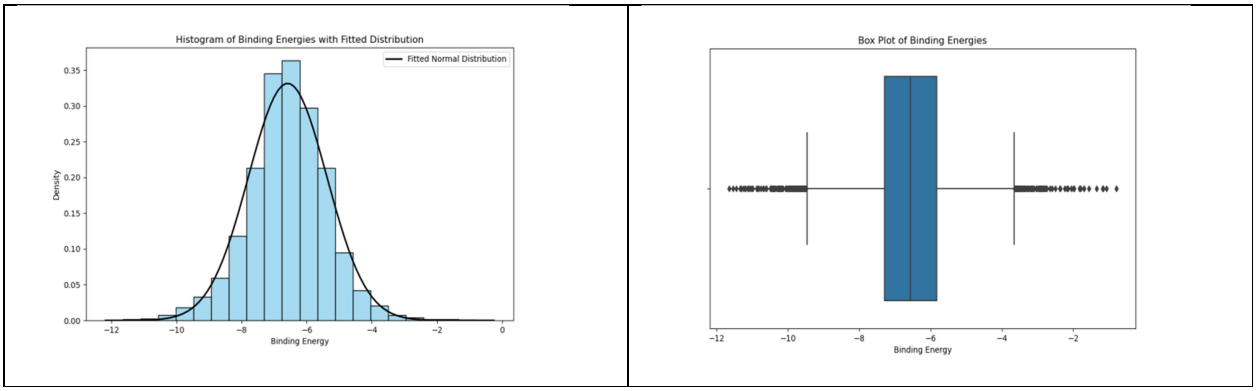

Figure.4.6.1: Statistical Insights into Novel Quorum Sensing Inhibitors — (a) Histogram with Fitted Normal Distribution Density Plot and (b) Box Plot of Binding Energies for all molecules of IMPPAT Database.

Ligands Name	Binding Energies (Kcal/mol)
ligand6885	-11.639
ligand7478	-11.532
ligand4407	-11.45
ligand7527	-11.34
ligand3805	-11.31
ligand4793	-11.239
ligand7785	-11.193
ligand1344	-11.181
ligand5734	-11.118
ligand4708	-11.101
ligand6668	-11.064
ligand5743	-11.019
ligand5412	-10.988
ligand5089	-10.868
ligand6324	-10.836
ligand8971	-10.819
ligand8460	-10.751
ligand8991	-10.694
ligand8941	-10.675
ligand449	-10.604
ligand7530	-10.591
ligand4884	-10.483
ligand3707	-10.478
ligand9055	-10.453
ligand6681	-10.452
ligand4518	-10.432
ligand4463	-10.414
ligand5852	-10.412
ligand4353	-10.396

ligand2520	-10.381
ligand6987	-10.373
ligand1296	-10.367
ligand6121	-10.33
ligand1469	-10.287
ligand980	-10.28
ligand3877	-10.275
ligand5733	-10.266
ligand4683	-10.261
ligand7334	-10.251
ligand8173	-10.246

Table.3.6.1: Pinnacle of Potency — Top 40 Molecules Showcasing Highest Binding Energies among all molecules of IMPPAT database.

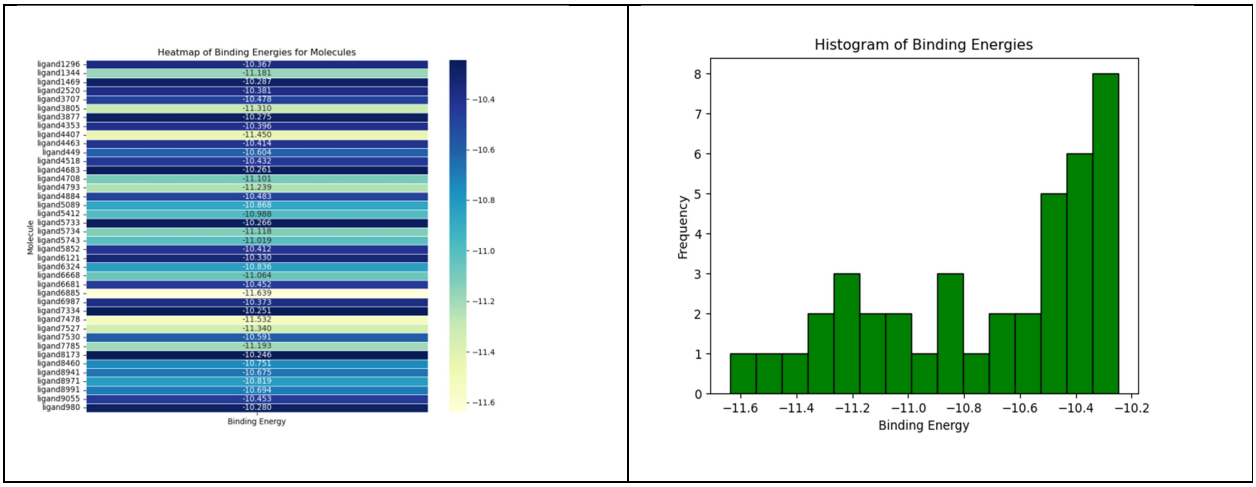

Figure.4.6.2: Insightful Visualization — (a) Heatmap and (b) Frequency distribution Illustrating the Binding Energies of the Top 40 Molecules among a Set of all molecules of IMPPAT Database.

7. 7QA0

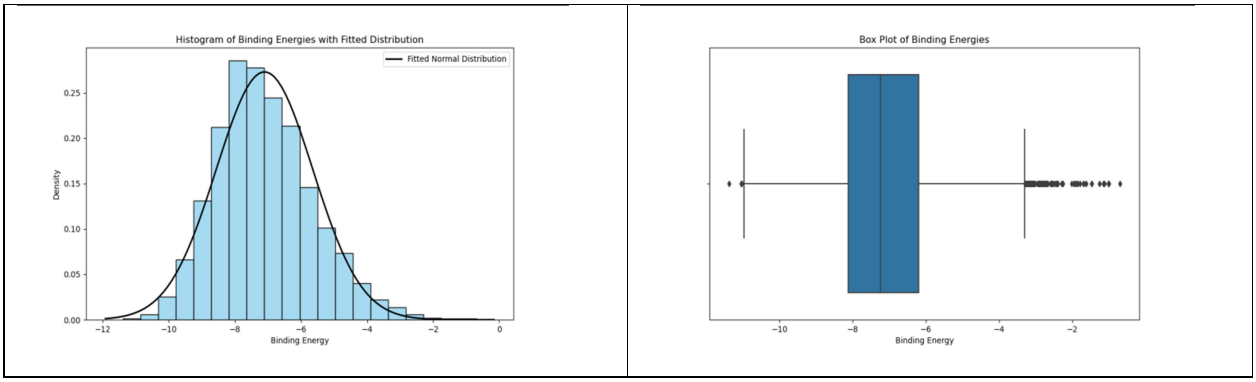

Figure.4.7.1: Statistical Insights into Novel Quorum Sensing Inhibitors — (a) Histogram with Fitted Normal Distribution Density Plot and (b) Box Plot of Binding Energies for all molecules of IMPPAT Database.

Ligands Name	Binding Energies (Kcal/mol)
ligand7530	-11.379
ligand8749	-11.033
ligand6342	-10.977
ligand7412	-10.843
ligand3758	-10.784
ligand5527	-10.782
ligand5916	-10.768
ligand8689	-10.717
ligand8488	-10.707
ligand6723	-10.706
ligand2482	-10.668
ligand3749	-10.657
ligand4468	-10.647
ligand7422	-10.608
ligand7159	-10.562
ligand3883	-10.531
ligand818	-10.475
ligand7548	-10.471
ligand548	-10.467
ligand4096	-10.461

ligand5036	-10.454
ligand6480	-10.409
ligand3740	-10.401
ligand5482	-10.391
ligand2337	-10.376
ligand6504	-10.366
ligand5056	-10.362
ligand184	-10.356
ligand7169	-10.354
ligand4128	-10.344
ligand8549	-10.339
ligand8441	-10.333
ligand8681	-10.317
ligand4357	-10.302
ligand7761	-10.299
ligand7342	-10.291
ligand8705	-10.266
ligand9045	-10.26

Table.3.7.1: Pinnacle of Potency — Top 40 Molecules Showcasing Highest Binding Energies among all molecules of IMPPAT database.

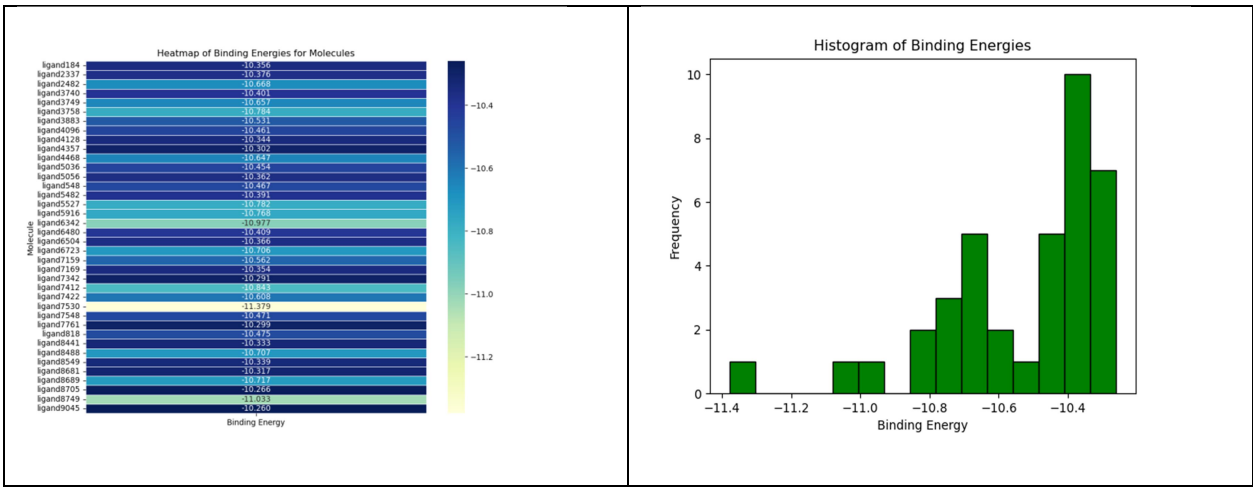

Figure.4.7.2: Insightful Visualization — (a) Heatmap and (b) Frequency distribution Illustrating the Binding Energies of the Top 40 Molecules among a Set of all molecules of IMPPAT Database.

8. 7R3J

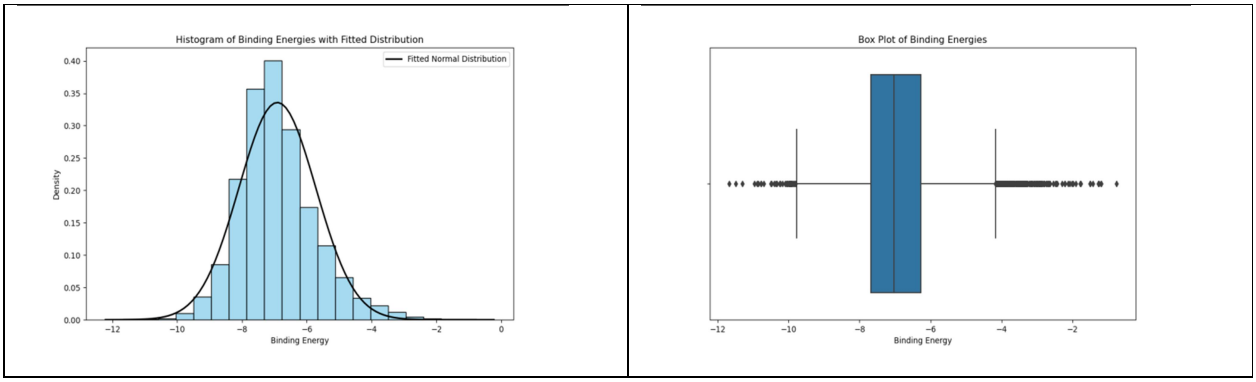

Figure.4.8.1: Statistical Insights into Novel Quorum Sensing Inhibitors — (a) Histogram with Fitted Normal Distribution Density Plot and (b) Box Plot of Binding Energies for all molecules of IMPPAT Database.

Ligands Name	Binding Energies (Kcal/mol)
ligand3764	-11.669
ligand4854	-11.486
ligand5718	-11.296
ligand5789	-10.955
ligand7530	-10.883
ligand5720	-10.852
ligand4612	-10.777
ligand526	-10.775
ligand6753	-10.692
ligand5623	-10.504
ligand7465	-10.488
ligand5338	-10.411
ligand3644	-10.362
ligand8735	-10.322
ligand7015	-10.251
ligand5536	-10.237
ligand247	-10.167
ligand8460	-10.094
ligand8488	-10.063
ligand6809	-10.04

ligand6752	-10.03
ligand5457	-10.029
ligand6342	-10.026
ligand2358	-9.989
ligand4388	-9.982
ligand8920	-9.981
ligand4866	-9.976
ligand5069	-9.961
ligand8409	-9.956
ligand8806	-9.949
ligand5550	-9.939
ligand7273	-9.928
ligand4689	-9.921
ligand8807	-9.909
ligand184	-9.888
ligand6956	-9.861
ligand4884	-9.851
ligand4407	-9.809
ligand5117	-9.796
ligand4309	-9.775

Table.3.8.1: Pinnacle of Potency — Top 40 Molecules Showcasing Highest Binding Energies among all molecules of IMPPAT database.

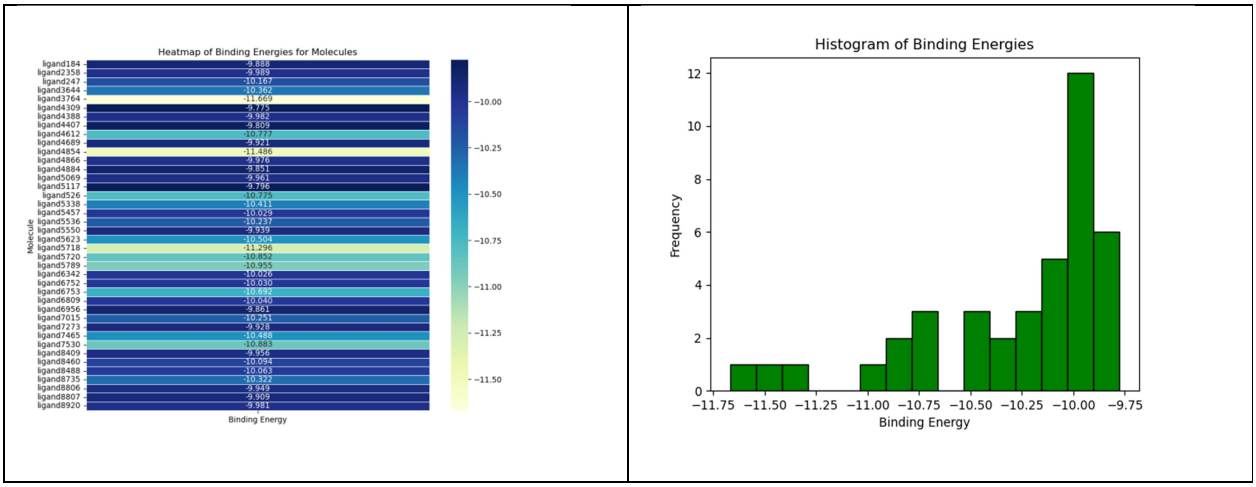

Figure.4.8.2: Insightful Visualization — (a) Heatmap and (b) Frequency distribution Illustrating the Binding Energies of the Top 40 Molecules among a Set of all molecules of IMPPAT Database.

9. 7R9X

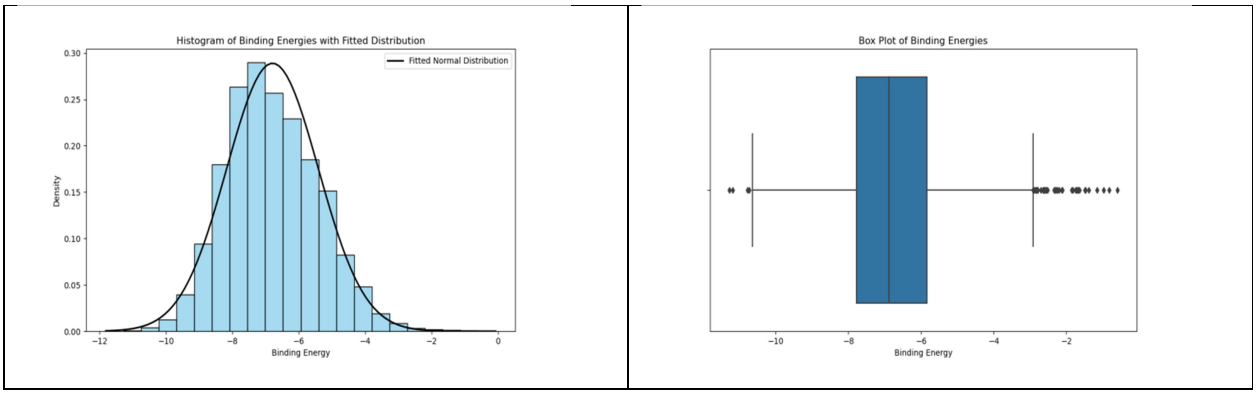

Figure.4.9.1: Statistical Insights into Novel Quorum Sensing Inhibitors — (a) Histogram with Fitted Normal Distribution Density Plot and (b) Box Plot of Binding Energies for all molecules of IMPPAT Database.

Ligands Name	Binding Energies (Kcal/mol)
ligand7530	-11.275
ligand6795	-11.18
ligand8831	-10.774
ligand8718	-10.729
ligand3083	-10.641
ligand6857	-10.535
ligand1610	-10.521
ligand6086	-10.501
ligand7190	-10.484
ligand8488	-10.476
ligand8946	-10.471
ligand3078	-10.456
ligand6746	-10.456
ligand2038	-10.434
ligand7548	-10.409
ligand8409	-10.297
ligand9045	-10.281

ligand8947	-10.276
ligand7412	-10.253
ligand3749	-10.226
ligand8445	-10.216
ligand8599	-10.21
ligand7169	-10.209
ligand8523	-10.203
ligand7603	-10.17
ligand8480	-10.169
ligand5909	-10.146
ligand6893	-10.134
ligand865	-10.133
ligand9080	-10.098
ligand4176	-10.092
ligand7469	-10.089
ligand5151	-10.088
ligand8527	-10.082
ligand7159	-10.072
ligand4145	-10.07
ligand8727	-10.058
ligand4120	-10.029
ligand7135	-10.024
ligand644	-9.994

Table.3.9.1: Pinnacle of Potency — Top 40 Molecules Showcasing Highest Binding Energies among all molecules of IMPPAT database.

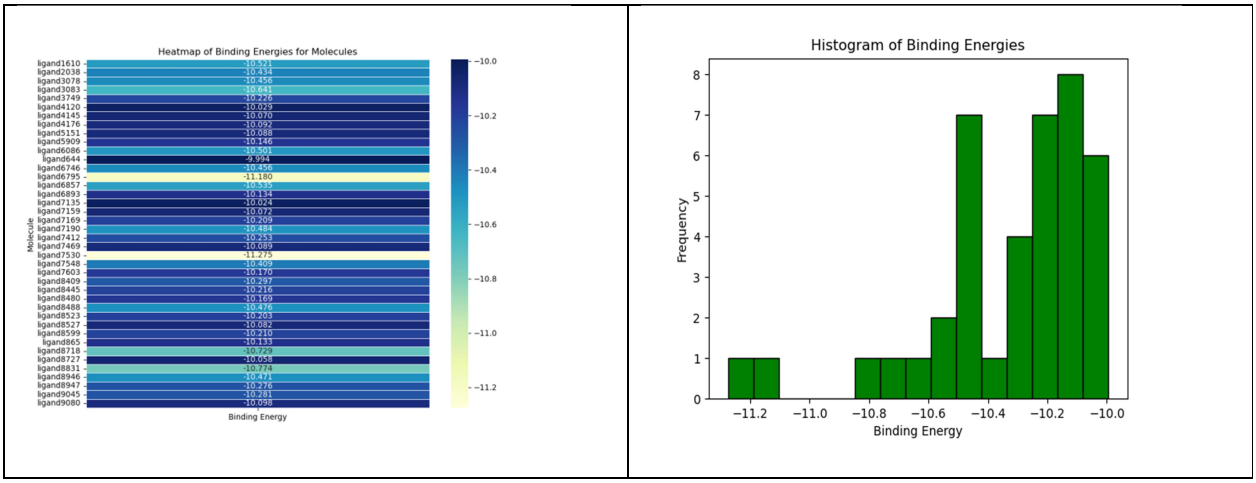

Figure.4.9.2: Insightful Visualization — (a) Heatmap and (b) Frequency distribution Illustrating the Binding Energies of the Top 40 Molecules among a Set of all molecules of IMPPAT Database.

10.7X17

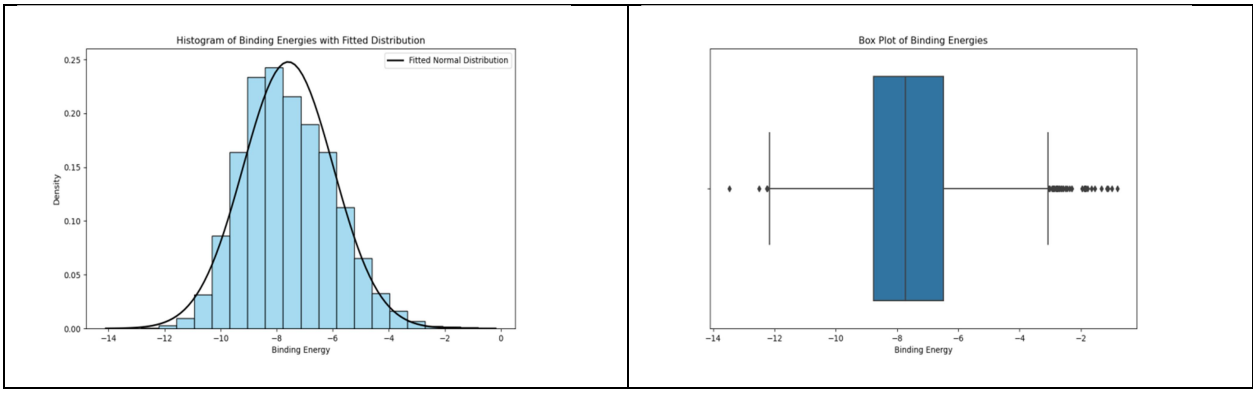

Figure.4.10.1: Statistical Insights into Novel Quorum Sensing Inhibitors — (a) Histogram with Fitted Normal Distribution Density Plot and (b) Box Plot of Binding Energies for all molecules of IMPPAT Database.

Ligands Name	Binding Energies (Kcal/mol)
ligand7530	-13.468
ligand4091	-12.504
ligand6851	-12.248
ligand7344	-12.231
ligand7412	-12.164
ligand8441	-12.101
ligand7169	-12.042
ligand8831	-11.97

ligand3556	-11.941
ligand548	-11.917
ligand1465	-11.848
ligand8946	-11.831
ligand8488	-11.766
ligand3749	-11.687
ligand6342	-11.679
ligand3811	-11.674
ligand7099	-11.673
ligand7571	-11.669
ligand1639	-11.648
ligand3736	-11.612
ligand4200	-11.6
ligand6802	-11.542
ligand7603	-11.464
ligand4620	-11.43
ligand8806	-11.43
ligand6795	-11.412
ligand4148	-11.392
ligand8683	-11.385
ligand9080	-11.349
ligand973	-11.338
ligand4998	-11.327
ligand7273	-11.324
ligand8545	-11.312
ligand4195	-11.287
ligand9031	-11.279
ligand3083	-11.261
ligand4138	-11.257
ligand494	-11.25
ligand7306	-11.248
ligand428	-11.231

Table.3.10.1: Pinnacle of Potency — Top 40 Molecules Showcasing Highest Binding Energies among all molecules of IMPPAT database.

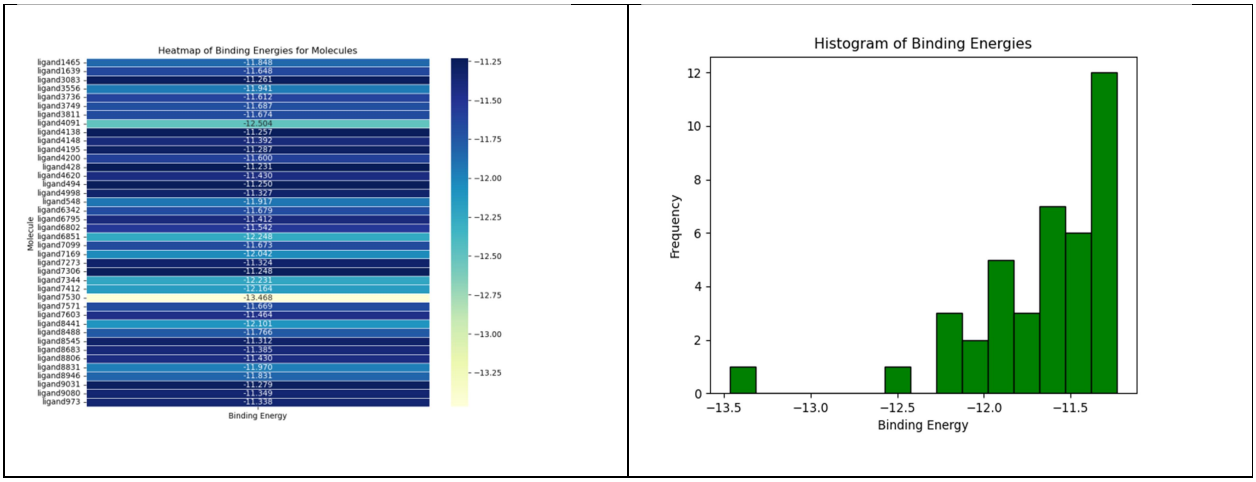

Figure.4.10.2: Insightful Visualization — (a) Heatmap and (b) Frequency distribution Illustrating the Binding Energies of the Top 40 Molecules among a Set of all molecules of IMPPAT Database.

11.Q02N79

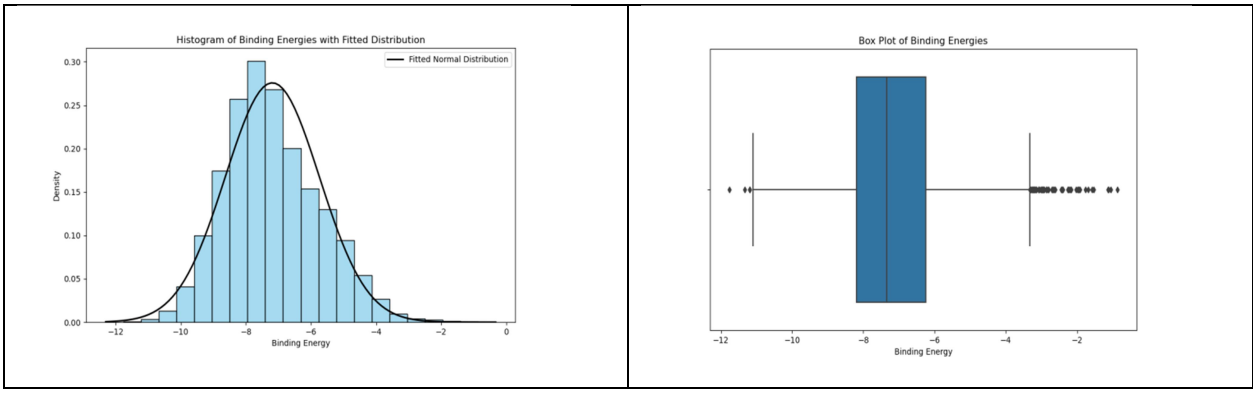

Figure.4.11.1: Statistical Insights into Novel Quorum Sensing Inhibitors — (a) Histogram with Fitted Normal Distribution Density Plot and (b) Box Plot of Binding Energies for all molecules of IMPPAT Database.

Ligands Name	Binding Energies (Kcal/mol)
ligand184	-11.758
ligand8806	-11.334
ligand8705	-11.193
ligand6809	-11.187
ligand7601	-11.096

ligand7412	-11.03
ligand1913	-10.988
ligand2482	-10.955
ligand3749	-10.936
ligand3078	-10.922
ligand6208	-10.877
ligand7169	-10.832
ligand6485	-10.824
ligand1399	-10.766
ligand9099	-10.759
ligand8791	-10.757
ligand8441	-10.753
ligand3976	-10.691
ligand8532	-10.67
ligand2520	-10.648
ligand8459	-10.63
ligand7530	-10.615
ligand5725	-10.577
ligand4038	-10.561
ligand7574	-10.555
ligand5373	-10.551
ligand7099	-10.536
ligand8488	-10.516
ligand5958	-10.509
ligand8493	-10.496
ligand7540	-10.482
ligand4620	-10.481
ligand5304	-10.479
ligand6851	-10.467
ligand5662	-10.46
ligand9128	-10.455
ligand4391	-10.404

ligand7422	-10.4
ligand3811	-10.386
ligand5411	-10.385

Table.3.11.1: Pinnacle of Potency — Top 40 Molecules Showcasing Highest Binding Energies among all molecules of IMPPAT database.

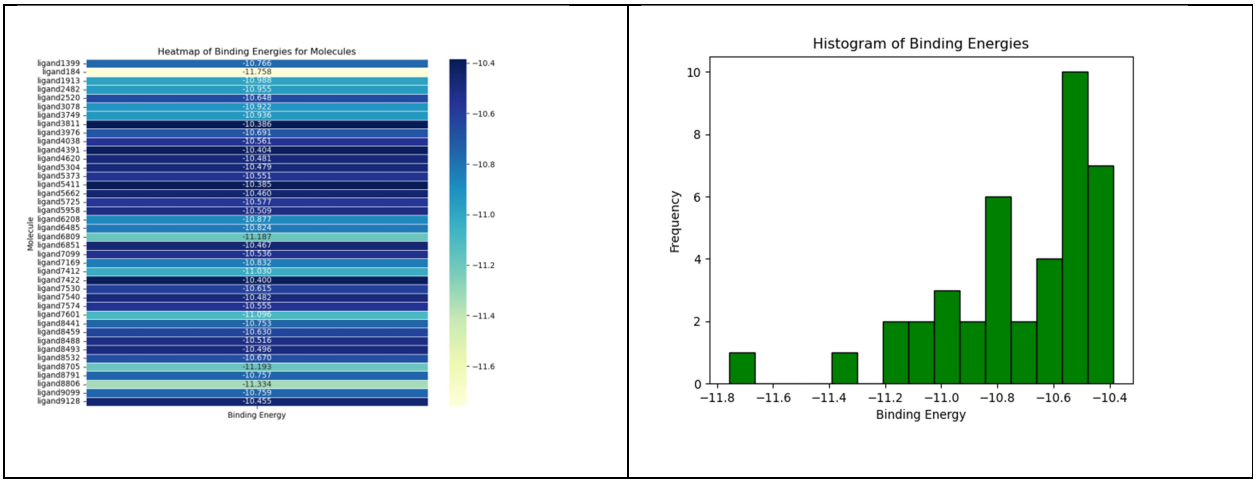

Figure.3.4.2: Insightful Visualization — (a) Heatmap and (b) Frequency distribution Illustrating the Binding Energies of the Top 40 Molecules among a Set of all molecules of IMPPAT Database.

Receptors	Ligands
Common Compounds between Receptor 1 and Receptor 2	[ligand8441, ligand8831, ligand1444, ligand3976, ligand6877, ligand6767, ligand8492]
Common Compounds between Receptor 1 and Receptor 3	[ligand8441, ligand6857, ligand8831, ligand1444, ligand8484, ligand7530, ligand3749, ligand6767]
Common Compounds between Receptor 1 and Receptor 4	set()
Common Compounds between Receptor 1 and Receptor 5	[ligand1433, ligand8441, ligand8831, ligand7412, ligand1444, ligand7159, ligand3976, ligand7530, ligand3749]
Common Compounds between Receptor 1 and Receptor 6	[ligand7530, ligand7478]
Common Compounds between Receptor 1 and Receptor 7	[ligand6342, ligand8441, ligand8549, ligand7412, ligand7159, ligand7530, ligand3749]
Common Compounds between Receptor 1 and Receptor 8	[ligand6342, ligand7530, ligand7465, ligan

	d5720]
Common Compounds between Receptor 1 and Receptor 9	[ligand6857, ligand8831, ligand7412, ligand3083, ligand7159, ligand7530, ligand3749]
Common Compounds between Receptor 1 and Receptor 10	[ligand6342, ligand8441, ligand8831, ligand7412, ligand3083, ligand7344, ligand7530, ligand3749]
Common Compounds between Receptor 1 and Receptor 11	[ligand8441, ligand7412, ligand3976, ligand7530, ligand3749]
Common Compounds between Receptor 2 and Receptor 3	[ligand4096, ligand8441, ligand8831, ligand1444, ligand9053, ligand6767, ligand4209, ligand5589, ligand3883]
Common Compounds between Receptor 2 and Receptor 4	[ligand4096, ligand5336]
Common Compounds between Receptor 2 and Receptor 5	[ligand8946, ligand8441, ligand8831, ligand1444, ligand984, ligand3976]
Common Compounds between Receptor 2 and Receptor 6	set()
Common Compounds between Receptor 2 and Receptor 7	[ligand8488, ligand4096, ligand8441, ligand8689, ligand3883]
Common Compounds between Receptor 2 and Receptor 8	[ligand526, ligand8488]
Common Compounds between Receptor 2 and Receptor 9	[ligand8946, ligand8488, ligand8831]
Common Compounds between Receptor 2 and Receptor 10	[ligand8441, ligand8946, ligand8488, ligand8831]
Common Compounds between Receptor 2 and Receptor 11	[ligand8488, ligand8441, ligand5662, ligand4038, ligand3976]
Common Compounds between Receptor 3 and Receptor 4	[ligand5772, ligand4096]
Common Compounds between Receptor 3 and Receptor 5	[ligand8441, ligand8831, ligand1444, ligand6893, ligand7530, ligand3749, ligand3638]
Common Compounds between Receptor 3 and Receptor 6	[ligand7530]
Common Compounds between Receptor 3 and Receptor 7	[ligand4096, ligand8441, ligand7530, ligand3749, ligand6723, ligand3883]
Common Compounds between Receptor 3 and Receptor 8	[ligand7530, ligand5718]
Common Compounds between Receptor 3 and Receptor 9	[ligand6857, ligand8831, ligand1610, ligand6893, ligand7530, ligand3749]
Common Compounds between Receptor 3 and Receptor 10	[ligand8441, ligand8831, ligand6851, ligand3736, ligand7530, ligand3749]

Common Compounds between Receptor 3 and Receptor 11	[ligand8441, ligand6851, ligand5304, ligand7530, ligand3749, ligand8459]
Common Compounds between Receptor 4 and Receptor 5	set()
Common Compounds between Receptor 4 and Receptor 6	set()
Common Compounds between Receptor 4 and Receptor 7	[ligand5036, ligand4096]
Common Compounds between Receptor 4 and Receptor 8	[ligand4612, ligand4854]
Common Compounds between Receptor 4 and Receptor 9	set()
Common Compounds between Receptor 4 and Receptor 10	set()
Common Compounds between Receptor 4 and Receptor 11	set()
Common Compounds between Receptor 5 and Receptor 6	[ligand7530, ligand6681]
Common Compounds between Receptor 5 and Receptor 7	[ligand8681, ligand7169, ligand8441, ligand7412, ligand6504, ligand7159, ligand7530, ligand3749, ligand184]
Common Compounds between Receptor 5 and Receptor 8	[ligand7530, ligand184]
Common Compounds between Receptor 5 and Receptor 9	[ligand4145, ligand8946, ligand7169, ligand8831, ligand7412, ligand7159, ligand8480, ligand7530, ligand6893, ligand3749]
Common Compounds between Receptor 5 and Receptor 10	[ligand8946, ligand7169, ligand8441, ligand8831, ligand7412, ligand7099, ligand7530, ligand3749]
Common Compounds between Receptor 5 and Receptor 11	[ligand7169, ligand6485, ligand8441, ligand7412, ligand1399, ligand3976, ligand7099, ligand7530, ligand3749, ligand184]
Common Compounds between Receptor 6 and Receptor 7	[ligand7530]
Common Compounds between Receptor 6 and Receptor 8	[ligand4884, ligand8460, ligand4407, ligand7530]
Common Compounds between Receptor 6 and Receptor 9	[ligand7530]
Common Compounds between Receptor 6 and Receptor 10	[ligand7530]
Common Compounds between Receptor 6 and Receptor 11	[ligand2520, ligand7530]
Common Compounds between Receptor 7 and Receptor 8	[ligand8488, ligand6342, ligand7530, ligand184]
Common Compounds between Receptor 7 and Receptor 9	[ligand8488, ligand7169, ligand9045, ligand7412, ligand7159, ligand7530, ligand3749, ligand7548]
Common Compounds between Receptor 7 and Receptor 10	[ligand8488, ligand7169, ligand6342, ligand8441, ligand7412, ligand7530, ligand374

	9, ligand548]
Common Compounds between Receptor 7 and Receptor 11	[ligand8488, ligand7169, ligand7422, ligand8441, ligand2482, ligand7412, ligand7530, ligand3749, ligand184, ligand8705]
Common Compounds between Receptor 8 and Receptor 9	[ligand8488, ligand7530, ligand8409]
Common Compounds between Receptor 8 and Receptor 10	[ligand8488, ligand6342, ligand7530, ligand7273, ligand8806]
Common Compounds between Receptor 8 and Receptor 11	[ligand8488, ligand6809, ligand7530, ligand184, ligand8806]
Common Compounds between Receptor 9 and Receptor 10	[ligand7603, ligand8488, ligand9080, ligand7169, ligand8946, ligand6795, ligand8831, ligand7412, ligand3083, ligand7530, ligand3749]
Common Compounds between Receptor 9 and Receptor 11	[ligand8488, ligand7169, ligand7412, ligand7530, ligand3749, ligand3078]
Common Compounds between Receptor 10 and Receptor 11	[ligand4620, ligand8488, ligand7169, ligand8441, ligand7412, ligand6851, ligand7099, ligand7530, ligand3811, ligand3749, ligand8806]

Table.3.(B): Comprehensive Analysis — Comparison List of Molecules Demonstrating Common Inhibitory Properties Across 11 Receptors, Derived from all molecules of IMPPAT database.

Receptors	**Ligands**
Common compounds in the majority of the Receptors	[ligand8488, ligand8441, ligand8831, ligand7412, ligand7530, ligand3749]

Table.3.(C): Unified Potency — Common Inhibitory Compounds Across 11 Receptors, Unveiling Consistency across all molecules of IMPPAT database.

S.NO	DRUG BANK Ligands	Ligands Structure
1.	ligand8488	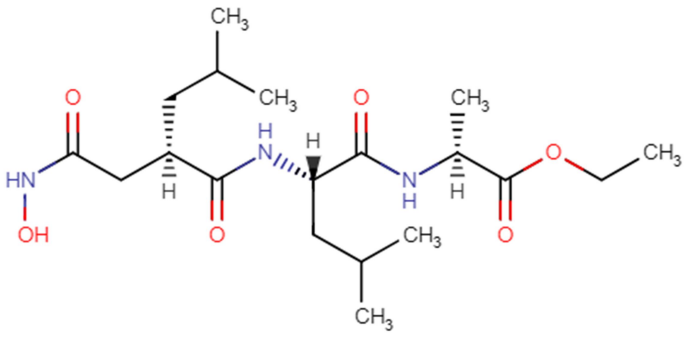
2.	ligand8441	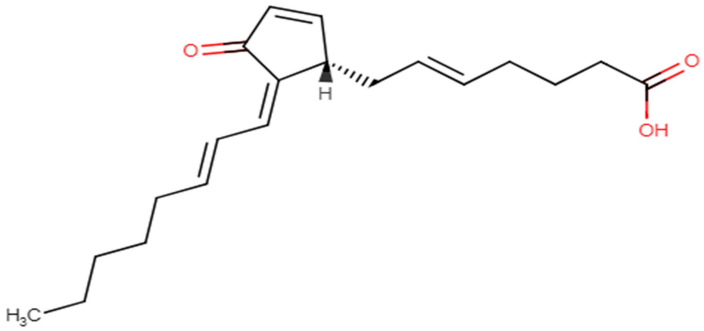
3.	ligand8831	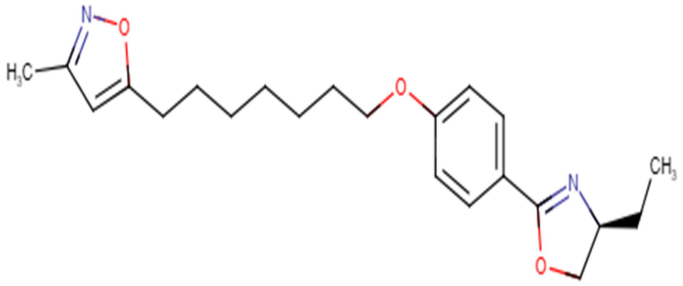
4.	ligand7412	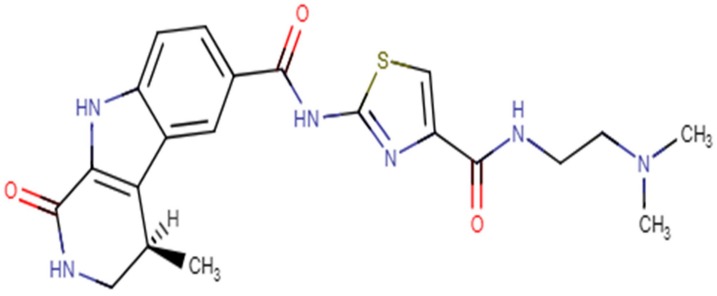

5.	ligand7530	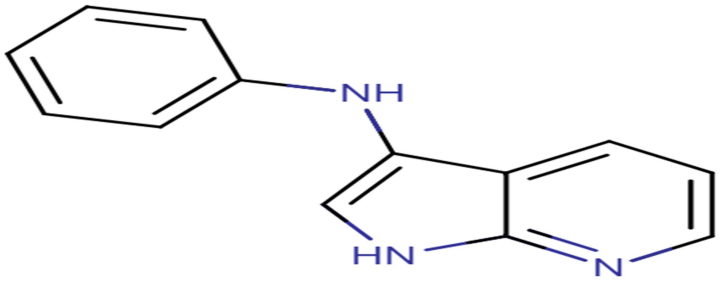
6.	ligand3749	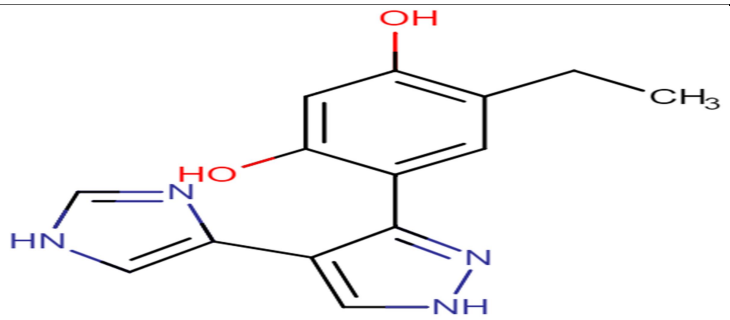

Table.3.(D): Unified Potency — Common Inhibitory Compounds with Structures Across 11 Receptors, Unveiling Consistency across all molecules of IMPPAT database

Chapter 5

In this Chapter, the study focused on a comparative analysis by employing the same set of 11 *Pseudomonas aeruginosa* quorum sensing receptors as in Chapter [3&4]. Consistent with the earlier chapters, PDBQT files were generated for these receptors, maintaining a grid box size of 40x40x40 for the molecular docking simulations. However, in this chapter, the exploration of potential inhibitors took a distinct direction, as 40 molecules were generated based on the literature's identification of Hydnocarpin, Flavonolignans, and Coumarin as prevalent compounds associated with inhibitory effects. The 40 molecules were initially generated using the PubChem Sketcher tool, yielding corresponding SMILES files. Subsequently, 3D PDB files for these molecules were generated using the NovoPro Bioscience online server. With a set of 40 PDB files in hand, the study utilized the Open Babel tool to convert them into PDBQT format, essential for the docking studies. Following the docking simulations, the study identified and analyzed the top molecules based on their binding energies. Plots were generated, and a comparative list was compiled to discern common compounds exhibiting inhibitory effects across multiple receptors. This comprehensive analysis aimed to identify molecules with consistent inhibitory potential against *Pseudomonas aeruginosa* quorum sensing receptors. The results of Chapter 5 were systematically compared with those from Chapters 3 and 4, aligning with the overarching goal of understanding how different databases and compounds influence the inhibitory profiles. The findings are presented in tables, graphs, and images, providing a visual representation of the outcomes. By following a structured and systematic approach, Chapter 5 contributes to a more holistic understanding of potential inhibitors against *Pseudomonas aeruginosa* quorum sensing receptors. The results pave the way for further investigations, aiding in the identification and development of effective compounds for combating quorum sensing mechanisms in P. aeruginosa.

Results:

S. No	Structure	SMILES
1.	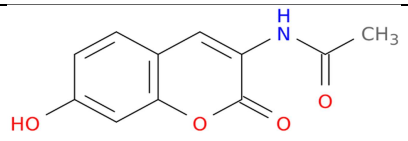	C1=C(C=CC2=C1OC(C(=C2)NC(=O)C)=O)O

2.	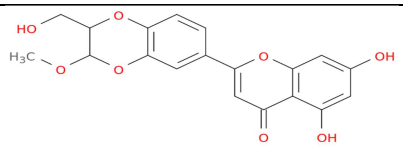	C1=C(C=C(C2=C1OC(=CC2=O)C3=CC4=C(C=C3)OC(C(O4)OC)CO)O)O
3.	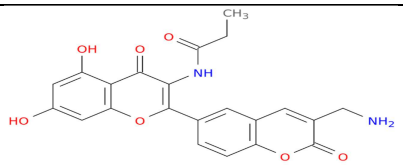	C1=C(C=C(C2=C1OC(=C(C2=O)NC(=O)CC)C3=CC4=C(C=C3)OC(C(=C4)CN)=O)O)O
4.	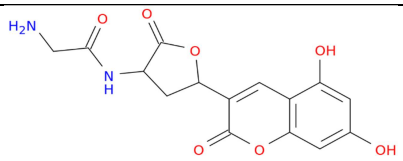	C1=C(C=C(C2=C1OC(C(=C2)C3CC(C(O3)=O)NC(=O)CN)=O)O)O
5.	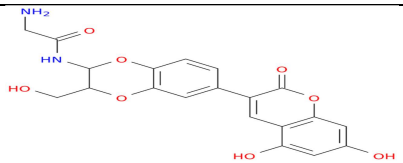	C1=C(C=C(C2=C1OC(C(=C2)C3=CC4=C(C=C3)OC(C(O4)CO)NC(=O)CN)=O)O)O
6.	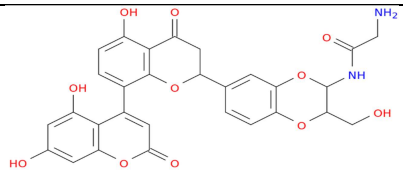	C1=C(C=C(C2=C1OC(C=C2C3=CC=C(C4=C3OC(CC4=O)C5=CC6=C(C=C5)OC(C(O6)NC(=O)CN)CO)O)=O)O)O
7.	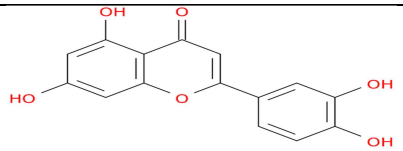	C1=C(C=C(C2=C1OC(=CC2=O)C3=CC(=C(C=C3)O)O)O)O
8.	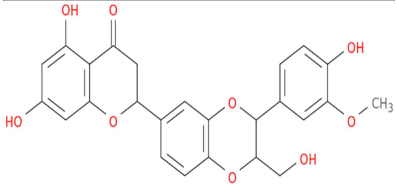	C1=C(C=C(C2=C1OC(CC2=O)C3=CC4=C(C=C3)OC(C(O4)C5=CC=C(C(=C5)OC)O)CO)O)O
9.	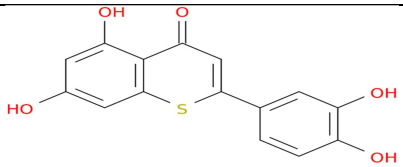	C1=C(C=C(C2=C1SC(=CC2=O)C3=CC(=C(C=C3)O)O)O)O
10.	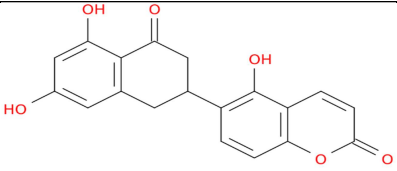	C1=C(C=C(C2=C1CC(CC2=O)C3=C(C4=C(C=C3)OC(C=C4)=O)O)O)O

11.	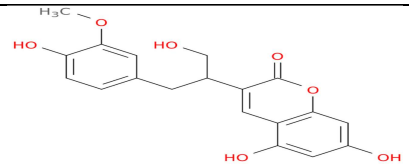	C1=C(C=C(C2=C1OC(C(=C2)C(CO)CC3=CC=C(C(=C3)OC)O)=O)O)O
12.	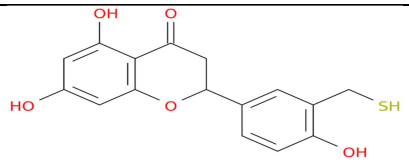	C1=C(C=C(C2=C1OC(CC2=O)C3=CC(=C(C=C3)O)CS)O)O
13.	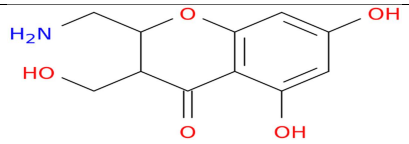	C1=C(C=C(C2=C1OC(C(CO)C2=O)CN)O)O
14.	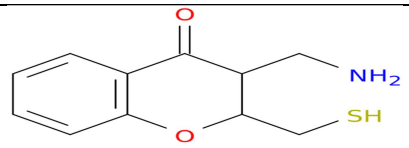	C1=CC=CC2=C1OC(C(CN)C2=O)CS
15.	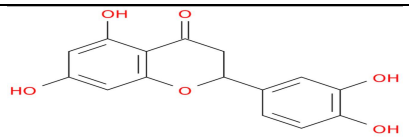	C1=C(C=C(C2=C1OC(CC2=O)C3=CC(=C(C=C3)O)O)O)O
16.	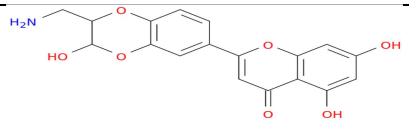	C1=C(C=C(C2=C1OC(=CC2=O)C3=CC4=C(C=C3)OC(C(O4)O)CN)O)O
17.	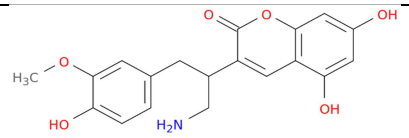	C1=C(C=C(C2=C1OC(C(=C2)C(CC3=CC=C(C(=C3)OC)O)CN)=O)O)O
18.	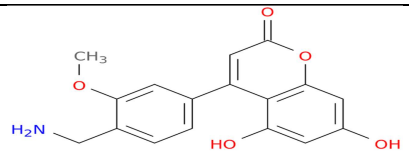	C1=C(C=C(C2=C1OC(C=C2C3=CC=C(C(=C3)OC)CN)=O)O)O
19.	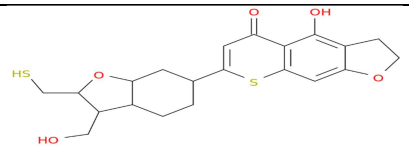	C1=C5C(=C(C2=C1SC(=CC2=O)C3CCC4C(C3)OC(C4CO)CS)O)CCO5
20.	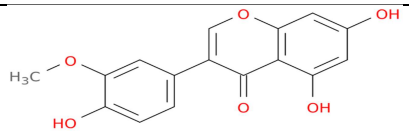	C1=C(C=C(C3=C1OC=C(C2=CC=C(C(=C2)OC)O)C3=O)O)O
21.	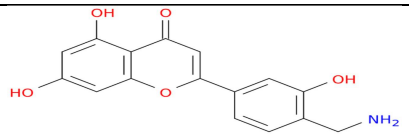	C1=C(C=C(C2=C1OC(=CC2=O)C3=CC(=C(C=C3)CN)O)O)O

22.	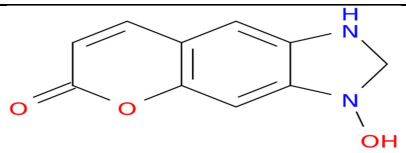	C1=C3C(=CC2=C1OC(C=C2)=O)NCN3O
23.	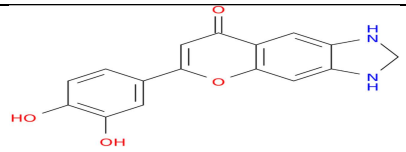	C1=C4C(=CC2=C1OC(=CC2=O)C3=CC(=C(C=C3)O)O)NCN4
24.	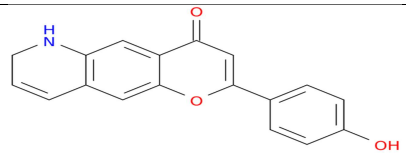	C1=CCNC2=C1C=C4C(=C2)C(C=C(C3=CC=C(C=C3)O)O4)=O
25.	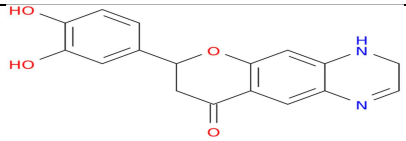	C1=C4C(=CC2=C1OC(CC2=O)C3=CC(=C(C=C3)O)O)N=CCN4
26.	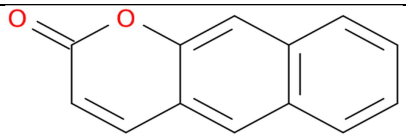	C1=CC=CC2=C1C=C3C(=C2)C=CC(O3)=O
27.	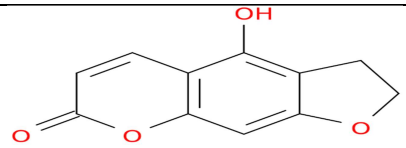	C1=C3C(=C(C2=C1OC(C=C2)=O)O)CCO3
28.	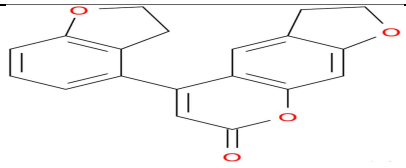	C1=C5C(=CC2=C1OC(C=C2C3=CC=CC4=C3CCO4)=O)CCO5
29.	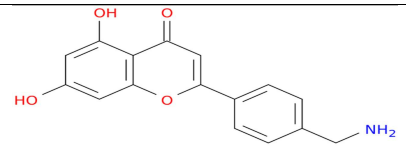	C1=C(C=C(C2=C1OC(=CC2=O)C3=CC=C(C=C3)CN)O)O
30.	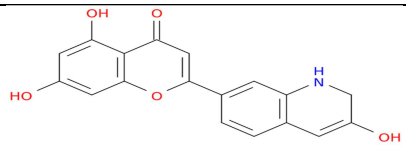	C1=C(C=C(C2=C1OC(=CC2=O)C3=CC4=C(C=C3)C=C(CN4)O)O)O
31.	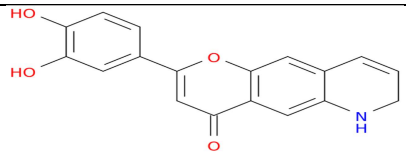	C1=C4C(=CC2=C1OC(=CC2=O)C3=CC(=C(C=C3)O)O)NCC=C4
32.	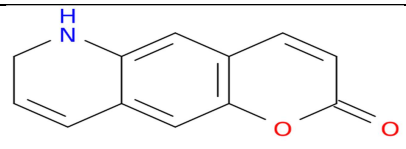	C1=C3C(=CC2=C1OC(C=C2)=O)NCC=C3

33.	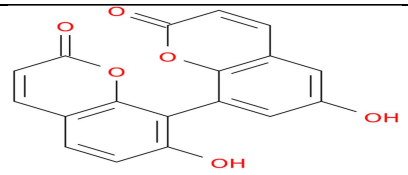	C1=C(C=C(C2=C1C=CC(=O)O2)C3=C(C=CC4=C3OC(C=C4)=O)O)O
34.	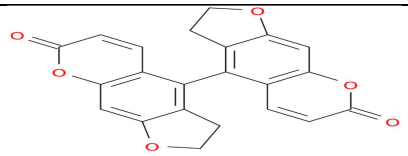	C1=C6C(=C(C2=C1OC(C=C2)=O)C3=C5C(=CC4=C3C=CC(O4)=O)OCC5)CCO6
35.	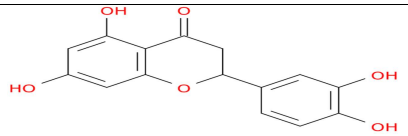	C1=C(C=C(C2=C1OC(CC2=O)C3=CC(=C(C=C3)O)O)O)O
36.	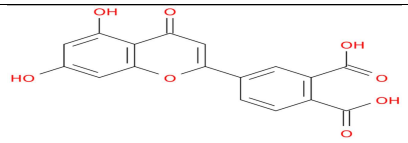	C1=C(C=C(C2=C1OC(=CC2=O)C3=CC(=C(C=C3)C(=O)O)C(=O)O)O)O
37.	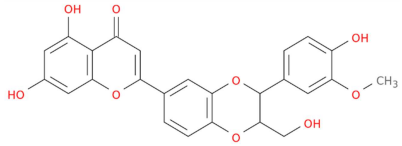	C1=C(C=C(C2=C1OC(=CC2=O)C3=CC5=C(C=C3)OC(C(C4=CC=C(C(=C4)OC)O)O5)CO)O)O
38.	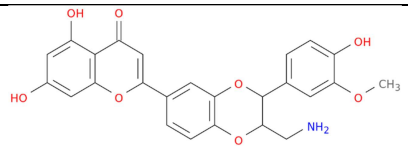	C1=C(C=C(C2=C1OC(=CC2=O)C3=CC5=C(C=C3)OC(C(C4=CC=C(C(=C4)OC)O)O5)CN)O)O
39.	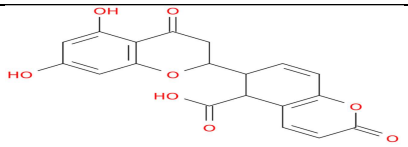	C1=C(C=C(C2=C1OC(CC2=O)C3C=CC4=C(C3C(O)=O)C=CC(O4)=O)O)O
40.	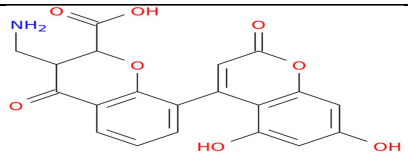	C1=C(C=C(C2=C1OC(C=C2C3=CC=CC4=C3OC(C(O)=O)C(C4=O)CN)=O)O)O
41.	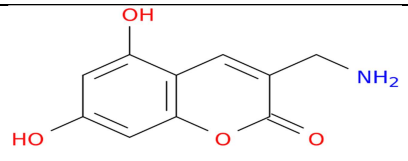	C1=C(C=C(C2=C1OC(C(=C2)CN)=O)O)O

Table.3.(A): Design of 41 Novel Molecules: Leveraging Hydnocarpin, Flavonolignans, and Coumarin as Building Blocks — SMILES Files and Structural Details.

S. No	Receptors& Ligand	Receptors Ligand Interaction (Ligplot+)	Binding Energy(Kcal/mol)
1.	1RO5 & 8	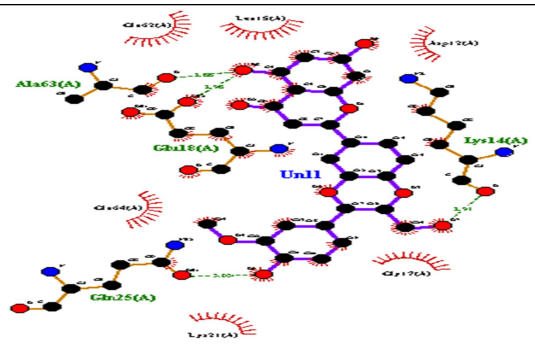	-7.702 (Kcal/mol)
2.	2Q0I & 10	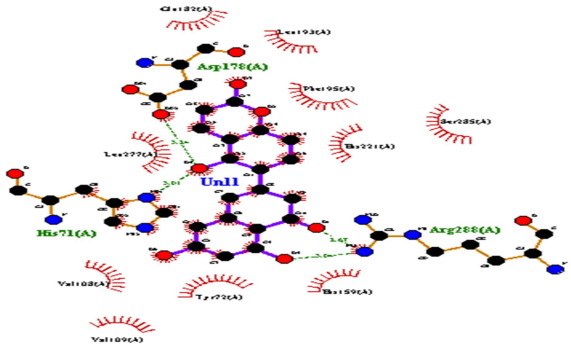	-10.859 (Kcal/mol)
3.	3H77 & 32	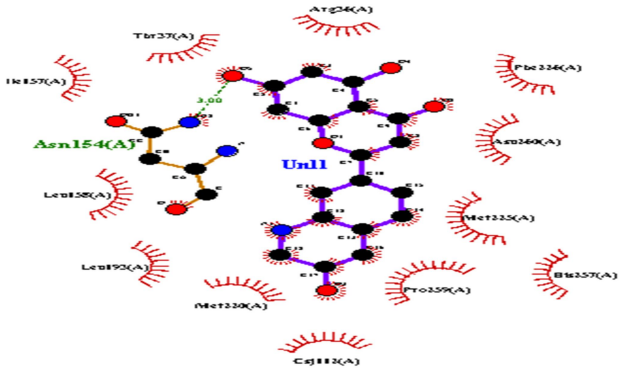	-9.491 (Kcal/mol)
4.	4ng2 &32	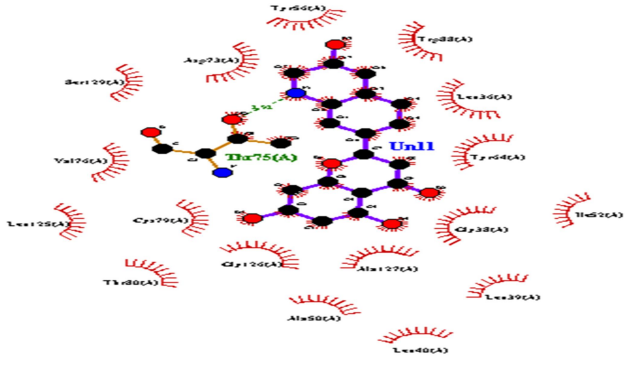	-11.743 (Kcal/mol)

5.	5OE3 & 5	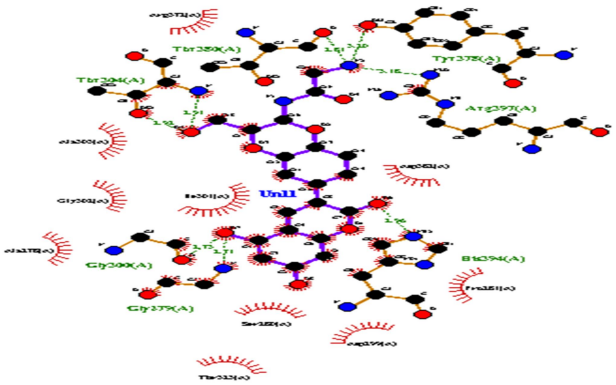	-9.824 (Kcal/mol)
6.	6CC0 & 33	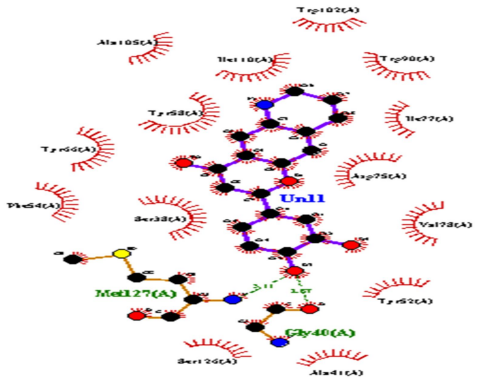	-9.67 (Kcal/mol)
7.	7QA0 & 40	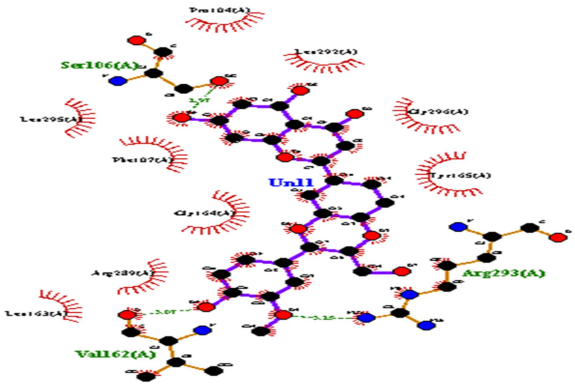	-9.346 (Kcal/mol)
8.	7r3j & 28	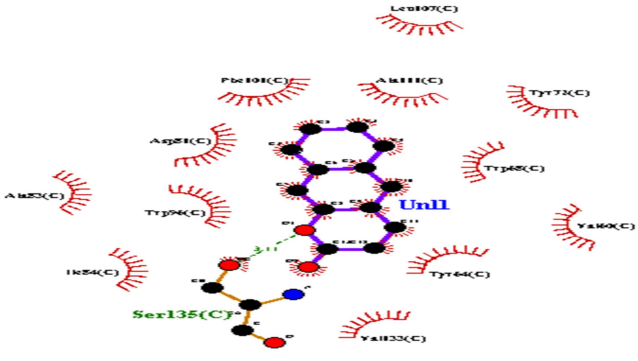	-9.662 (Kcal/mol)

9.	7R9X & 6	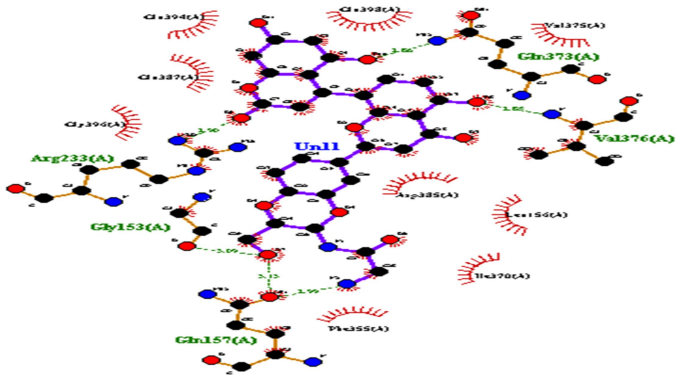	-10.381 (Kcal/mol)
10.	7x17 & 6	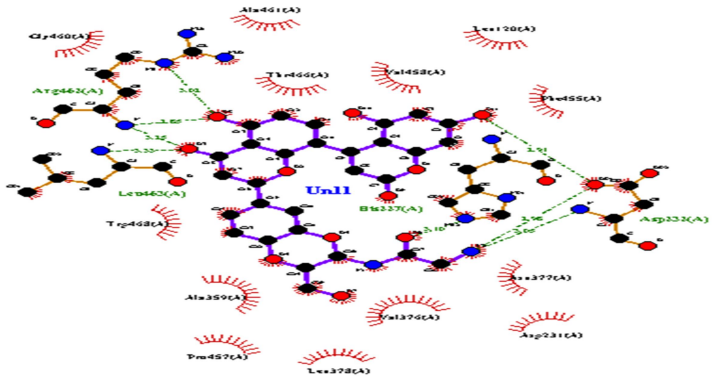	-10.57 (Kcal/mol)
11.	Q02N79 & 8	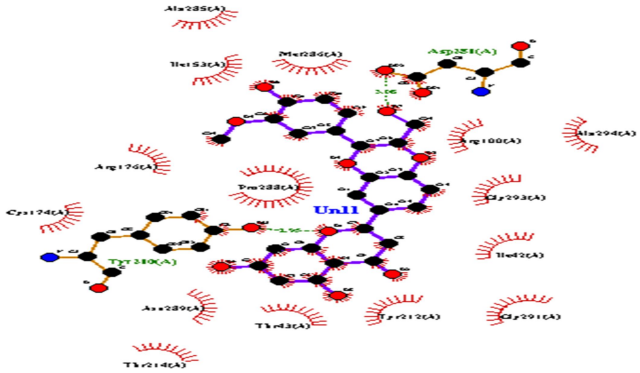	-10.2 (Kcal/mol)

Table.3.(B): Quantifying Inhibitory Potency: Top Molecules with Peak Binding Energy and Detailed Receptor-Ligand Interactions Across All 11 Receptors, Visualized Using LigPlot.

1. 1RO5

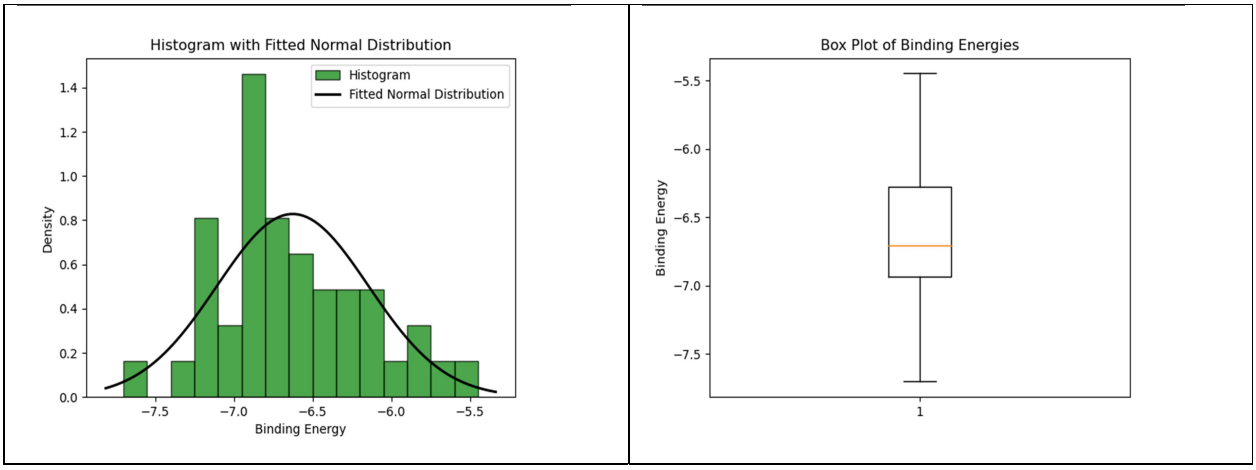

Figure.5.1.1: Statistical Insights into Novel Quorum Sensing Inhibitors — (a) Histogram with Fitted Normal Distribution Density Plot and (b) Box Plot of Binding Energies for 41 Molecules Designed with Flavonolignans, Hydnocarpin, and Coumarin Building Blocks.

Ligands Name	Binding Energies (Kcal/mol)
itatGU_8	- 7.702
WkWiws_33	-7.361
qEWdZ2_24	-7.219
hj06k4_32	-7.178
0uP1Ww_26	-7.157
nvDPzM_40	-7.14
Zhq913_41	-7.105
pNwq3c_10	-7.029
LgSS5g_17	-6.998
asmIyX_27	-6.938

Table.3.1.1: Pinnacle of Potency — Top 40 Molecules Showcasing Highest Binding Energies among 41 Novel Compounds Engineered with Flavonolignans, Hydnocarpin, and Coumarin as Fundamental Building Blocks.

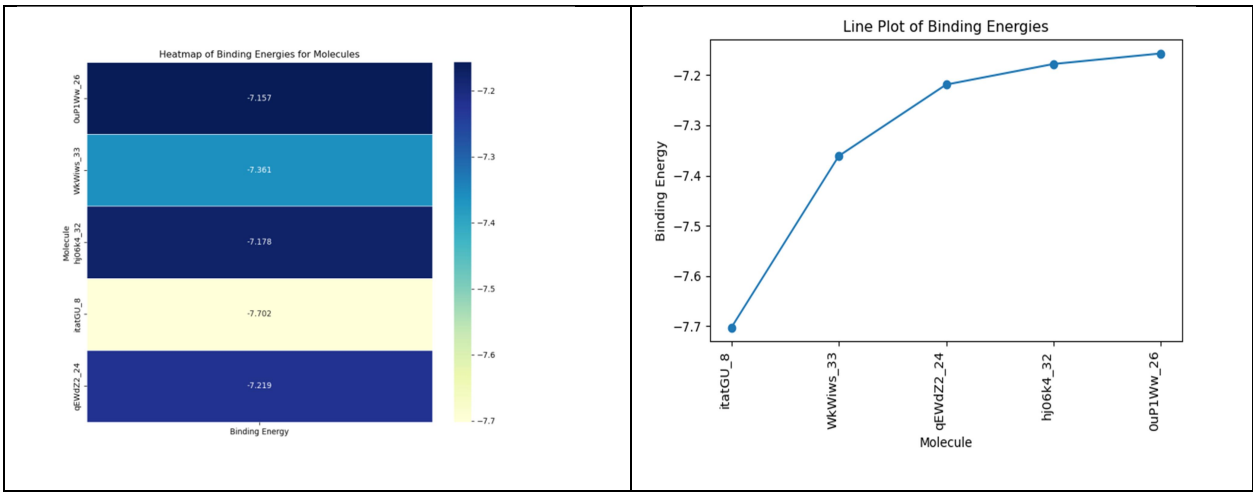

Figure.5.1.2: Insightful Visualization — (a) Heatmap and (b) Line Plot Illustrating the Binding Energies of the Top 40 Molecules among a Set of 41 Novel Compounds Crafted with Flavonolignans, Hydnocarpin, and Coumarin as Fundamental Building Blocks.

2. 2Q0I

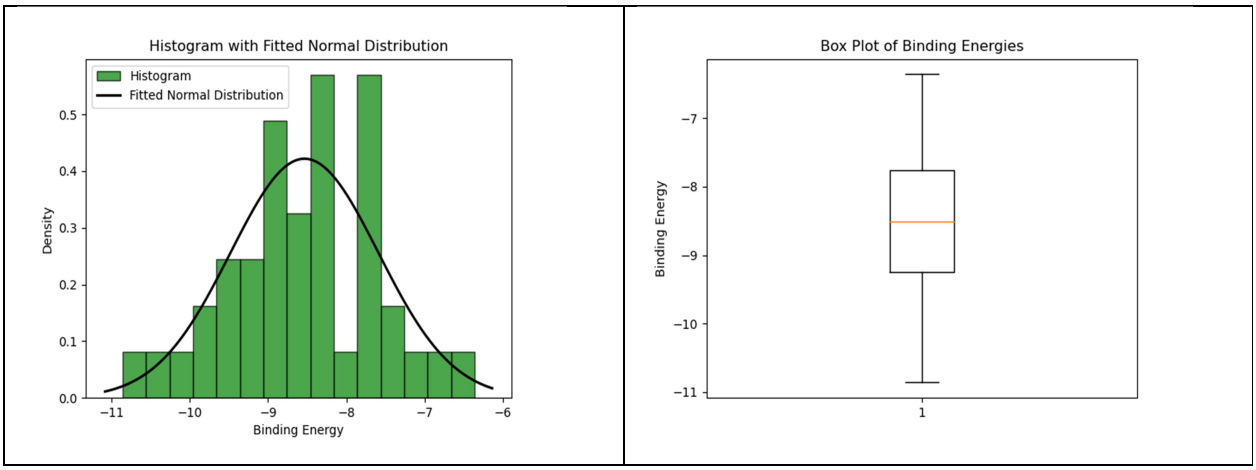

Figure.5.2.1: Statistical Insights into Novel Quorum Sensing Inhibitors — (a) Histogram with Fitted Normal Distribution Density Plot and (b) Box Plot of Binding Energies for 41 Molecules Designed with Flavonolignans, Hydnocarpin, and Coumarin Building Blocks.

Ligands Name	Binding Energies (Kcal/mol)
pNwq3c_10	-10.859
WkWiws_33	-10.264
0uP1Ww_26	-10.239
hj06k4_32	-9.806

ACPsBE_5	-9.754
nvDPzM_40	-9.476
IwWypR_28	-9.397
FS4Kx3_2	-9.382
qEWdZ2_24	-9.343
Zhq913_41	-9.296

Table.3.2.1: Pinnacle of Potency — Top 40 Molecules Showcasing Highest Binding Energies among 41 Novel Compounds Engineered with Flavonolignans, Hydnocarpin, and Coumarin as Fundamental Building Blocks.

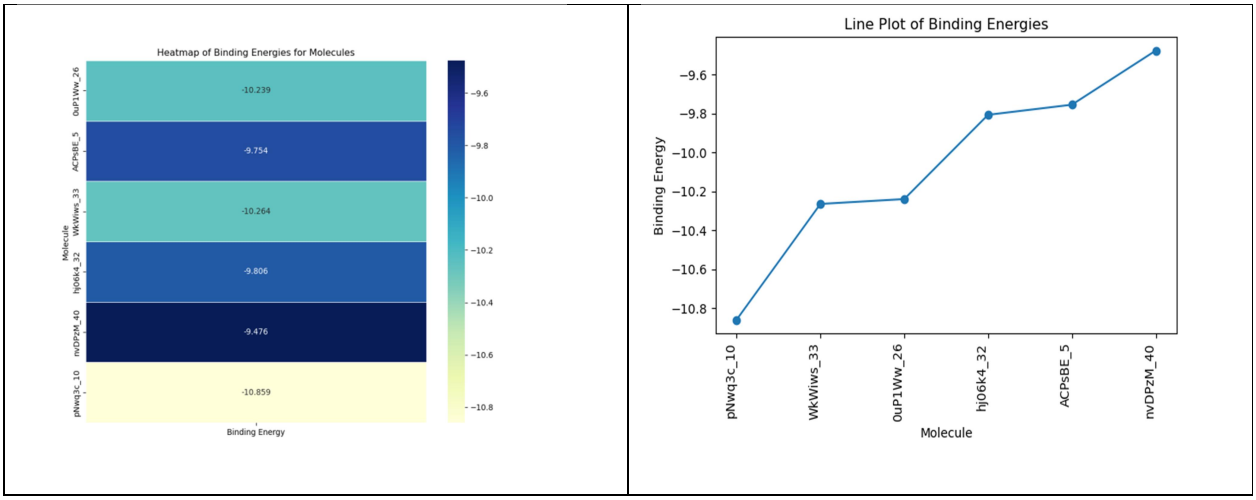

Figure.5.2.2: Insightful Visualization — (a) Heatmap and (b) Line Plot Illustrating the Binding Energies of the Top 40 Molecules among a Set of 41 Novel Compounds Crafted with Flavonolignans, Hydnocarpin, and Coumarin as Fundamental Building Blocks.

3. 3H77

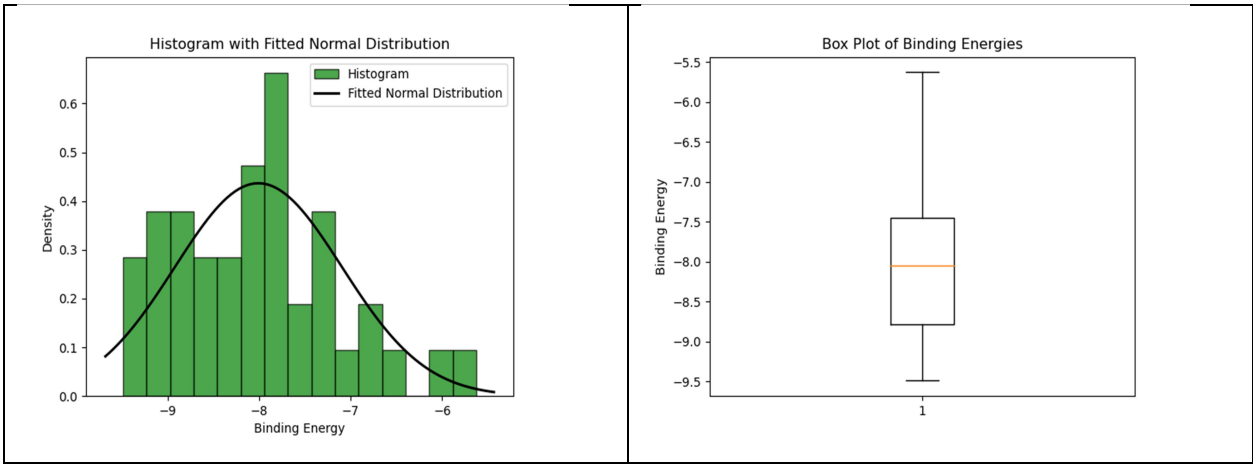

Figure.5.3.1: Statistical Insights into Novel Quorum Sensing Inhibitors — (a) Histogram with Fitted Normal Distribution Density Plot and (b) Box Plot of Binding Energies for 41 Molecules Designed with Flavonolignans, Hydnocarpin, and Coumarin Building Blocks.

Ligands Name	Binding Energies (Kcal/mol)
pNwq3c_10	-9.328
hj06k4_32	-9.491
nvDPzM_40	-9.428
eHlV2f_30	-9.165
WkWiws_33	-9.152
0uP1Ww_26	-9.114
LgSS5g_17	-9.02
qEWdZ2_24	-8.948
FS4Kx3_2	-8.912
zxfWXn_7	-8.818

Table.3.3.1: Pinnacle of Potency — Top 40 Molecules Showcasing Highest Binding Energies among 41 Novel Compounds Engineered with Flavonolignans, Hydnocarpin, and Coumarin as Fundamental Building Blocks.

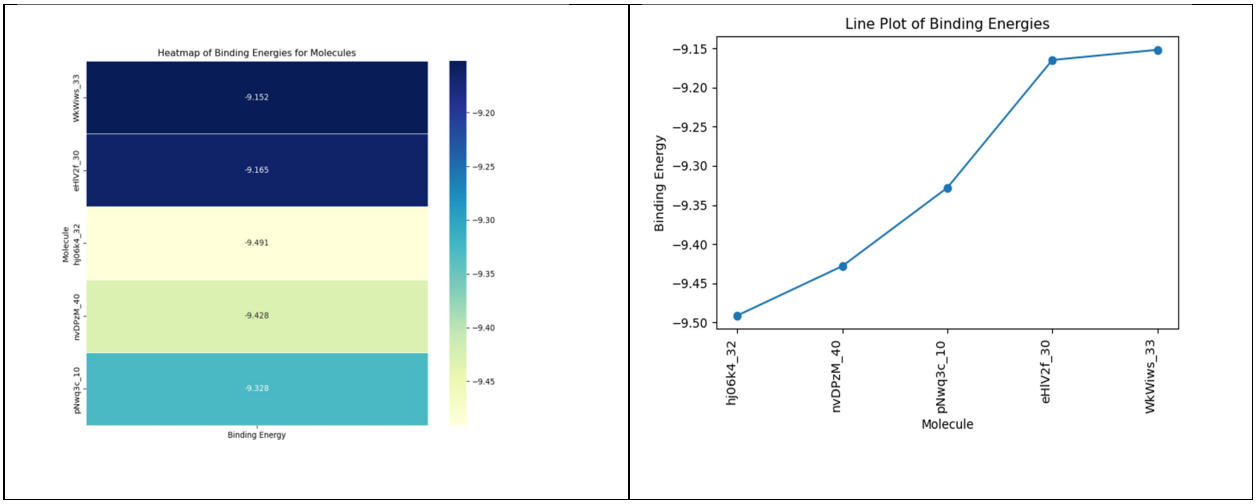

Figure.5.3.2: Insightful Visualization — (a) Heatmap and (b) Line Plot Illustrating the Binding Energies of the Top 40 Molecules among a Set of 41 Novel Compounds Crafted with Flavonolignans, Hydnocarpin, and Coumarin as Fundamental Building Blocks.

4. 4NG2

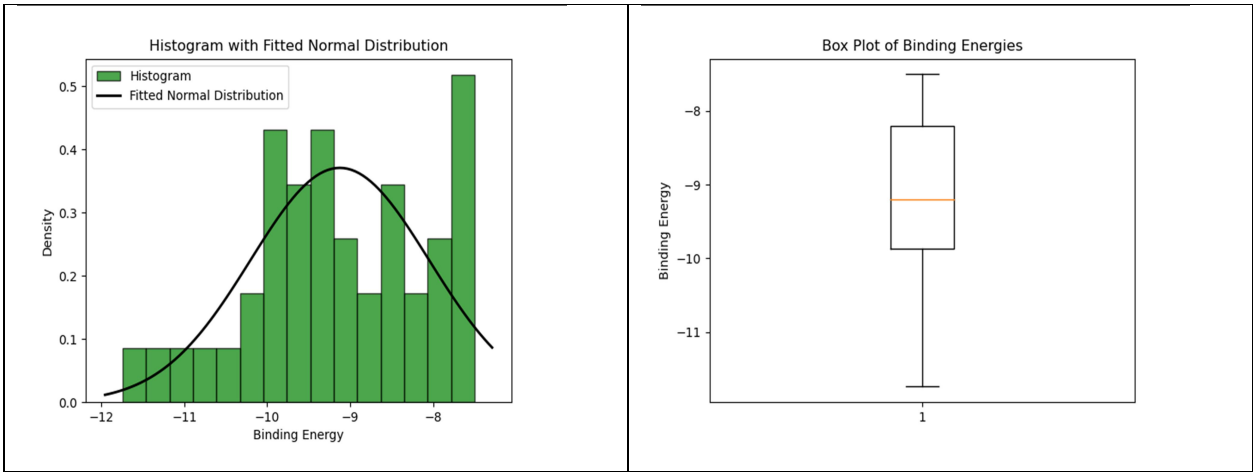

Figure.5.4.1: Statistical Insights into Novel Quorum Sensing Inhibitors — (a) Histogram with Fitted Normal Distribution Density Plot and (b) Box Plot of Binding Energies for 41 Molecules Designed with Flavonolignans, Hydnocarpin, and Coumarin Building Blocks

Ligands Name	Binding Energies (Kcal/mol)
hj06k4_32	-11.743
qEWdZ2_24	-11.209
0uP1Ww_26	-11.094
WkWiws_33	-10.631
zxfWXn_7	-10.433
6v93Ak_18	-10.196
vdx6SF_22	-10.154
fXdld0_38	-10.045
btPB1h_9	-9.982
eHlV2f_30	-9.917

Table.3.4.1: Pinnacle of Potency — Top 40 Molecules Showcasing Highest Binding Energies among 41 Novel Compounds Engineered with Flavonolignans, Hydnocarpin, and Coumarin as Fundamental Building Blocks.

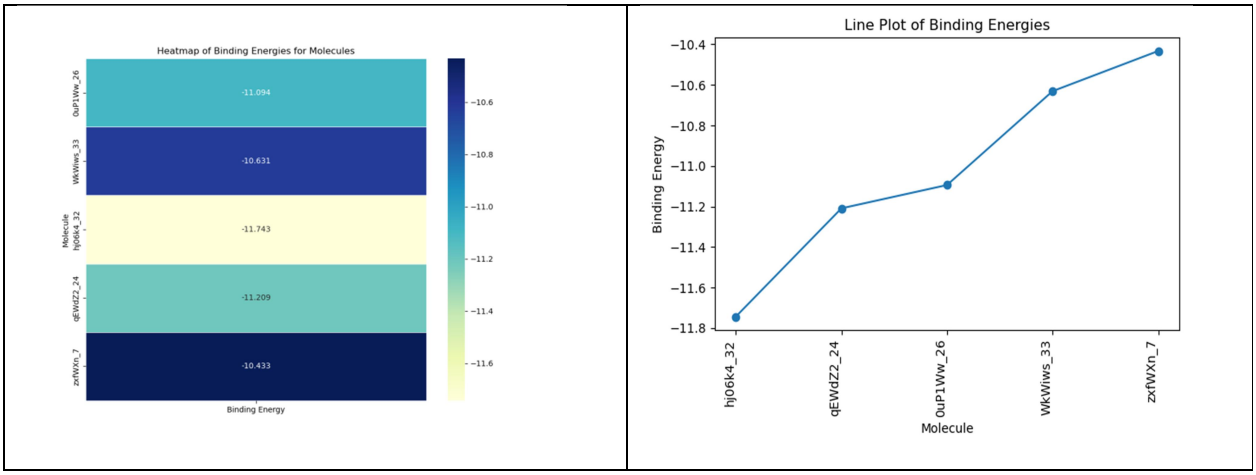

Figure.5.4.2: Insightful Visualization — (a) Heatmap and (b) Line Plot Illustrating the Binding Energies of the Top 40 Molecules among a Set of 41 Novel Compounds Crafted with Flavonolignans, Hydnocarpin, and Coumarin as Fundamental Building Blocks

5. 5OE3

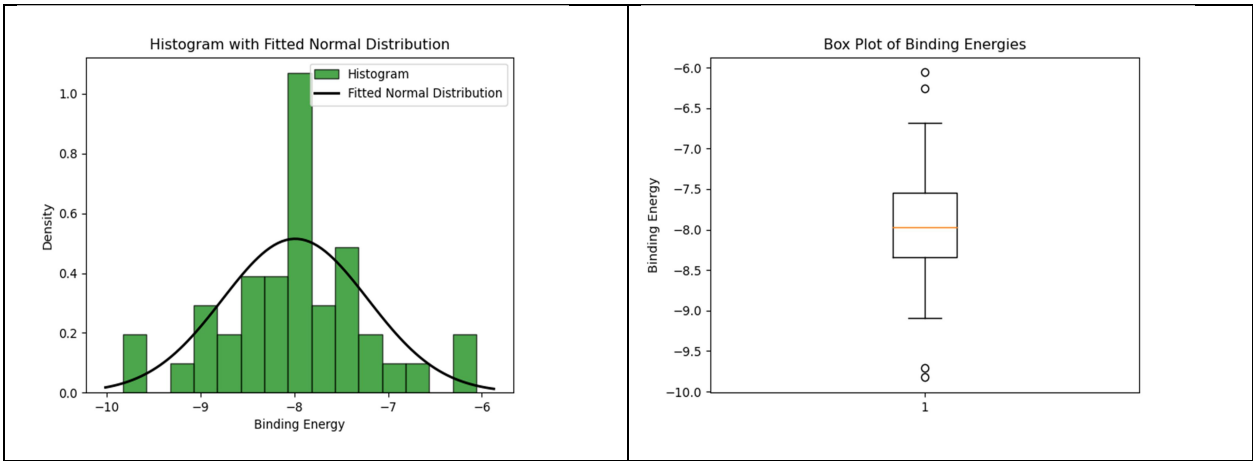

Figure.5.5.1: Statistical Insights into Novel Quorum Sensing Inhibitors — (a) Histogram with Fitted Normal Distribution Density Plot and (b) Box Plot of Binding Energies for 41 Molecules Designed with Flavonolignans, Hydnocarpin, and Coumarin Building Blocks.

Ligands Name	Binding Energies (Kcal/mol)
ACPsBE_5	-9.824
K8mQm6_6	-9.705
zW12h9_11	-9.091
tBWQv5_4	-9.039
pNwq3c_10	-8.961

WkWiws_33	-8.909
asmIyX_27	-8.675
hj06k4_32	-8.582
kjDXIC_19	-8.565
kWYzEw_36	-8.366

Table.3.5.1: Pinnacle of Potency — Top 40 Molecules Showcasing Highest Binding Energies among 41 Novel Compounds Engineered with Flavonolignans, Hydnocarpin, and Coumarin as Fundamental Building Blocks.

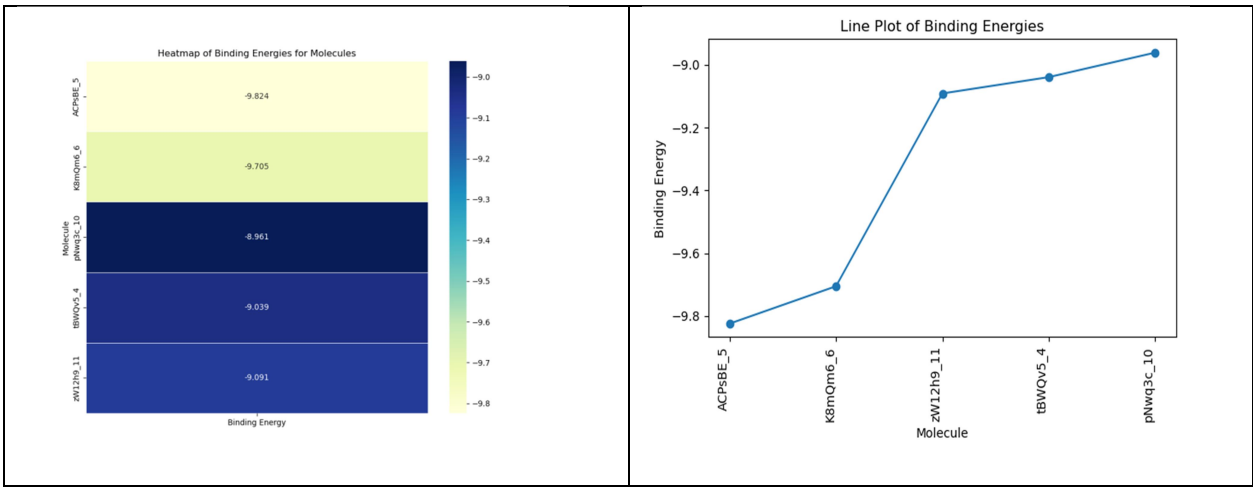

Figure.5.5.2: Insightful Visualization — (a) Heatmap and (b) Line Plot Illustrating the Binding Energies of the Top 40 Molecules among a Set of 41 Novel Compounds Crafted with Flavonolignans, Hydnocarpin, and Coumarin as Fundamental Building Blocks.

6. 6CC0

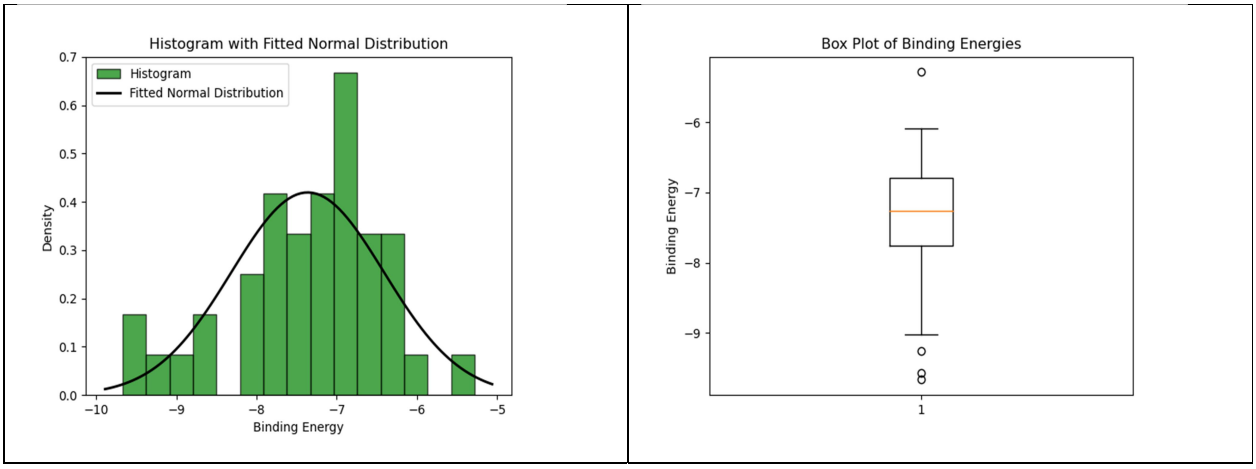

Figure.5.6.1: Statistical Insights into Novel Quorum Sensing Inhibitors — (a) Histogram with Fitted Normal Distribution Density Plot and (b) Box Plot of Binding Energies for 41 Molecules Designed with Flavonolignans, Hydnocarpin, and Coumarin Building Blocks.

Ligands Name	Binding Energies (Kcal/mol)
WkWiws_33	-9.67
6v93Ak_18	-9.577
IwWypR_28	-9.255
zxfWXn_7	-9.024
qEWdZ2_24	-8.693
eicPcb_34	-8.565
hVjcNi_23	-8.189
h43Ld7_1	-8.127
LMukwA_21	-8.032
nvDPzM_40	-7.775

Table.3.6.1: Pinnacle of Potency — Top 40 Molecules Showcasing Highest Binding Energies among 41 Novel Compounds Engineered with Flavonolignans, Hydnocarpin, and Coumarin as Fundamental Building Blocks.

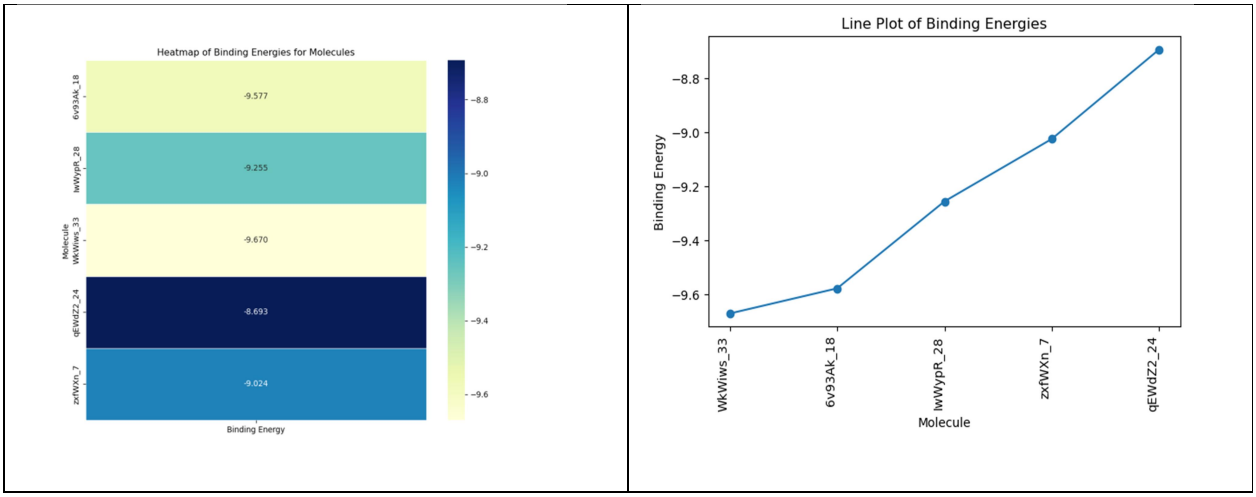

Figure.5.6.2: Insightful Visualization — (a) Heatmap and (b) Line Plot Illustrating the Binding Energies of the Top 40 Molecules among a Set of 41 Novel Compounds Crafted with Flavonolignans, Hydnocarpin, and Coumarin as Fundamental Building Blocks.

7. 7QA0

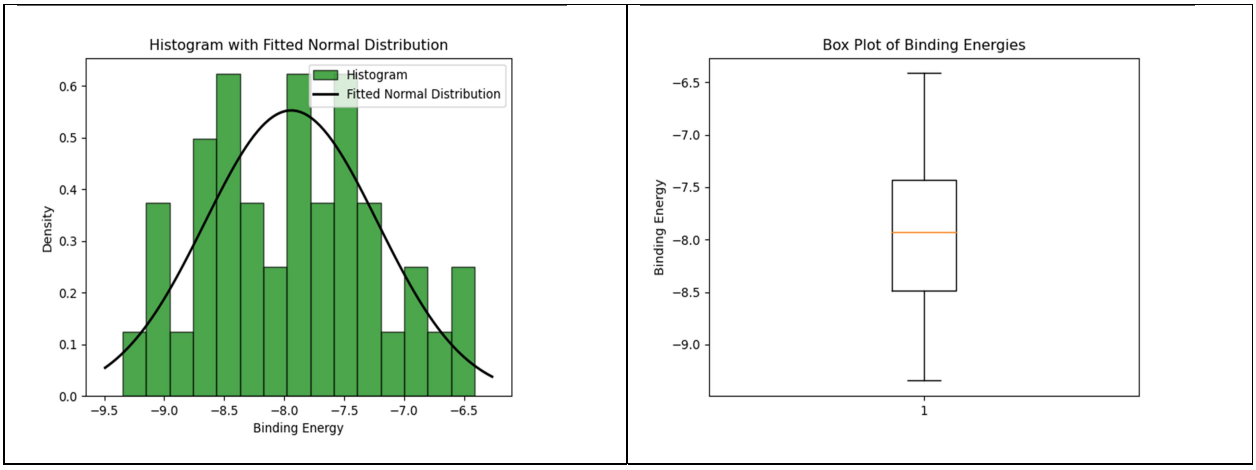

Figure.5.7.1: Statistical Insights into Novel Quorum Sensing Inhibitors — (a) Histogram with Fitted Normal Distribution Density Plot and (b) Box Plot of Binding Energies for 41 Molecules Designed with Flavonolignans, Hydnocarpin, and Coumarin Building Blocks.

Ligands Name	Binding Energies (Kcal/mol)
nvDPzM_40	-9.346
hj06k4_32	-9.098
Zhq913_41	-9.018
WkWiws_33	-8.966
eHlV2f_30	-8.837
0uP1Ww_26	-8.72
gYYRjv_3	-8.686
K8mQm6_6	-8.655
itatGU_8	-8.625
qUMSeM_35	-8.507

Table.3.7.1: Pinnacle of Potency — Top 40 Molecules Showcasing Highest Binding Energies among 41 Novel Compounds Engineered with Flavonolignans, Hydnocarpin, and Coumarin as Fundamental Building Blocks.

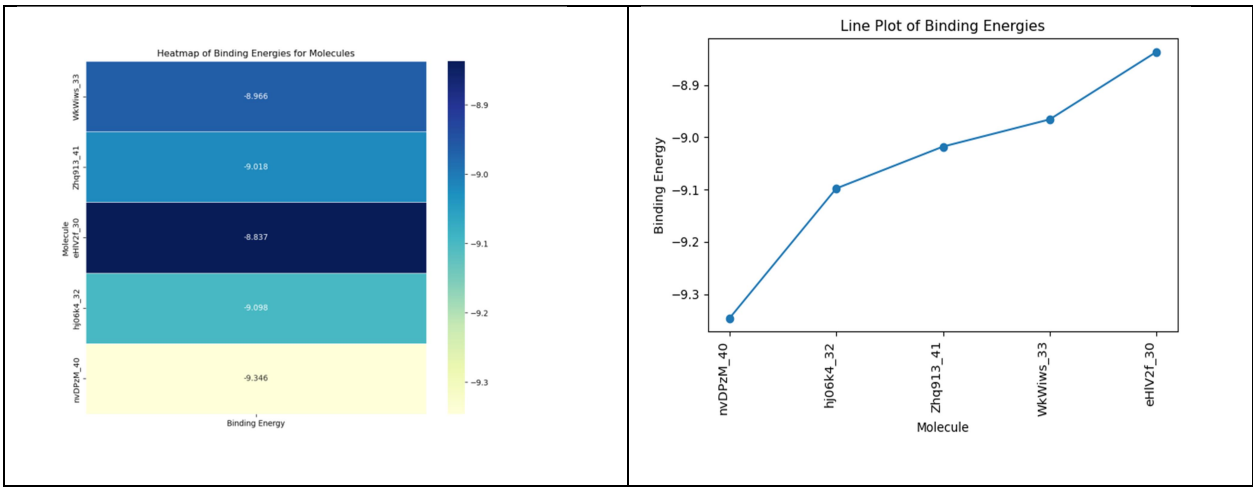

Figure.5.7.2: Insightful Visualization — (a) Heatmap and (b) Line Plot Illustrating the Binding Energies of the Top 40 Molecules among a Set of 41 Novel Compounds Crafted with Flavonolignans, Hydnocarpin, and Coumarin as Fundamental Building Blocks.

8. 7R3J

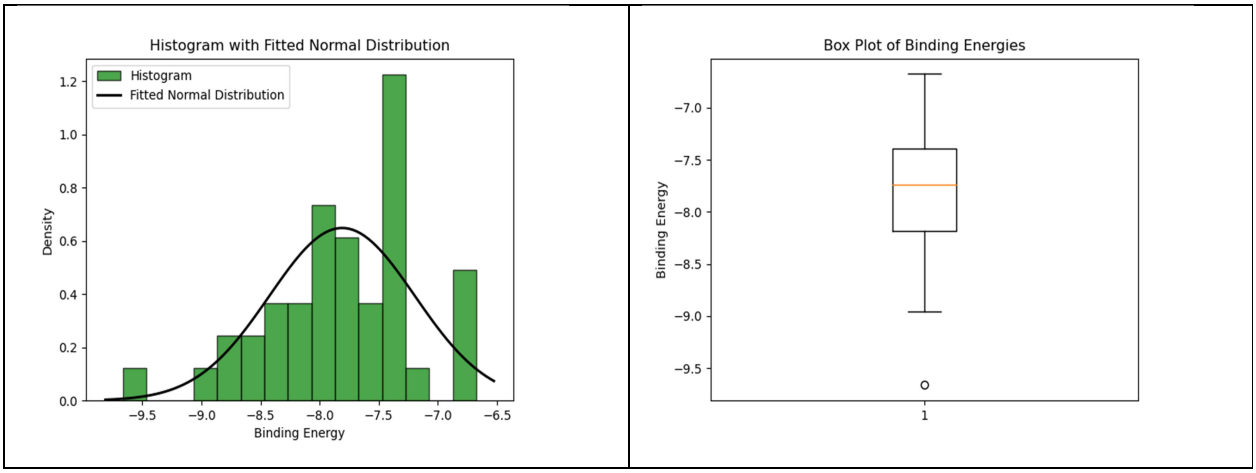

Figure.5.8.1: Statistical Insights into Novel Quorum Sensing Inhibitors — (a) Histogram with Fitted Normal Distribution Density Plot and (b) Box Plot of Binding Energies for 41 Molecules Designed with Flavonolignans, Hydnocarpin, and Coumarin Building Blocks.

Ligands Name	Binding Energies (Kcal/mol)
IwWypR_28	-9.662
kWYzEw_36	-8.952
eicPcb_34	-8.754
LgSS5g_17	-8.676

itatGU_8	-8.618
hg3zym_29	-8.5
K8mQm6_6	-8.339
FS4Kx3_2	-8.326
KRIoAO_44	-8.308
eHlV2f_30	-8.226

Table.3.8.1: Pinnacle of Potency — Top 40 Molecules Showcasing Highest Binding Energies among 41 Novel Compounds Engineered with Flavonolignans, Hydnocarpin, and Coumarin as Fundamental Building Blocks.

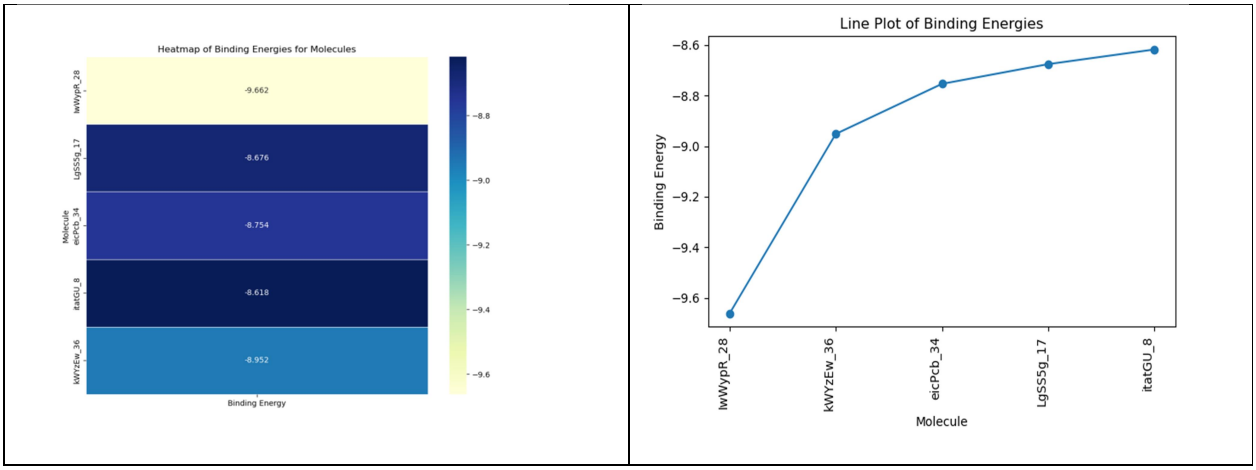

Figure 5.8.2: Insightful Visualization — (a) Heatmap and (b) Line Plot Illustrating the Binding Energies of the Top 40 Molecules among a Set of 41 Novel Compounds Crafted with Flavonolignans, Hydnocarpin, and Coumarin as Fundamental Building Blocks.

9. 7R9X

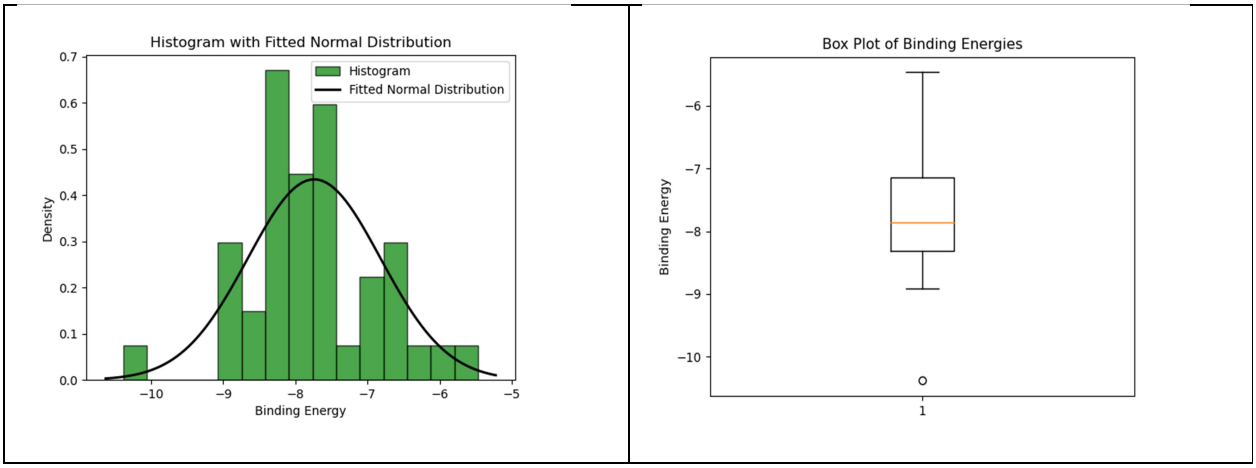

Figure.5.9.1: Statistical Insights into Novel Quorum Sensing Inhibitors — (a) Histogram with Fitted Normal Distribution Density Plot and (b) Box Plot of Binding Energies for 41 Molecules Designed with Flavonolignans, Hydnocarpin, and Coumarin Building Blocks.

Ligands Name	Binding Energies (Kcal/mol)
K8mQm6_6	-10.381
itatGU_8	-8.911
gYYRjv_3	-8.838
pNwq3c_10	-8.828
kWYzEw_36	-8.811
nvDPzM_40	-8.728
Zhq913_41	-8.571
LgSS5g_17	-8.415
eHlV2f_30	-8.348
6v93Ak_18	-8.338

Table.3.9.1: Pinnacle of Potency — Top 40 Molecules Showcasing Highest Binding Energies among 41 Novel Compounds Engineered with Flavonolignans, Hydnocarpin, and Coumarin as Fundamental Building Blocks.

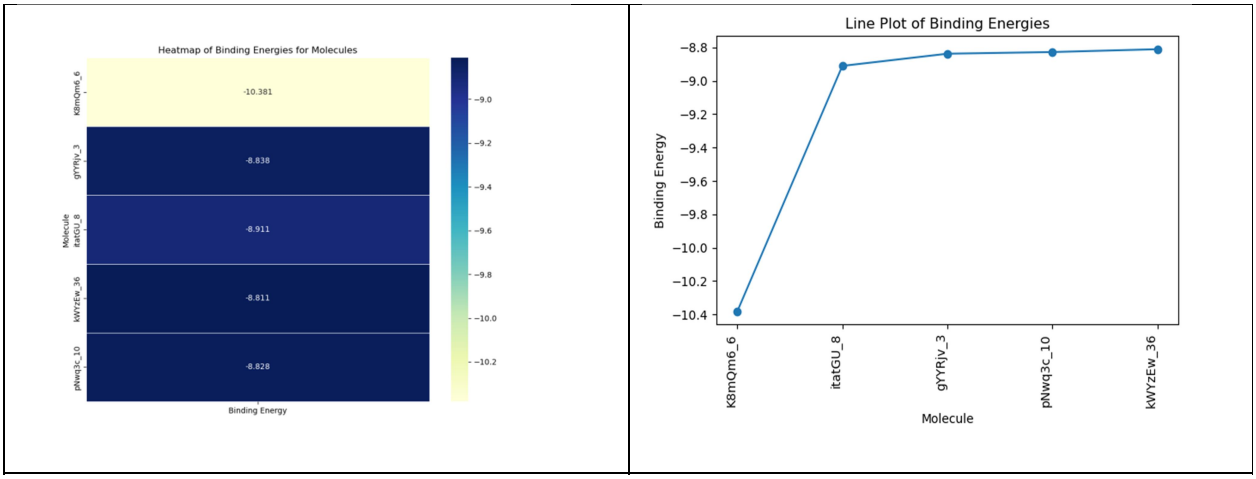

Figure.5.9.2: Insightful Visualization — (a) Heatmap and (b) Line Plot Illustrating the Binding Energies of the Top 40 Molecules among a Set of 41 Novel Compounds Crafted with Flavonolignans, Hydnocarpin, and Coumarin as Fundamental Building Blocks.

10.7X17

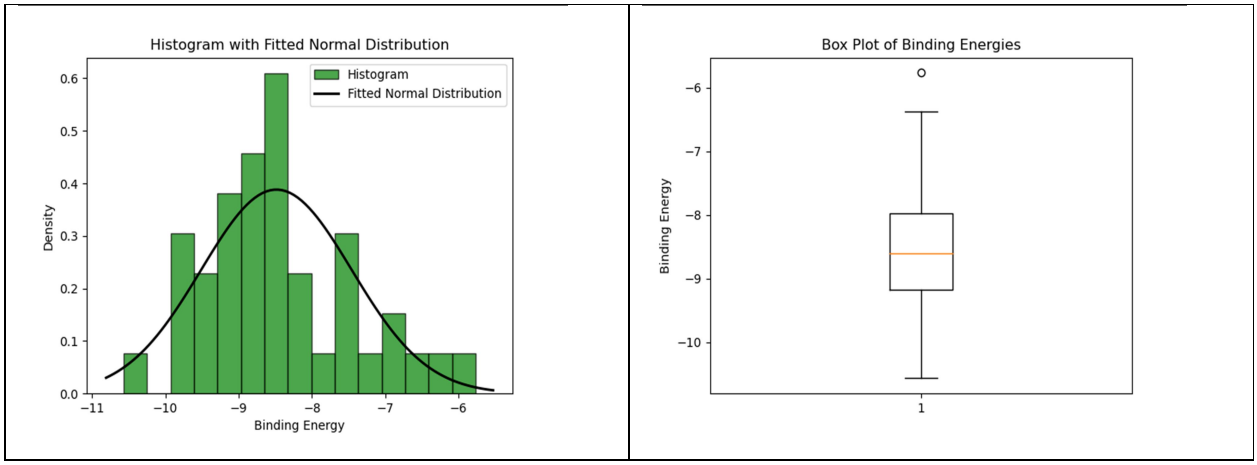

Figure 5.10.1: Statistical Insights into Novel Quorum Sensing Inhibitors — (a) Histogram with Fitted Normal Distribution Density Plot and (b) Box Plot of Binding Energies for 41 Molecules Designed with Flavonolignans, Hydnocarpin, and Coumarin Building Blocks.

Ligands Name	Binding Energies (Kcal/mol)
K8mQm6_6	-10.57
gYYRjv_3	-9.928
Zhq913_41	-9.866
ACPsBE_5	-9.827
nvDPzM_40	-9.664
itatGU_8	-9.603
kWYzEw_36	-9.511
0uP1Ww_26	-9.352
pNwq3c_10	-9.272
WkWiws_33	-9.241

Table.3.10.1: Pinnacle of Potency — Top 40 Molecules Showcasing Highest Binding Energies among 41 Novel Compounds Engineered with Flavonolignans, Hydnocarpin, and Coumarin as Fundamental Building Blocks.

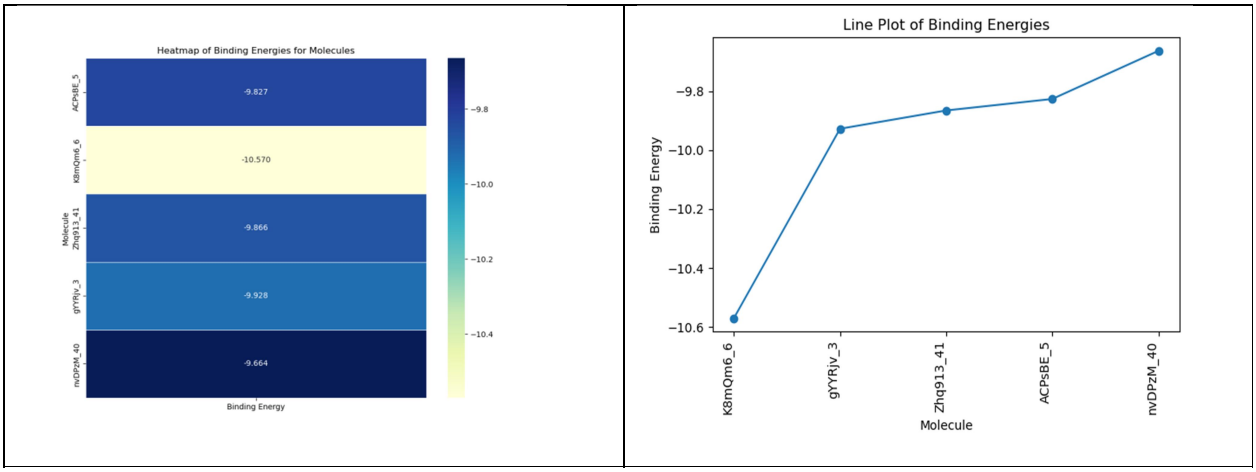

Figure 5.10.2: Insightful Visualization — (a) Heatmap and (b) Line Plot Illustrating the Binding Energies of the Top 40 Molecules among a Set of 41 Novel Compounds Crafted with Flavonolignans, Hydnocarpin, and Coumarin as Fundamental Building Blocks.

11.Q02N79

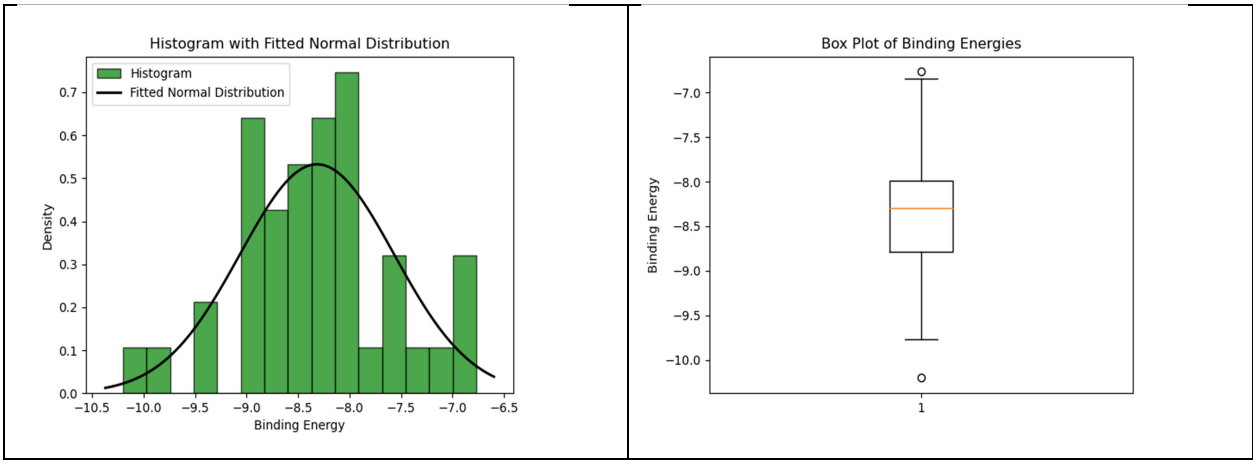

Figure 5.11.1: Statistical Insights into Novel Quorum Sensing Inhibitors — (a) Histogram with Fitted Normal Distribution Density Plot and (b) Box Plot of Binding Energies for 41 Molecules Designed with Flavonolignans, Hydnocarpin, and Coumarin Building Blocks.

Ligands Name	Binding Energies (Kcal/mol)
itatGU_8	-10.2
KRIoAO_44	-9.764
eHlV2f_30	-9.314
qUMSeM_35	-9.288
kWYzEw_36	-9.053

nvDPzM_40	-9.051
K8mQm6_6	-8.999
Zhq913_41	-8.944
pNwq3c_10	-8.93
asmIyX_27	-8.92

Table 5.11.1: Pinnacle of Potency — Top 40 Molecules Showcasing Highest Binding Energies among 41 Novel Compounds Engineered with Flavonolignans, Hydnocarpin, and Coumarin as Fundamental Building Blocks.

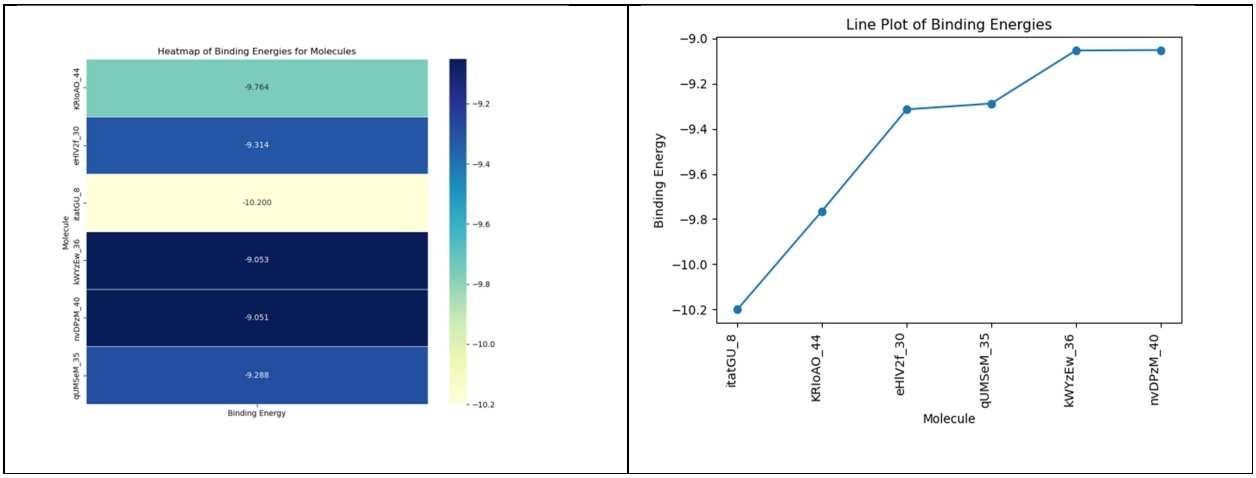

Figure.5.11.2: Insightful Visualization — (a) Heatmap and (b) Line Plot Illustrating the Binding Energies of the Top 40 Molecules among a Set of 41 Novel Compounds Crafted with Flavonolignans, Hydnocarpin, and Coumarin as Fundamental Building Blocks.

Receptors	**Ligands**
Common Compounds between Receptor 1 and Receptor 2	['qEWdZ2_24', 'WkWiws_33', '0uP1Ww_26', 'pNwq3c_10', 'Zhq913_41', 'hj06k4_32', 'nvDPzM_40']
Common Compounds between Receptor 1 and Receptor 3	['qEWdZ2_24', 'WkWiws_33', '0uP1Ww_26', 'pNwq3c_10', 'LgSS5g_17', 'hj06k4_32', 'nvDPzM_40']
Common Compounds between Receptor 1 and Receptor 4	['qEWdZ2_24', 'WkWiws_33', 'hj06k4_32', '0uP1Ww_26']
Common Compounds between Receptor 1 and Receptor 5	['WkWiws_33', 'hj06k4_32', 'asmIyX_27', 'pNwq3c_10']
Common Compounds between Receptor 1 and Receptor 6	['qEWdZ2_24', 'WkWiws_33', 'nvDPzM_40']

Common Compounds between Receptor 1 and Receptor 7	['WkWiws_33', '0uP1Ww_26', 'Zhq913_41' , 'itatGU_8', 'hj06k4_32', 'nvDPzM_40']
Common Compounds between Receptor 1 and Receptor 8	['LgSS5g_17', 'itatGU_8']
Common Compounds between Receptor 1 and Receptor 9	['pNwq3c_10', 'LgSS5g_17', 'Zhq913_41', 'i tatGU_8', 'nvDPzM_40']
Common Compounds between Receptor 1 and Receptor 10	['WkWiws_33', '0uP1Ww_26', 'pNwq3c_10 ', 'Zhq913_41', 'itatGU_8', 'nvDPzM_40']
Common Compounds between Receptor 1 and Receptor 11	['pNwq3c_10', 'Zhq913_41', 'itatGU_8', 'as mIyX_27', 'nvDPzM_40']
Common Compounds between Receptor 2 and Receptor 3	['qEWdZ2_24', 'WkWiws_33', '0uP1Ww_2 6', 'pNwq3c_10', 'FS4Kx3_2', 'hj06k4_32', ' nvDPzM_40']
Common Compounds between Receptor 2 and Receptor 4	['qEWdZ2_24', 'WkWiws_33', 'hj06k4_32', '0uP1Ww_26']
Common Compounds between Receptor 2 and Receptor 5	['WkWiws_33', 'hj06k4_32', 'ACPsBE_5', ' pNwq3c_10']
Common Compounds between Receptor 2 and Receptor 6	['IwWypR_28', 'qEWdZ2_24', 'WkWiws_3 3', 'nvDPzM_40']
Common Compounds between Receptor 2 and Receptor 7	['WkWiws_33', '0uP1Ww_26', 'Zhq913_41' , 'hj06k4_32', 'nvDPzM_40']
Common Compounds between Receptor 2 and Receptor 8	['IwWypR_28', 'FS4Kx3_2']
Common Compounds between Receptor 2 and Receptor 9	['nvDPzM_40', 'Zhq913_41', 'pNwq3c_10']
Common Compounds between Receptor 2 and Receptor 10	['WkWiws_33', '0uP1Ww_26', 'pNwq3c_10 ', 'ACPsBE_5', 'Zhq913_41', 'nvDPzM_40']
Common Compounds between Receptor 2 and Receptor 11	['nvDPzM_40', 'Zhq913_41', 'pNwq3c_10']
Common Compounds between Receptor 3 and Receptor 4	['qEWdZ2_24', 'WkWiws_33', '0uP1Ww_2 6', 'eHlV2f_30', 'zxfWXn_7', 'hj06k4_32']
Common Compounds between Receptor 3 and Receptor 5	['WkWiws_33', 'hj06k4_32', 'pNwq3c_10']
Common Compounds between Receptor 3 and Receptor 6	['qEWdZ2_24', 'WkWiws_33', 'zxfWXn_7', 'nvDPzM_40']
Common Compounds between Receptor 3 and Receptor 7	['WkWiws_33', '0uP1Ww_26', 'eHlV2f_30', 'hj06k4_32', 'nvDPzM_40']
Common Compounds between Receptor 3 and Receptor 8	['LgSS5g_17', 'eHlV2f_30', 'FS4Kx3_2']
Common Compounds between Receptor 3 and Receptor 9	['LgSS5g_17', 'eHlV2f_30', 'nvDPzM_40', ' pNwq3c_10']
Common Compounds between Receptor 3 and Receptor 10	['WkWiws_33', '0uP1Ww_26', 'nvDPzM_4

	0', 'pNwq3c_10']
Common Compounds between Receptor 3 and Receptor 11	['eHlV2f_30', 'nvDPzM_40', 'pNwq3c_10']
Common Compounds between Receptor 4 and Receptor 5	['WkWiws_33', 'hj06k4_32']
Common Compounds between Receptor 4 and Receptor 6	['qEWdZ2_24', 'WkWiws_33', 'zxfWXn_7', '6v93Ak_18']
Common Compounds between Receptor 4 and Receptor 7	['WkWiws_33', '0uP1Ww_26', 'eHlV2f_30', 'hj06k4_32']
Common Compounds between Receptor 4 and Receptor 8	['eHlV2f_30']
Common Compounds between Receptor 4 and Receptor 9	['eHlV2f_30', '6v93Ak_18']
Common Compounds between Receptor 4 and Receptor 10	['WkWiws_33', '0uP1Ww_26']
Common Compounds between Receptor 4 and Receptor 11	['eHlV2f_30']
Common Compounds between Receptor 5 and Receptor 6	['WkWiws_33']
Common Compounds between Receptor 5 and Receptor 7	['WkWiws_33', 'hj06k4_32', 'K8mQm6_6']
Common Compounds between Receptor 5 and Receptor 8	['K8mQm6_6', 'kWYzEw_36']
Common Compounds between Receptor 5 and Receptor 9	['K8mQm6_6', 'pNwq3c_10', 'kWYzEw_36']
Common Compounds between Receptor 5 and Receptor 10	['WkWiws_33', 'K8mQm6_6', 'pNwq3c_10', 'ACPsBE_5', 'kWYzEw_36']
Common Compounds between Receptor 5 and Receptor 11	['asmIyX_27', 'K8mQm6_6', 'pNwq3c_10', 'kWYzEw_36']
Common Compounds between Receptor 6 and Receptor 7	['WkWiws_33', 'nvDPzM_40']
Common Compounds between Receptor 6 and Receptor 8	['IwWypR_28', 'eicPcb_34']
Common Compounds between Receptor 6 and Receptor 9	['6v93Ak_18', 'nvDPzM_40']
Common Compounds between Receptor 6 and Receptor 10	['WkWiws_33', 'nvDPzM_40']
Common Compounds between Receptor 6 and Receptor 11	['nvDPzM_40']
Common Compounds between Receptor 7 and Receptor 8	['itatGU_8', 'eHlV2f_30', 'K8mQm6_6']
Common Compounds between Receptor 7 and Receptor 9	['eHlV2f_30', 'K8mQm6_6', 'gYYRjv_3', 'Zhq913_41', 'itatGU_8', 'nvDPzM_40']
Common Compounds between Receptor 7 and Receptor 10	['WkWiws_33', '0uP1Ww_26', 'K8mQm6_6', 'gYYRjv_3', 'Zhq913_41', 'itatGU_8', 'nvDPzM_40']
Common Compounds between Receptor 7 and Receptor 11	['eHlV2f_30', 'K8mQm6_6', 'Zhq913_41', 'itatGU_8', 'qUMSeM_35', 'nvDPzM_40']
Common Compounds between Receptor 8 and Receptor 9	['eHlV2f_30', 'K8mQm6_6', 'LgSS5g_17', 'itatGU_8', 'kWYzEw_36']
Common Compounds between Receptor 8 and Receptor 10	['itatGU_8', 'K8mQm6_6', 'kWYzEw_36']

Common Compounds between Receptor 8 and Receptor 11	['eHlV2f_30', 'K8mQm6_6', 'itatGU_8', 'KRIoAO_44', 'kWYzEw_36']
Common Compounds between Receptor 9 and Receptor 10	['K8mQm6_6', 'pNwq3c_10', 'gYYRjv_3', 'Zhq913_41', 'itatGU_8', 'nvDPzM_40', 'kWYzEw_36']
Common Compounds between Receptor 9 and Receptor 11	['eHlV2f_30', 'K8mQm6_6', 'pNwq3c_10', 'Zhq913_41', 'itatGU_8', 'nvDPzM_40', 'kWYzEw_36']
Common Compounds between Receptor 10 and Receptor 11	['K8mQm6_6', 'pNwq3c_10', 'Zhq913_41', 'itatGU_8', 'nvDPzM_40', 'kWYzEw_36']

Table.3.(B): Comprehensive Analysis — Comparison List of Molecules Demonstrating Common Inhibitory Properties Across 11 Receptors, Derived from 41 Novel Compounds Engineered with Flavonolignans, Hydnocarpin, and Coumarin as Fundamental Building Blocks.

Receptors	**Ligands**
Common compounds in the majority of the Receptors	[WkWiws_**33**, 0uP1Ww_**26**, eHlV2f_**30**, K8mQm6_**6**, pNwq3c_**10**, Zhq913_**41**, itatGU_**8**, hj06k4_**32**, nvDPzM_**40**]

Table.3.(C): Unified Potency — Common Inhibitory Compounds Across 11 Receptors, Unveiling Consistency in 41 Novel Compounds Engineered with Flavonolignans, Hydnocarpin, and Coumarin as Fundamental Building Blocks

S.No	**Ligand**	**Structure**
1.	WkWiws_**33**	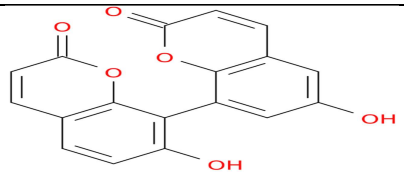
2.	0uP1Ww_**26**	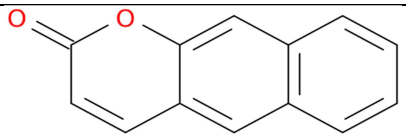
3.	eHlV2f_**30**	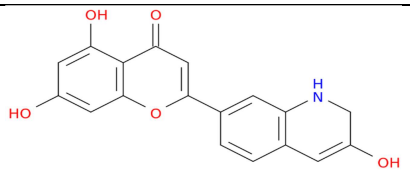

4.	K8mQm6_**6**	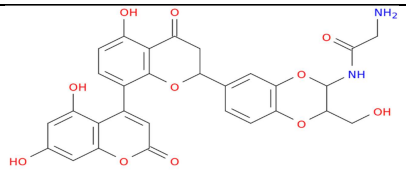
5.	pNwq3c_**10**	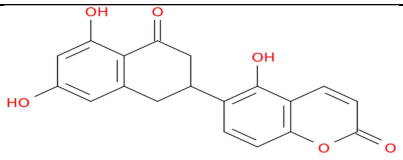
6.	Zhq913_**41**	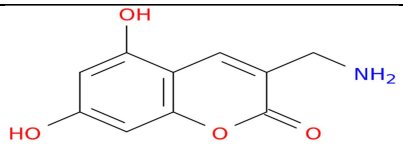
7.	itatGU_**8**	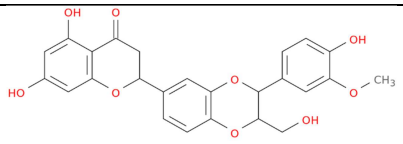
8.	hj06k4_**32**	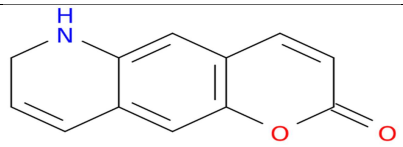
9.	nvDPzM_**40**	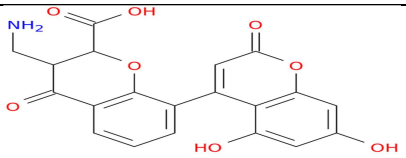

[Table.3.(E)] : Unified Potency — Common Inhibitory Compounds with Structures Across 11 Receptors, Unveiling Consistency in 41 Novel Compounds Engineered with Flavonolignans, Hydnocarpin, and Coumarin as Fundamental Building Blocks

Chapter 6

Conclusion

In the exploration of *Pseudomonas aeruginosa* quorum sensing pathways, four pivotal systems were identified, namely LAS, RHL, PQS, and IQS. In-depth investigations within these systems targeted specific components such as LASI and LASR in the LAS system, RHLR as the crucial receptor in the RHL system, and potential targets including PQSE, PQSD, PQSA, PQSR (MVFR), and PQSH within the PQS system. Additionally, the IQS system featured AMBE, AMBB, and the LuxR-type transcription factor QscR as significant components. In Chapter 3, utilizing the IMPATT database, the study identified molecules with potential inhibitory properties against the majority of receptors. Notable common molecules included IMPHY009207, IMPHY007725, IMPHY008591, IMPHY013460, and IMPHY007982. Similarly, in Chapter 4, employing the DRUG BANK, the study revealed common molecules exhibiting potential inhibition across the majority of receptors. Prominent among these were ligand8488, ligand8441, ligand8831, ligand7412, ligand7530, and ligand3749. Continuing this pattern of exploration, Chapter 5 aimed to identify common molecules demonstrating inhibitory potential across the majority of receptors. The study focused on molecules synthesized using flavonolignans, Hydnocarpin, and Coumarin as fundamental building blocks. Notable common molecules included WkWiws_33, 0uP1Ww_26, eHlV2f_30, K8mQm6_6, pNwq3c_10, Zhq913_41, itatGU_8, hj06k4_32, and nvDPzM_40. These findings underscore the consistency and reproducibility of potential inhibitors across different databases and compound designs. The study provides valuable insights for the development of targeted strategies against *Pseudomonas aeruginosa* quorum sensing pathways, showcasing promising molecules with broad spectrum inhibitory effects against *Pseudomonas aeruginosa* which is having very high MDR.

Future Scope

The comprehensive exploration of *Pseudomonas aeruginosa* quorum sensing pathways in this study has identified four crucial systems: LAS, RHL, PQS, and IQS. Delving into the intricacies of these systems, specific components were targeted, such as LASI and LASR in the LAS system, RHLR as the pivotal receptor in the RHL system, and potential targets within the PQS system, including PQSE, PQSD, PQSA, PQSR (MVFR), and PQSH. The IQS system featured significant components such as AMBE, AMBB, and the LuxR-type transcription factor QscR. The success of this research opens avenues for several promising future endeavors. Further investigations into the biological

mechanisms underlying the identified inhibitors can provide a deeper understanding of their mode of action and potential applications in real-world scenarios. The study's findings could pave the way for addressing the critical issue of MDR in bacterial infections. Understanding how these inhibitors affect multiple drug-resistant strains can lead to the development of more effective treatment strategies. The compounds identified in this study may exhibit broader antimicrobial properties, making them potential candidates for the treatment of various bacterial infections beyond *Pseudomonas aeruginosa*. Exploring cost-effective and time-efficient methods for synthesizing the identified compounds can enhance their practical applicability, potentially lowering the overall cost of drug development. Optimizing the productivity of the synthesis process and studying the scalability of production can contribute to the potential translational success of the identified inhibitors. Investigating the synergistic effects of the identified compounds with existing antibiotics or other antimicrobial agents can open new avenues for combination therapies, potentially enhancing treatment efficacy. Moving towards clinical trials and translational research is a natural progression, taking the study findings from the laboratory bench to the bedside for the benefit of patients. In conclusion, the culmination of this research not only provides valuable insights into quorum sensing inhibition in *Pseudomonas aeruginosa* but also lays the groundwork for addressing broader challenges in antimicrobial research and therapeutics. The future holds exciting possibilities for translating these findings into practical solutions for combating bacterial infections and advancing the field of antimicrobial drug discovery.

References

1. Keegan NR, Colón Torres NJ, Stringer AM, et al. Promoter selectivity of the RhlR quorum-sensing transcription factor receptor in Pseudomonas aeruginosa is coordinated by distinct and overlapping dependencies on C4-homoserine lactone and PqsE. PLoS Genet. 2023; 19:e1010900

2. Chioro A, Coll-Seck AM, Høie B, et al. Antimicrobial resistance: a priority for global health action. Bull. World Health Organ. 2015; 93:439–439

3. Abdula N, Macharia J, Motsoaledi A, et al. National action for global gains in antimicrobial resistance. Lancet 2016; 387:e3–e5

4. Laxminarayan R, Duse A, Wattal C, et al. Antibiotic resistance—the need for global solutions. Lancet Infect. Dis. 2013; 13:1057–1098

5. . Guidelines for the prevention and control of carbapenem-resistant Enterobacteriaceae, Acinetobacter baumannii, and Pseudomonas aeruginosa in health care facilities. 2017;

6. Hagiya H, Tanaka T, Takimoto K, et al. Non-nosocomial healthcare-associated left-sided Pseudomonas aeruginosa endocarditis: a case report and literature review. BMC Infect. Dis. 2016; 16:

7. Marcus N, Ashkenazi S, Samra Z, et al. Community-acquired Pseudomonas aeruginosa urinary tract infections in children hospitalized in a tertiary center: Relative frequency, risk factors, antimicrobial resistance and treatment. Infection 2008; 36:421–426

8. Sonmezer MC, Ertem G, Erdinc FS, et al. Evaluation of risk factors for antibiotic resistance in patients with nosocomial infections caused by*Pseudomonas aeruginosa*. Can. J. Infect. Dis. Med. Microbiol. 2016; 2016:1–9

9. Kalia VC, Wood TK, Kumar P. Evolution of resistance to quorum-sensing inhibitors. Microb. Ecol. 2014; 68:13–23

10. Peacock SJ, Paterson GK. Mechanisms of methicillin resistance in *staphylococcus aureus*. Annu. Rev. Biochem. 2015; 84:577–601

11. Rezaie P, Pourhajibagher M, Chiniforush N, et al. The effect of quorum-sensing and efflux pumps interactions in Pseudomonas aeruginosa against photooxidative stress. J. Lasers Med. Sci. 2018; 9:161–167

12. Zhong J, Zhao X. Transcriptomic analysis of viable but non-culturable Escherichia coli O157:H7 formation induced by low temperature. Microorganisms 2019; 7:634

13. Schweizer HP. Efflux as a mechanism of resistance to antimicrobials in Pseudomonas aeruginosa and related bacteria: unanswered questions. Genet. Mol. Res. 2003; 2:48–62

14. Breidenstein EBM, de la Fuente-Núñez C, Hancock REW. Pseudomonas aeruginosa: all roads lead to resistance. Trends Microbiol. 2011; 19:419–426

15. Høiby N, Bjarnsholt T, Givskov M, et al. Antibiotic resistance of bacterial biofilms. Int. J. Antimicrob. Agents 2010; 35:322–332

16. Welsh MA, Blackwell HE. Chemical genetics reveals environment-specific roles for quorum sensing circuits in Pseudomonas aeruginosa. Cell Chem. Biol. 2016; 23:361–369

17. Papaioannou E, Utari P, Quax W. Choosing an appropriate infection model to study quorum sensing inhibition in Pseudomonas infections. Int. J. Mol. Sci. 2013; 14:19309–19340

18. Diggle SP, Matthijs S, Wright VJ, et al. The Pseudomonas aeruginosa 4-quinolone signal molecules HHQ and PQS play multifunctional roles in quorum sensing and iron entrapment. Chem. Biol. 2007; 14:87–96

19. Schertzer JW, Brown SA, Whiteley M. Oxygen levels rapidly modulate Pseudomonas aeruginosa social behaviours via substrate limitation of PqsH. Mol. Microbiol. 2010; 77:1527–1538

20. Rampioni G, Falcone M, Heeb S, et al. Unravelling the genome-wide contributions of specific 2-alkyl-4-quinolones and PqsE to quorum sensing in Pseudomonas aeruginosa. PLoS Pathog. 2016; 12:e1006029

21. Drees SL, Fetzner S. PqsE of Pseudomonas aeruginosa acts as pathway-specific thioesterase in the biosynthesis of alkylquinolone signaling molecules. Chem. Biol. 2015; 22:611–618

22. Steindler L, Bertani I, De Sordi L, et al. LasI/R and RhlI/R quorum sensing in a strain of *Pseudomonas aeruginosa* beneficial to plants. Appl. Environ. Microbiol. 2009; 75:5131–5140

23. Bokhari SN. The Linux operating system. Computer (Long Beach Calif.) 1995; 28:74–79

24. Hasija Y, Chakraborty R. Python: Introduction and Environment Setup. Hands-On Data Science for Biologists Using Python 2021; 1–6

25. Beg M, Taka J, Kluyver T, et al. Using jupyter for reproducible scientific workflows. Comput. Sci. Eng. 2021; 23:36–46

26. Ossom Williamson P, Minter CIJ. Exploring PubMed as a reliable resource for scholarly communications services. J. Med. Libr. Assoc. 2019; 107:

27. Berman HM. The Protein Data Bank. Nucleic Acids Res. 2000; 28:235–242

28. Apweiler R. UniProt: The universal protein knowledgebase. Nucleic Acids Res. 2004; 32:115D – 119

29. Schwede T. SWISS-MODEL: an automated protein homology-modeling server. Nucleic Acids Res. 2003; 31:3381–3385

30. Trott O, Olson AJ. AutoDock Vina: improving the speed and accuracy of docking with a new scoring function, efficient optimization, and multithreading. J. Comput. Chem. 2010; 31:455–461

31. Seeliger D, de Groot BL. Ligand docking and binding site analysis with PyMOL and Autodock/Vina. J. Comput. Aided Mol. Des. 2010; 24:417–422

32. Forli S, Huey R, Pique ME, et al. Computational protein–ligand docking and virtual drug screening with the AutoDock suite. Nat. Protoc. 2016; 11:905–919

33. Binkowski TA, Naghibzadeh S, Liang J. CASTp: Computed Atlas of Surface Topography of proteins. Nucleic Acids Res. 2003; 31:3352–3355

34. O'Boyle NM, Banck M, James CA, et al. Open Babel: An open chemical toolbox. J. Cheminform. 2011; 3:33

35. Ihlenfeldt WD, Bolton EE, Bryant SH. The PubChem chemical structure sketcher. J. Cheminform. 2009; 1:

36. Laskowski RA, Swindells MB. LigPlot+: Multiple ligand–protein interaction diagrams for drug discovery. J. Chem. Inf. Model. 2011; 51:2778–2786

37. . National Center for Biotechnology Information. Springer Reference Medizin 2019; 1723–1723

38. Soukarieh F, Williams P, Stocks MJ, et al. *Pseudomonas aeruginosa* quorum sensing systems as drug discovery targets: Current position and future perspectives. J. Med. Chem. 2018; 61:10385–10402

39. Chegini Z, Khoshbayan A, Taati Moghadam M, et al. Bacteriophage therapy against Pseudomonas aeruginosa biofilms: a review. Ann. Clin. Microbiol. Antimicrob. 2020; 19:

40. McKnight SL, Iglewski BH, Pesci EC. The *Pseudomonas* quinolone signal regulates *rhl* quorum sensing in *Pseudomonas aeruginosa*. J. Bacteriol. 2000; 182:2702–2708

41. Sterling T, Irwin JJ. ZINC 15 – ligand discovery for everyone. J. Chem. Inf. Model. 2015; 55:2324–2337

42. Kim S, Thiessen PA, Bolton EE, et al. PubChem substance and compound databases. Nucleic Acids Res. 2016; 44:D1202–D1213

43. Gaulton A, Bellis LJ, Bento AP, et al. ChEMBL: a large-scale bioactivity database for drug discovery. Nucleic Acids Res. 2012; 40:D1100–D1107

44. Pence HE, Williams A. ChemSpider: An online chemical information resource. J. Chem. Educ. 2010; 87:1123–1124

45. Mohanraj K, Karthikeyan BS, Vivek-Ananth RP, et al. IMPPAT: A curated database of Indian Medicinal Plants, Phytochemistry And Therapeutics. Sci. Rep. 2018; 8:

46. Wishart DS. DrugBank: a comprehensive resource for in silico drug discovery and exploration. Nucleic Acids Res. 2006; 34:D668–D672

47. van Santen JA, Poynton EF, Iskakova D, et al. The Natural Products Atlas 2.0: a database of microbially-derived natural products. Nucleic Acids Res. 2022; 50:D1317–D1323

48. Banerjee P, Erehman J, Gohlke B-O, et al. Super Natural II—a database of natural products. Nucleic Acids Res. 2015; 43:D935–D939

49. Glessner A, Smith RS, Iglewski BH, et al. Roles of *Pseudomonas aeruginosa las* and *rhl* Quorum-Sensing Systems in Control of Twitching Motility. J. Bacteriol. 1999; 181:1623–1629

50. Li Q, Mao S, Wang H, et al. The Molecular Architecture of Pseudomonas aeruginosa Quorum-Sensing Inhibitors. Mar. Drugs 2022; 20:488

51. García-Reyes S, Soberón-Chávez G, Cocotl-Yanez M. The third quorum-sensing system of Pseudomonas aeruginosa: Pseudomonas quinolone signal and the enigmatic PqsE protein. J. Med. Microbiol. 2020; 69:25–34

52. Pearson JP, Pesci EC, Iglewski BH. Roles of Pseudomonas aeruginosa las and rhl quorum-sensing systems in control of elastase and rhamnolipid biosynthesis genes. J. Bacteriol. 1997; 179:5756–5767

53. Cao Q, Wang Y, Chen F, et al. A Novel Signal Transduction Pathway that Modulates rhl Quorum Sensing and Bacterial Virulence in Pseudomonas aeruginosa. PLoS Pathog. 2014; 10:e1004340